KADRI TOOME

Homing peptides for targeting of
brain diseases

KADRI TOOME

Homing peptides for targeting of brain diseases

Cancer Biology Research Group, Institute of Biomedicine and Translational Medicine, University of Tartu, Estonia.

The dissertation is accepted for the commencement of the degree of Doctor of Philosophy in Medicine on the 22nd of May 2020 by the council of the Faculty of Medicine, University of Tartu, Estonia.

Supervisor:	Professor Tambet Teesalu Lab of Cancer Biology, Institute of Biomedicine and Translational Medicine, Faculty of Medicine, University of Tartu
Reviewers:	Professor Margus Pooga, Institute of Technology, Faculty of Science and Technology, University of Tartu
	Kalle Kilk, MD, PhD, Department of Biochemistry, Institute of Biomedicine and Translational Medicine, University of Tartu
Opponent:	Cornelis F.M. Sier, PhD, Department of Surgery, Leiden University Medical Centre, Leiden, Holland
Commencement:	22nd of May 2020

Publication of this dissertation is granted by University of Tartu.

European Union
European Regional
Development Fund

Investing
in your future

TABLE OF CONTENTS

LIST OF ORIGINAL PUBLICATIONS

I   **Toome, K**; Willmore, AA.; Paiste, P.; Tobi, A.; Sugahara, KN.; Ruoslahti, E.; Braun, GB.; Teesalu, T.: **Ratiometric in vivo auditioning of targeted silver nanoparticles**. *Nanoscale*. 2017, 9(28)

II   Willmore, AA.; Simón-Gracia, L.; **Toome, K.**; Paiste, P.; Kotamraju, VR.; Mölder, T.; Sugahara; KN.; Ruoslahti, E.; Braun, GB.; Teesalu, T.: **Targeted silver nanoparticles for ratiometric cell phenotyping**. *Nanoscale*. 2016, 8(17)

III Säälik, P; Lingasamy, P.; **Toome, K**.; Mastandrea, I.; Rousso-Noori, L.; Tobi, A.; Simón-Gracia, L.; Hunt, H.; Paiste, P.; Kotamraju, VR.; Bergers, G.; Asser, T.; Rätsep, T.; Ruoslahti, E.; Bjerkvig, R.; Friedmann-Morvinski, D.; Teesalu, T.: **Peptide-guided nanoparticles for glioblastoma targeting.** *J Control Release.* 2019, 28(308)

IV   Mann, AP.; Scodeller, P.; Hussain, S.; Braun, GB.; Mölder T.; **Toome, K.**; Ambasudhan, R.; Teesalu, T.; Lipton, SA.; Ruoslahti, E.: **Identification of a peptide recognizing cerebrovascular changes in mouse models of Alzheimer's disease**. *Nat Commun.* 2017, 8(1)

My contribution to the articles referred to in this study is following:

Ref I
1. Designed all the experiments and developed the methodology by having discussions with T. Teesalu and A.A. Willmore.
2. Experimental part:
   - Ag nanoparticle coupling with linkers and relevant peptides
   - Performed all the animal experiments (including optimization experiments): injection of nanoparticles (including prior coupling of dye and peptides), termination of mice, extraction of relevant organs
   - Performed cryosectioning of tissues, antibody stainings and other necessary preparations for confocal microscopy, performed the confocal imaging of the tissue sections
   - Performed silver enhancement to visualize silver in the tissue sections, performed dark-field microscopy
   - Quantified fluorescent confocal images and dark-field microphotographs with proper software
   - Injected animals for ICP-MS/LA-ICP-MS analysis and conducted necessary tissue preparations
3. Data analysis and interpretation: Analyzed all the data in the article by using relevant software and interpreted the data. Had regular discussions with T.Teesalu and A.A. Willmore about the data and next steps.
4. Wrote the manuscript.

Ref II
1. Participated in the design of study and development of methodology by attending regular meetings with T. Teesalu, A. A. Willmore and L. Simón-Gracia.
2. Experimental part:
   a. Coupling of dye and peptides to AgNPs
   b. Cell culturing, seeding, AgNP binding experiments, antibody stainings and other necessary preparations for confocal microscopy, performed the confocal imaging
   c. Prepared samples for in vivo ICP-MS with 3 types of isotopic particles (injection of peptide, termination of mice and extraction of relevant organs followed by preparing samples for ICP-MS) – results were not included into the publication
3. Data analysis and interpretation: analyzed and interpreted the results from *in vivo* ICP-MS
4. Participated in writing of the manuscript.

Ref III
1. Participated in the design of study and development of methodology by attending meetings with T.Teesalu and P.Säälik
2. Experimental part:
   a. Established glioblastoma models in the Laboratory of Cancer Biology
   b. Performed phage display screens on GBM tumor bearing mice to identify new GBM homing peptides
   c. Tested multiple homing peptides in different GBM models to select the best suited one for subsequent experiments and treatment study – most of the results from 2a–2c were not included in this publication
   d. Induced GBM tumors for the experiments and experimental study (cell culturing for tumor induction in mice, monitoring of tumor growth in mice)
   e. Coupling of dye and peptides to AgNPs
   f. Preparing tissues for ICP-MS experiments
3. Participated in writing of the manuscript.

Ref IV
1. Experimental part:
   • Performed all the GBM experiments (including optimization experiments with different GBM models): Cell culturing for tumor induction in mice, monitoring of tumor growth in mice, injection of peptide, termination of mice and extraction of relevant organs followed by cryosectioning of the tissues, staining tissues with antibodies, and confocal microscopy.
2. Data analysis and interpretation: collected and interpreted confocal microscopy image from *in vivo* GBM homing experiments
3. Wrote the methodology and results part for GBM homing experiments and reviewed manuscript drafts.

ABBREVIATIONS

2D	two-dimensional
ABX	Abraxane
AD	Alzheimer's disease
Ag107	silver isotope 107
Ag109	silver isotope 109
AgNP	silver nanoparticle
APP	amyloid precursor protein
ATP	adenosine triphosphate
Aβ	β-amyloid peptide
B	bronchiole
B/biot	biotin
B-AgNP	silver nanoparticle blocked with biotin
BBB	blood-brain barrier
BBTB	blood-brain tumor barrier
Br	brain
BSA	bovine serum albumin
BSCB	blood-spinal cord barrier
CF555	succinimidyl ester, fluorescent dye
CendR	C-end Rule
CNS	central nervous system
CSF	cerebrospinal fluid
CTGF	connective tissue growth factor
DAPI	4`6-diamidino-2-phenylindole fluorescent dye
DMEM	Dulbecco's Modified Eagle Medium
DLS	Dynamic Light Scattering
EC	endothelial cell
EGF	epidermal growth factor
FAM	5(6)-carboxyfluorescein fluorescent dye
FDA	The Food and Drug Administration of the United States
FGF	fibroblast growth factor
FT	fibrillary tract
GBM	glioblastoma multiforme
GEMM	genetically engineered mouse model
GFAP	glial fibrillary acidic protein
GL	granular layer
GLUT1	glucose transporter 1
HEPES	4-(2-hydroxyethyl)-1-piperazineethanesulfonic acid
HPLC	High Performance Liquid Chromatography
ICP-MS	inductively coupled plasma mass spectroscopy
IMAC	immobilized metal affinity chromatography
IONW	iron oxide nanoworm
IV	intravenous

K-AgNP	silver nanoparticle functionalized with SGKRK
LA-ICP-MS	laser ablation inductively coupled plasma mass spectroscopy
LB	lysogeny broth
LinTT1	linearTT1, p32-directed tumor penetrating peptide, sequence [AKRGARSTA]
LRP	low-density lipoprotein receptor-related protein
mAbs	monoclonal antibodies
MEM	Minimum Essential Medium
MeOH	methanol
ML	molecular layer
MR	magnetic resonance
NA	neutravidin
NHS	N-hydroxysuccinimide
NTA	nitrilotriacetic acid
NP	nanoparticle
NP40	nonyl phenoxypolyethoxylethanol
NRP-1	neuropilin-1
NW	nanoworm
OBOC	one-bead-one-compound
OCT	Optimal Cutting Temperature compound
p32	protein 32
PAGE	polyacrylamide gel electrophoresis
PD	Parkinson's disease
PDGC	patient-derived glioma cell
PDX	patient-derived xenograft
PEG	polyethylene glycol
PFU	plaque-forming unit
PV	pulmonary vessel
RAGE	receptor for advanced glycation end products
RPAR/R	prototypic CendR peptide, sequence [RPARPAR]
R-AgNP	silver nanoparticle functionalized with RPARPAR peptide
RT	room temperature
SC	subcutaneous
SD	standard deviation
SDS	sodium dodecyl sulfate
SM	smooth muscle
TEM	transmission electron microscopy
TFA	trifluoroacetic acid
Tu/T	tumor
UV-vis	ultraviolet-visible
VEGF	vascular endothelial growth factor
Wt	wild type
X	aminohexanoic acid

1. INTRODUCTION

Already at the end of 19th century Paul Ehrlich discovered the vascular barrier between blood circulation and central nervous system as he observed that certain dyes when injected into vascular system stain all the organs except brain and spinal cord (Ehrlich 2013). Now it is well-known that protecting barriers exist in order to help maintain brain homeostasis and prevent the entrance of pathogens and toxic compounds (Engelhardt and Sorokin 2009). The same barriers limit the entrance of 98% of molecules, including most of the drugs into the brain tissue (Wolburg et al. 2009). This is the reason why improving diagnosis and treatment of brain disorders has remained a challenge compared to diseases in other parts of body. Enormous effort has been put into developing new drugs for CNS disorders but over 90% of drug candidates have proven inefficient, mainly because insufficient amount of drug was able to reach extravascular brain parenchyma (Cummings et al. 2015).

Actively targeted nanodrugs hold a great promise to improve the treatment of neurological disorders by precision delivery to disease site in CNS (Saraiva et al. 2016). Targeted nanomedicine approach requires excellent targeting ligands that would enable to transport adequate amount of cargo to lesion site. Phage display can be used for agnostic identification of peptide ligands that target receptors in the vascular beds in the CNS (Ghosh et al. 2018). Such homing peptides can be readily conjugated to drugs and nanoparticles to improve their biodistribution and activity. Using nanoparticles for the delivery has several advantages over the transport of free drugs, such as attachment of multiple copies of targeting peptides for enhanced avidity, prevention of the degradation of drugs during delivery and controlled release at disease site (VanDyke et al. 2016; Hua et al. 2018).

The thesis summarizes our work on identification and characterization of brain targeting peptides that could be used to improve the diagnosis and treatment of various neurological disorders. To enhance the validation process of homing peptides and to select the best performing peptides, an ultrasensitive quantification system based on isotopic silver nanoparticles and ICP-MS analysis was developed. Phage display on Alzheimer`s disease (AD) model was used to identify new peptides to target vascular changes in AD and studied suitability of a previously identified targeting peptide for malignant glioma nanodrug delivery.

2. LITERATURE REVIEW

2.1. Drug delivery challenge

Drug concentration at the biological receptor site determines the magnitude of the pharmacological response (Campbell and Cohall 2017). Even the agents with excellent bioavailability, long plasma half-lives and favorable receptor binding properties do not pass clinical testing if not able to reach the target at required concentration. Therefore, efforts to develop more efficacious drugs focus increasingly on optimizing drug biodistribution in tissues, cells, and on subcellular level. Encapsulating drugs into nanoparticles (NPs) can overcome some of the limitations of conventional medicine by promoting more desirable pharmacokinetics and biodistribution (Ventola 2017). The encapsulation in NPs can increase drug concentration at the intended site(s) of action (Vieira and Gamarra 2016). Loading a drug in nanocarriers can increase its stability, prolong the circulation time, extend the release of drug, and finally, decrease immunogenicity and systemic toxicity (Bobo et al. 2016).

NPs target tissues passively by taking advantage of longer circulation half-life and/or actively by using affinity ligands that bind to specific receptors expressed in a target tissue (Bertrand et al. 2014). Passive targeting to solid tumors relies on leaky vessels and poor lymphatic drainage that result in the extravasation and accumulation of drug in the tumor tissue (Maeda, Nakamura, and Fang 2013). Coating targeting ligands on NPs enables to fully exploit their potential as delivery vehicles. Active targeting improves accumulation of nano-therapeutics in target tissue and their uptake in target cells, leading to increased therapeutic efficacy and reduced off-target side effects (Danhier 2016; Ruoslahti 2012). By increasing the local drug concentration, active targeting helps to lower the risk of developing drug resistance (Andrieu et al. 2019).

The first nanodrug on the clinical market – Doxil (PEGylated liposomal doxorubicin) was approved by Food and Drug Administration (FDA) of the United States in 1995 for the treatment of Kaposi's sarcoma (Barenholz 2012; Harris et al. 2002). Compared with free doxorubicin, Doxil had fewer side effects. Approved nanodrugs are based on existing drugs that have been nano-formulated to improve their biodistribution or pharmacodynamic properties. Nanoparticle-based therapeutics have been approved for a variety of pathologies: cancer, hepatitis, multiple sclerosis, chronic kidney disease, macular degeneration, and hemophilia. All clinically approved nanoparticles are non-targeted passive drug delivery vehicles (Bobo et al. 2016).

2.1.1. Vascular heterogeneity and its targeting with affinity ligands

Blood and lymphatic vessels are morphologically, molecularly and physiologically diverse and specialized according to the site and physiological status of the tissue that they supply (Potente and Mäkinen 2017). In blood vessels, the luminal side of the vessels is covered by a single layer of endothelial cells (ECs), which form a continuous monolayer in arteries and veins, but can be fenestrated or discontinuous in capillaries. Endothelial layer permeability in the vasculature in different organs is not uniform. In the brain, ECs in conjunction with the supporting cells establish a highly selective blood-brain barrier with very low baseline permeability, whereas in the kidney glomerular endothelial cells enable rapid filtering of water and unbound drug molecules of less than 20 kDa. Above mentioned water and unbound drug molecules of less than 20 kDa are filtered through the glomerulus with the primary urine. Depending on tissue and its physiological status, endothelial cells also vary in their ability to mediate transport of nutrients and in expression of membrane receptors and transporters (Aird 2012). For example, neuronal cells need high levels of glucose and the ECs in the brain overexpress GLUT1 that transports glucose from blood to the brain parenchyma (Zhao et al. 2015). The ECs in the heart express high levels of the fatty acid transporter CD36, because cardiac muscles rely on fatty acid catabolism for ATP synthesis (Coppiello et al. 2015). Molecular heterogeneity of vascular endothelium has led to the identification of tissue and organ specific ligands that could be used for active targeting of drugs and nanoparticles into these tissues (Teesalu, Sugahara, and Ruoslahti 2012).

Normal vascular morphology, permeability, and gene expression are altered by many diseases, such as cancer, neurodegenerative disorders, cardiovascular disorders, and diabetes. Solid tumors depend on formation of new blood vessels to supply malignant tissue with nutrients and oxygen, leading to development of disorganized "leaky" vessels. Tumor neovasculature has molecular expression pattern different from the normal vessels in the same tissue; several molecular markers, like VEGF, integrins, and CD105, are upregulated on angiogenic vessels (Chen and Cai 2014). Alzheimer's lesions express elevated levels of RAGE receptor and decreased amount of LRP1 in their brain capillaries. Changes in RAGE and LRP1 expression promote disease progression by triggering accumulation of Aβ peptide and compromised BBB (Saraiva et al. 2016).

Molecular heterogeneity of blood vessels in normal tissues and elevated expression of systemically accessible molecular markers at disease sites allow affinity-based targeting to enhance drug concentration at disease-site, at the same time attenuating off-target side-effects (Ruoslahti 2004).

2.1.2. Classes of affinity ligands

A variety of molecules, such as antibodies, peptides, aptamers, vitamins and other low molecular weight compounds, can be used as affinity ligands (Liu et al. 2017).

Antibodies and antibody fragments are widely used as targeting ligands because of their high affinity and specificity. Several targeting antibodies have been approved by FDA for the delivery of radionuclides (e.g. Zevalin or Bexxar, anti-CD20 antibodies loaded with ^{90}Y or ^{131}I) and cytotoxic drugs (e.g. Trastuzumab emtasine) (Liu et al. 2017). However, most of the monoclonal antibodies (mAbs) penetrate poorly into tumor tissue because they are too big to extravasate and efficiently diffuse into tissue (Kue et al. 2016). Antibodies with high affinity to, e.g. tumor antigens, will stably bind to the first encountered antigen; this effect is called "binding site barrier", it will lead to uneven distribution inside the tumor tissue and suboptimal therapeutic effect. Thus, antibodies with moderate affinity are more favorable to be used as targeting ligands (Adams et al. 2001). The use of antibodies have several disadvantages; slow clearance of mAbs results in high normal tissue exposure, the Fc region of antibodies binds to reticuloendothelial system and can cause toxicities to liver, spleen and bone marrow (Liu et al. 2017). Their size makes large scale manufacturing process difficult and expensive (Liu et al. 2017). Antibody fragments can offer several advantages over the use of full-length mAbs; due to their smaller size antibody fragments can more effectively penetrate into tissues and access challenging epitopes and have potentially reduced immunogenicity (Bates and Power 2019).

Peptides are efficient alternative targeting ligands for selective delivery of drugs and nanoparticles. Several peptide hormones have already been used for tumor targeting, e.g. octreotide, an octapeptide that mimics natural somatostatin, has been used to target neuroendocrine tumor (Lopci et al. 2008). The size of targeting peptides falls in between the size of small molecule ligands and antibodies. Due to their larger size, they possess much higher binding affinity and specificity than small molecule ligands, but still being small enough to possess increased diffusion and tissue penetration (Jiang et al. 2019). The major problem of peptide ligands is their poor stability. Several modifications such as, cyclization, backbone/side chain modification, and unnatural residue substitution can be used to improve peptide stability against proteolysis (Chen et al. 2017). Peptide ligands are typically non-immunogenic, and the multivalent presentation on a NP provides high avidity for the target (Ruoslahti 2012). In addition, they can be readily conjugated to different drugs, nanoparticles, or radionuclides. Peptides can be synthesized on large scale at low cost (Zhao et al. 2007).

Aptamers are nucleic acid macromolecules with high affinity and specificity to their targets (Alshaer, Hillaireau, and Fattal 2018). DNA and RNA aptamers have been selected against different targets –small molecules, membrane receptors and whole living cells (Pereira et al. 2018). Aptamers can be readily

conjugated to drugs and nanoparticles and their chemical properties provide good solubility with low toxicity and immunogenicity. Additional advantage of aptamers is low cost of production. The main disadvantage of aptamers is sensitivity to degradation by nucleases and rapid clearance from the circulation (Alshaer, Hillaireau, and Fattal 2018). Additionally, aptamer-target interactions are strongly influenced by slight changes in the microenvironment that can alter the secondary and tertiary conformation of aptamers (Jiang et al. 2019).

Low molecular weight affinity ligands extravasate easily and quickly reach their target *in vivo*. Furthermore, small molecules are rapidly cleared from the circulation, if they fail to reach target cells, reducing the possibility of off-site toxicity (Srinivasarao and Low 2017; Vlashi et al. 2009). However, limited binding interfaces between low molecular compounds and their receptors restrict specificity of interaction (Jiang et al 2019). Small molecule ligands are amenable to chemical synthesis, making their production cost-effective (Kue et al. 2016). Some of the most promising small molecule ligands that have been used for tumor targeting are folate derivatives, glutamic acid urea derivatives, and low molecular weight analogues of peptide hormone somatostatin (Casi and Neri 2015).

2.1.3. Agnostic exploration of vascular heterogeneity by peptide phage display

Receptor-specific targeting peptides can be identified using various approaches: by using receptor's native ligands or their analogues (such as folic acid against folate receptor (Cheng et al. 2013)); by computer aided design based on the structure of the receptor (Chen et al. 2018); or by screening combinatorial libraries, such as OBOC combinatorial peptide library (Lam et al. 1991), peptide microarray (Xu and Lam 2003), phage-display peptide library (Krumpe et al. 2006), and other biological-display peptide libraries (Liu et al. 2017). Phage display is a powerful method that can be used to identify peptide ligands against simple and complex targets, including proteins, cells, and tissues. Phages are bacterial viruses that can be genetically engineered to express foreign peptides as fusions to the coat protein. Peptide phage library consist of a large number (typically about a billion) of bacteriophages, displaying different peptides on its surface (Smith and Petrenko 1997). Selection of phages that bind to specific target, "biopanning", can be performed *in vitro*, *ex vivo* and *in vivo* (Liu et al. 2017). Sequential biopanning rounds enrich the library with target-binding peptides, whereas the background phages are eliminated (Fig. 2). *In vivo* phage display can be used to identify peptides that target systemically accessible receptors that can be reached from the vasculature.
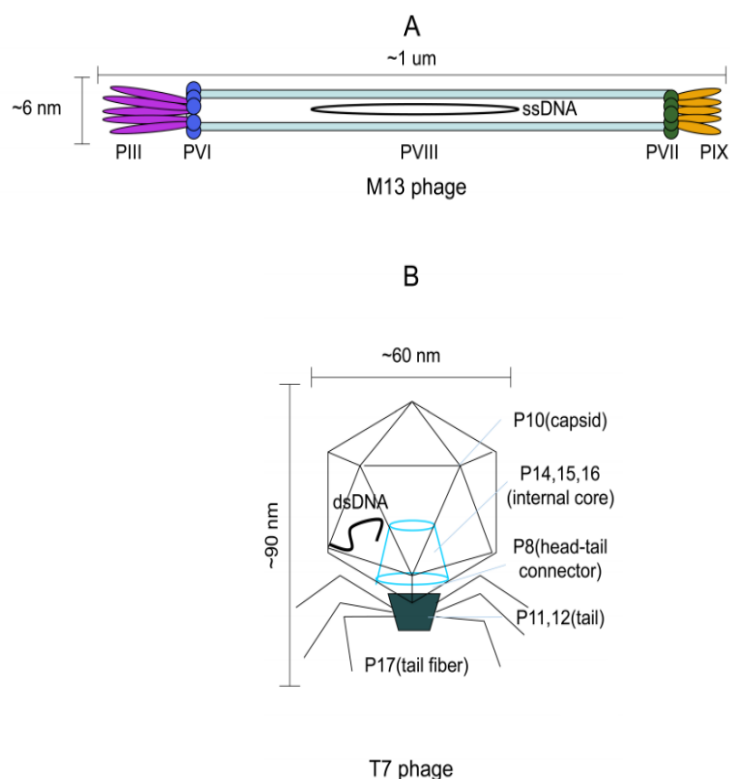
Figure 1: The schematic representation of (A) M13 phage and (B) T7 phage.
Adapted from Tan et al. (2016).

Numerous bacteriophage species have been employed in phage display systems, including f1, fd, T4, M13 and T7 (Deng et al. 2018).

T7 is a lytic coliphage with double-stranded DNA, which exhibits increased stability and low mutation rate during replication (Deng et al. 2018). Compared to filamentous phage-based systems, the peptide libraries constructed with the T7 display system retain fewer amino acid biases and have increased diversity of displayed peptides (Krumpe et al. 2006). Importantly, the size (~60 nm diameter) and shape of T7 particles and density of displayed peptides are similar to what is typically seen for (pre)clinical nanoparticles (Fig. 1b). Density of C-terminally exposed foreign peptides on T7 particle can be modulated across a wide range (1–415 peptides/particle) by amplifying peptide-phages in *E. coli* strains with different expression of wild-type p10 coat protein (T7Select® System Manual). As peptide density on phage particle is similar to the density on nanoparticles, it means that the novel peptides discovered using T7 display system are suitable for multivalent use on the nanoparticles. Multivalent presentation of peptides on biological phage particles and synthetic nanoparticles

increases the avidity and ensures strong target binding even with relatively low affinity (Ruoslahti 2012).
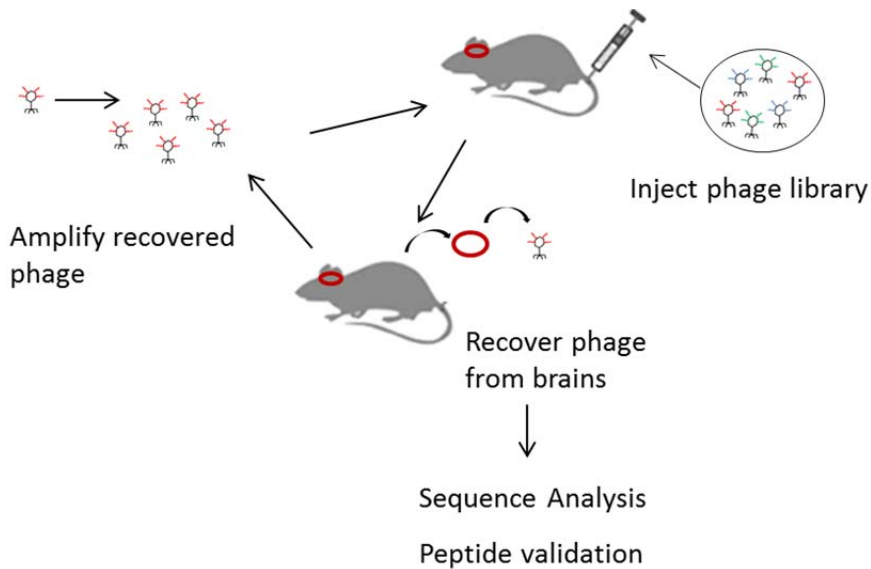
Figure 2: *In vivo* **phage display for brain homing peptides.** Peptide phage library is injected into blood circulation. After 10–60 min circulation, the brain and other organs are collected and homogenized in a buffered non-ionic detergent solution. The bound phage pool from the brain is amplified and used as input in the next biopanning round. After several rounds of selection, phages are recovered from brains and the peptide-encoding portion of the phage genome is sequenced. Enriched peptides are identified and validated further in individual phage homing assays and as synthetic peptides labeled with fluorophores or coated on nanoparticles.

The M13 phage is another widely used phage-display system with high capacity for replication and nonessential regions that allow exogenous gene insertions (Liu et al. 2017). M13 phage is a filamentous phage containing single-stranded DNA. M13 phage particles (Fig. 1a) are 6.5 nm in diameter and 1μm in length, and the peptides are displayed at one end of the phage particle (Tan et al. 2016). The use of filamentous phage systems have several disadvantages compared to lytic phage, filamentous phage vectors are associated with a limited cloning capacity, which in the case of M13 is < 1500 bp, and their genome exhibits markedly reduced stability following insertion of foreign DNA (Deng et al. 2018). Filamentous phage morphogenesis: phage assembly, secretion, and in-fection processes, limits significantly the diversity of peptides propagated in the M13 libraries as displayed peptides need to be compatible with *E.coli* secretory system (Krumpe et al. 2006).

2.1.4. Drug delivery to the brain. Blood-brain barrier

Already in the 1880s Paul Ehrlich observed that intravenously injected hydrophilic dyes stain all organs except the brain and the spinal cord (Dyrna 2013). It has become well established that the central nervous system has evolved different barriers that are important for protecting it from foreign substances and to maintain homeostasis. These protective structures include blood-brain barrier (BBB), blood-cerebrospinal fluid (CSF) barrier, blood-spinal cord barrier and blood-retinal barrier. The most selective of these barriers is the blood-brain barrier (Cipolla 2009). The BBB is crucial for protecting brain cells against circulating toxic or infectious agents and preserving the CNS homeostasis (Hawkins and Davis 2005). The BBB is impermeable to all large molecules and >95% of small molecules. Only a few molecules with specific characteristics are able to cross the barrier, such as water, some gases, and some lipophilic compounds (Saraiva et al. 2016). Small-molecule drugs need to have molecular mass under a 400- to 500-Da threshold, and high lipid solubility to cross the BBB in pharmacologically significant amounts (Pardridge 2003). Most low molecular weight drugs, mAbs, recombinant proteins, or gene therapeutics, do not cross the BBB (Pardridge 2005).

For most CNS diseases there are candidate drugs that show efficacy *in vitro* and when directly injected in the brain, however these compounds do not cross the BBB and are not effective upon systemic administration. For example, catalase could be potentially used to treat patients with chronic neurodegenerative diseases, as this enzyme binds to amyloid-β plaques and is a potent antioxidant able to fight oxidative stress seen at chronic inflammation (Singhal et al. 2013). However, inability of catalase to cross the BBB (and some other features such as a short half-life and poor cellular uptake) are not compatible with its therapeutic use (Jaffer et al. 2011). Curcumin, a polyphenol derived from turmeric herb, has a high affinity for the Aβ peptides and promotes the disaggregation of amyloid-β plaques. However, low bioavailability of curcumin excludes its uses for diagnosis and treatment of AD (Tang, Taghibiglou, and Liu 2017). Therapeutic hypothermia induced by neurotensin peptide has a neuroprotective effect and thereby could improve neurological outcome at severe liver failure, stroke, or neonatal ischemia. However, the clinical use of neurotensin is hampered because the peptide is not able to cross the BBB and enter the CNS to reach its target neurons in the lateral hypothalamus (Tang and Yenari 2010).

2.1.4.1. Anatomy and physiology of the BBB

Structurally, the BBB is composed of endothelial cells, astrocytes, pericytes and neurons (Fig. 3). Polarized endothelial cells lining the lumen of the cerebral capillaries are connected by tight junctions that form selective interface between blood and brain (Hawkins and Davis 2005).
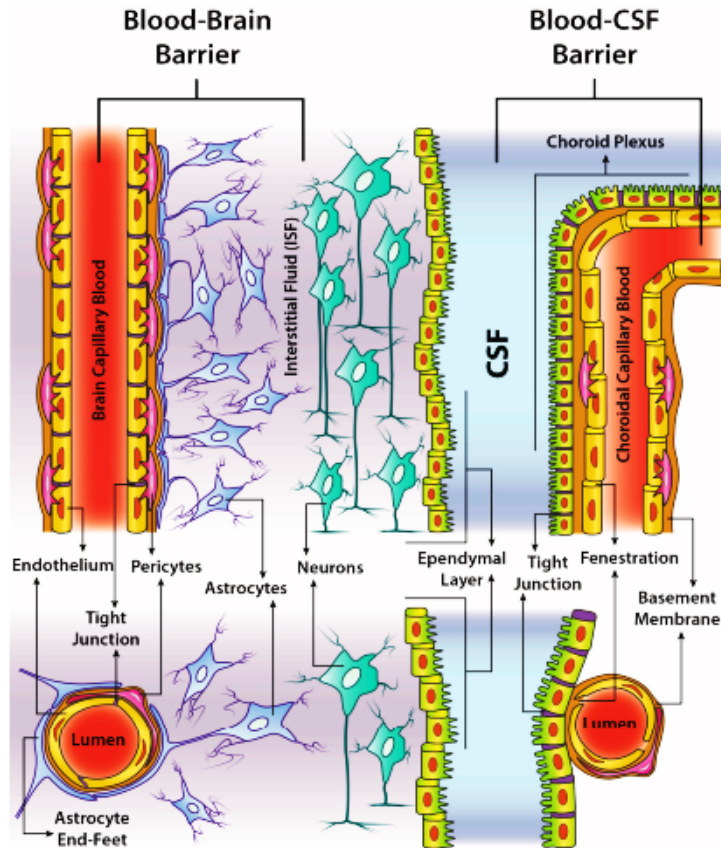
Figure 3: Structure of the BBB and the blood-CSF barrier. (Left) BBB is a highly selective barrier that separates blood from the brain parenchyma. BBB is composed of network of astrocytes, pericytes, neurons, and endothelial cells. (Right) The blood-CSF barrier is a more permissive barrier found in the choroid plexus of each ventricle of the brain. The blood-CSF barrier is composed of epithelium-like ependymal cells covering fenestrated capillaries. Tight junctions between ependymal cells are leakier to small molecules compared to the tight junctions forming the BBB. Adapted from D'Agata et al. (2018).
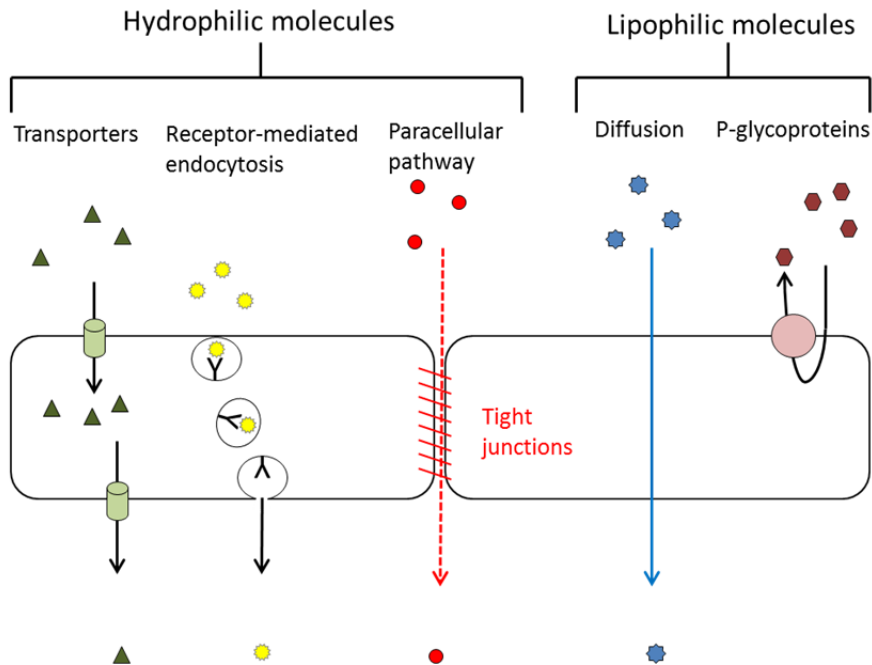
Figure 4: Pathways of transport across the BBB. Adapted from Gabathuler (2010).

Brain capillary endothelial cells express active transport mechanisms that ensure the transport of nutrients into the CNS and exclusion of blood-borne molecules (Fig. 4) (Engelhardt and Sorokin 2009). Small hydrophilic molecules that are essential for the brain cells to function, like amino acids and glucose, use transporters at the luminal and basolateral side of the endothelial cells. Larger and/or hydrophilic molecules such as hormones, transferrin and lipoproteins use specific receptors expressed in high numbers on the luminal side of the endothelial cells. These receptors facilitate endocytosis and transcytosis of compounds across the barrier. Small lipophilic molecules are able to diffuse passively across the BBB but are exposed to efflux pumps such as P-glycoprotein and Multidrug Resistance Proteins (Gabathuler 2010).

Some regions of the brain require a more permissive barrier for proper functioning, such as ventricular and circumventricular areas of the brain. Ventricular system is comprised of two lateral ventricles, and a third and fourth ventricle. Cerebrospinal fluid (CSF) is produced in the third and fourth ventricles by the choroid plexuses and capillaries. CSF protects the brain and spinal cord and provides them with important nutrients. Structurally, the choroid plexus is composed of capillaries covered by epithelium-like ependymal cells. Capillaries of the choroid plexus are fenestrated and allow direct passage from blood to the brain parenchyma. Tight junctions of the ependymal cells that cover the capillaries form the blood-CSF barrier (Fig. 3). Tight junctions between the

ependymal cells are leakier than between the cells of BBB (Cipolla 2009; Saraiva et al. 2016). Transport of compounds from blood into the CSF is similar to that into brain, with many of the transporters shared between the tissues. Due to the different properties of the two barriers, some compounds predominantly enter the brain by crossing the BBB, such as O_2, CO_2, glucose and amino acids, but others like Ca-ions and several hormones have choroid plexus as the major site of entry (Laterra et al. 1999). It has been shown that nanoparticles, which have been injected intravenously, will accumulate in these leakier areas irrespective of their cargo (Xin et al 2012).

Blood-spinal cord barrier (BSCB) protects and regulates the homeostasis of the spinal cord parenchyma. BSCB has similar structure as the BBB: it is composed of endothelial cells, basement membrane, pericytes, and astrocytic end-feet processes. However, the BSCB has several functional and morpho-logical differences when compared to the BBB. The microvessels in the spinal cord contain glycogen deposits not present in brain capillaries. Compared to the BBB, the BSCB is more permeable to variable tracers and cytokines (Pan, Banks, and Kastin 1997), potentially due to low expression of tight junction and adherens junction proteins in the spinal cord (Bartanusz et al. 2011).

BBB organization and function are severely altered in brain tumors and at neurodegenerative disorders, the disrupted BBB in case of brain tumors is called blood-brain tumor barrier (BBTB). BBTB limits the access of anticancer drugs to the brain tumor. In low grade diffuse gliomas the tumor cells are present as oligocellular aggregates in the brain parenchyma and the BBTB resembles structurally and functionally the BBB (Van Tellingen et al. 2015). In contrast, high grade gliomas are highly angiogenic tumors with leaky BBTB, as has been shown by contrast-enhanced MRI (Dhermain et al. 2010). BBTB shows elevated expression of receptors that mediate ligand-dependent drug delivery and could be targeted to improve drug delivery to tumor tissue (Ningaraj 2002). The BBB is formed by capillaries without fenestrations, but the BBTB can be comprised of non-fenestrated capillaries, capillaries with fenestrations and capillaries containing inter-endothelial gaps (Schlageter et al. 1999). BBTB capillaries present overexpression of drug efflux pumps and multidrug resistance-associated proteins, which function against the leaky vasculature and prevent the uptake of drugs by cancer cells (Ningaraj 2006). In addition, the tumor growth results in increased pressure to the surrounding tissue and leads to formation of intracranial edema that also limits the delivery of drugs to tumor (Wolburg et al. 2012).

2.1.4.2. Affinity targeting of the CNS

The presence of intact BBB is a major obstacle in treating CNS diseases. As less than 2% of the drug candidates are able to penetrate the BBB and to enter the cerebral tissue, more efficient CNS delivery strategies are needed to „by-pass" the protective BBB shield (Pardridge 2005). The concept of BBB shuttles –

application of molecular vectors for penetration from systemic circulation into brain parenchyma without disrupting the protective barrier – was introduced already more than three decades ago (Pardridge 1986). Most commonly used CNS delivery approach is receptor-mediated transport that takes advantage of highly expressed transport receptors on the luminal side of brain endothelial cells, such as transferrin receptor, insulin receptor, low-density lipoprotein receptor and LRP1 (Lajoie and Shusta 2014). Over the years, a number of BBB shuttle peptides have been published that bind to the receptors and thereby allow the transport of different cargoes, including small molecules, nano-particles and genetic material beyond the BBB (Table 1) (Urich et al. 2015; Zarebkohan et al. 2015). Despite the discovery of numerous BBB shuttle peptides, crossing the BBB to deliver drugs and diagnostic agents to the brain remains still a major hurdle. The shortage of brain selectivity and poor penetration capacity across the BBB are the two main problems current BBB crossing strategies are facing (Ross et al. 2018). Intensive research is ongoing in two main directions: firstly, to find new brain-specific markers to improve drug transport across the blood-brain barrier and more selectively to diseased cells, in order to minimize distribution into normal brain cells (Gao 2016). And secondly, to develop new nanocarriers with long plasma circulation that are nontoxic, biocompatible, and biodegradable, since the brain has very limited capability for elimination and metabolization of the translocated nanoparticles (Mi, Cabral, and Kataoka 2019).

Table 1: Brain homing peptides and evidence for the BBB penetration.

Peptide	Identification	Evidence for BBB penetration	Reference
CLSSRLDA	*In vivo* phage display for mouse brain homing peptides	Barrier penetration in an *in vitro* cell-based rat BBB model	(Pasqualini and Ruoslahti 1996)
LSSRLDAC	*In vivo* phage display for mouse brain homing peptides	Barrier penetration in an *in vitro* cell-based rat BBB model	(Pasqualini and Ruoslahti 1996)
CGHKAKG	*In vitro* phage display on extracellular domain of hTfR	Neuronal delivery of therapeutic payload in mouse AD model	(Xia et al. 2000)
THRPPMWSPVWP	*In vitro* phage display on cells that constitutively express the hTfR	Barrier penetration in an *in vitro* cell-based rat/bovine BBB model Demonstartion of the BBB penetration by transmission electron microscopy on rat brain sections	(Lee et al. 2001)
CAGALCY	*In vivo* phage display for mouse brain homing peptides	n.a.	(Fan et al. 2007)
TFFYGGSRGKRNNFKTEEYC	Neurotropic endogenous protein derived from the Kunitz domain of aprotinin	*In vivo* delivery of paclitaxel to mouse model of glioblastoma	(Demeule et al. 2008)
CMPRLRGCC	*In vitro* phage display on extracellular domain of human LDLR	Optical demonstration of BBB penetration by multiphoton microscopy in live mice	(Malcor et al. 2012)
RLSSVDSDLSGC	*In vivo* phage display for rat brain homing peptides	Peptide-phage recovered from the rat CSF	(Urich et al. 2015)
TPSYDTYAAELR	*In vivo* phage display for rat brain homing peptides	Peptide-phage recovered from the rat CSF	(Li, Feng, and Jiang 2015)

2.1.5. Brain diseases with unmet drug delivery challenge

2.1.5.1. Neurological disorders: Alzheimer's disease

The frequency of neurological diseases is expected to reach epidemic scale in the next decades as the average life expectancy is increasing globally. Neuropathies and neurodegenerative diseases such as Alzheimer's disease (AD) and Parkinson's disease (PD) lead to adverse health outcomes in patients and put immense load on healthcare system (Heemels et al. 2016). Already now, the morbidity and mortality caused by brain-related disorders is higher than that of cardiovascular diseases and cancer (Sharma et al. 2017). Improved diagnostic tools and treatments need to be developed to decrease the burden on affected individuals and society (Kevadiya et al. 2018). Current treatments fail to cure the neurodegenerative diseases or even slow down their progression and only deal with the symptoms (Kevadiya et al. 2018). Treatment with neuroprotective agents is likely to be an effective strategy to prevent neuronal degeneration, but typically these bioactive compounds are not able to cross the BBB (Levi and Brimble 2004). There are clinically approved drugs that have been reported to be effective in treating neurodegenerative disorders on experimental models, but they lack the ability to cross the BBB or require very high doses causing severe off-target side effects. One of the examples is minocycline; it is a broad-spectrum antibiotic, which has been used over 30 years to treat infections caused by Gram-negative and Gram-positive bacteria. Several groups have shown it to have neuroprotective effect in various experimental models of CNS diseases. Whereas minocycline is able to penetrate the BBB to some degree, it must be administered at high doses (with serious side effects) to achieve therapeutic concentration in the brain (Sharma et al. 2017). Using targeted delivery strategies to transport minocycline and other neuroprotective agents selectively to the brain and across the BBB could be the way treat neurodegeneration in patients.

AD is the most common age-related neurological disorder. AD causes widespread neuronal and synaptic loss, amnesia, cognitive impairment, hallucinations, and social deficits. AD is characterized by progressive and irreversible damage to neurons (Kevadiya et al. 2018). The most prevalent hypothesis regarding AD pathogenesis suggests that the accumulation of β-amyloid peptide (Aβ) is the key mechanism causing the disease (de la Torre and Ceña 2018). Overproduction of Aβ peptide isoforms causes aggregation of peptide fragments into large fibrils that become deposited as insoluble plaques (Golde, Eckman, and Younkin 2000). The Aβ plaques form first in the basal cortex but are at later stages detected in most neocortical regions except in the hippocampus (Braunstein et al. 2016). Aβ plaque toxicity is caused by multiple mechanisms, including increased membrane permeability, oxidative stress, synaptic dysfunction and microglial activation (Lin et al. 2001, Butterfield et al. 2007, Parameshwaran et al. 2008).

Whereas in most cases the AD begins after the age of 65 years, approximately 6% of patients have early-onset AD, an autosomal-dominant genetic disease that manifests in patients at ages 30–50 (Bateman et al. 2011; Dzamba et al. 2016). The clinical diagnosis of AD is based on family history, symptoms of dementia, imaging by computerized tomography (or magnetic resonance imaging), and blood biomarkers (Hane et al. 2017). However, a conclusive AD diagnosis can only be obtained post-mortem by autopsy (Kelley et al. 2007).

Currently, there are only five medications approved for the treatment of AD; four cholinesterase inhibitors and N-methyl-D-aspartate receptor antagonist (Cummings et al. 2014). These drugs are used to treat cognitive symptoms but fail to stop the progression of neuronal damage and loss. Discovery of new drugs able to slow down or reverse the progression of the AD is challenging, and disappointingly most of the clinical studies using investigational new drugs have failed to demonstrate clinical efficacy (Salloway et al. 2014). New cellular pathways and molecules involved in AD pathogenesis need to be identified to improve diagnosis and treatment.

2.1.5.2. Gliomas

Malignant glial tumors are the most common primary brain tumors. Gliomas are characterized by heterogeneity inside the tumors and between the tumors of different patients (Parsons et al. 2008). Gliomas originate from the glial cells: astrocytes, oligodendrocytes or ependymal cells. Depending on the cell of origin gliomas are classified into 3 groups: astrocytomas (including glioblastomas), oligodendrogliomas, and ependymomas; some tumors display a mixed phenotype of these different cells (Louis et al. 2016). Glioblastomas (GBM) are the most frequent and aggressive of the glial tumors. Despite intense research, GBM remains highly malignant with very poor prognosis in the patients. The current median survival of the patients is less than 15 months after GBM diagnosis (Stupp et al. 2005). GBM treatment combines maximum surgical resection of the tumor tissue with the radiation therapy and/or chemotherapy. Despite the aggressive treatment, the prognosis remains low due to high recurrence rate. Complete resection of the tumor is impossible because of anatomical location and highly infiltrative nature of these tumors (Stupp et al. 2005; Shirahata et al. 2007). Radiation and chemotherapy kill actively proliferating glioma cells but are unable to reach to the quiescent glioma stem cells that are hiding in hypoxic regions and behind the blood brain barrier. Recurrent GBM that develops from the guerilla cells away from tumor bulk grows rapidly and spreads to more distant regions and is more resistant to chemotherapy than the initial tumor (Yip et al. 2009).

Although GBM is highly angiogenic with leaky blood vessels and BBB disruption in the core of the tumor, most of the approved anticancer therapeutics are not able to cross the BBB or the BBTB (Van Tellingen et al. 2015). Currently there are only two anticancer agents, temozolomide and nitrosourea, that are able to cross the BBB and reach the cerebral tissue. Neither of these

agents is highly effective against GBM and new strategies for GBM management are actively sought for with >400 glioblastoma studies ongoing all over the world in late 2019 (Argyriou and Kalofonos 2009; clinicaltrials.gov).

2.2. Preclinical modeling of glioma and neurodegenerative disease

2.2.1. Glioma modeling in mice

Tumor modeling in small animals has a crucial role for development of new therapeutic strategies, to study tumor biology, and predict efficacy and toxicities of potential new therapies. Implantable brain tumor models have been widely used and well characterized (Assi et al. 2012).

Commercially available tumor cell lines are extensively used for both *in vitro* and *in vivo* research. These cell lines were initially derived from patient GBM tumor tissue and are commonly cultivated in 2D in serum-containing medium (Kijima and Kanemura 2017). Human-derived glioma cells have to be xenografted into immunodeficient animals; transplantation of cancer cells into rodents by stereotactic injection enables to induce tumors at specific anatomical structures within the brain (Assi et al. 2012). Patient-derived glioma cells (PDGCs) give rise to tumors that grow rapidly, have high engraftment rate, and good reproducibility (Fig. 5b) (Huszthy et al. 2012). However, xenografts induced by PDGCs often fail to reflect important clinical characteristics of real patient tumors, as the cell-line derived tumors are often circumscribed and fail to exhibit the hallmarks of clinical glioma: the presence of necrotic areas and single-cell invasion into surrounding brain tissue (Mahesparan et al. 2003).

Patient-derived xenografts (PDX) are established by implanting fresh tumor tissue or cultured tumor spheroids into immunodeficient animals (Fig. 5b) (Bjerkvig et al. 1990; Tentler et al. 2012). PDX models are maintained by serial passaging in animals or by producing tumor spheroids, often under serum-free neurosphere-culture conditions (Bjerkvig et al. 1990). PDX models are widely used in translational research, as they preserve both the genetic and histological features of parental tumors. Array-comparative genomic hybridization analysis has shown that in contrast to cell line xenografts, which genetically do not resemble patient tumors, PDX spheroids retain the genetic profile of parental tumors even after multiple *in vitro*/*in vivo* passages. Importantly, the PDX tumors maintain tumor heterogeneity; they remain infiltrative and have necrotic areas, which are main characteristics of clinical GBM (De Witt Hamer et al. 2008). However, not all human gliomas are tumorigenic when injected to animals; and some tumors fail to produce tumor spheroids. The time needed to establish the tumor varies between passages and different PDX tumors, making experimental planning challenging (Huszthy et al. 2012). Despite the disadvantages, PDX models are the way to move towards personalized treatment of tumors (Kijima and Kanemura 2017).
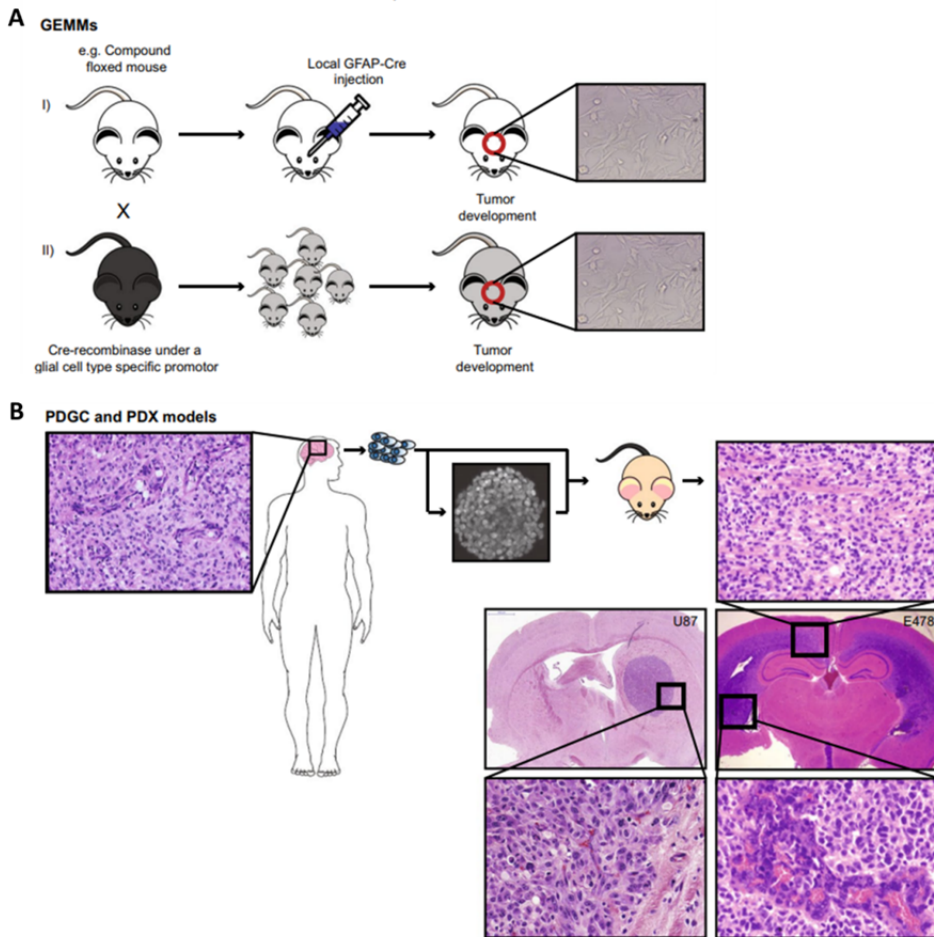
Figure 5: *In vivo* **GBM modeling.** (A) Genetically engineered mouse models are generated using Tet-regulation or Cre-inducible gene alleles. These GBM models are molecularly highly defined but fail to reflect biological heterogeneity seen in human GBM. (B) Patient-derived glioma cells (PDGCs) give rise to tumors that grow rapidly, have high engraftment rate, and good reproducibility. Tumors derived from PDGCs are often circumscribed without the presence of necrotic areas and single-cell invasion into surrounding tissue. Patient-derived xenografts (PDX) are generated by implanting fresh tumor tissue or cultured tumor spheroids into immunocompromised animals. Ideally, PDX models preserve both the genetic and histological features of parental tumors; florid microvascular proliferation (lower right panel) and diffuse infiltrative growth in the white matter (upper right image). Of note, as illustrated by a xenograft derived from U87 cells (lower left panel), PDGC models often fail to show diffuse infiltration in brain parenchyma. Adapted from Lenting et al. (2017).

Genetically engineered mouse models (GEMMs) resemble the histopathology and molecular features of human tumors (Fig. 5a). In genetically engineered models, gene expression has been manipulated often by using Tet-regulation or Cre-inducible gene alleles. GEMMs are especially useful to verify genetic alterations which are important for tumor initiation and progression (Kijima and Kanemura 2017). A disadvantage is that as the GEMM tumors are formed by cells with specific genetic changes, the tumors do not exhibit the biological heterogeneity seen in clinical GBM (Lenting et al. 2017).

2.2.2. Preclinical modeling of neurodegenerative diseases

To better understand AD pathology and progression, several human amyloid precursor protein (APP) transgenic models have been developed, these mouse lines express various mutations identified from patients with familial AD (Saraiva et al. 2016). hAPP-J20 model overexpresses human APP with Swedish mutation (K670N/ M671L) and Indiana mutation (V717F); Tg2576 model expresses human APP with the Swedish mutation (K670N/ M671L) (www.alzforum.org/research-models/j20-pdgf-appswind; Van Dam and De Deyn 2011). As these models rely on mutations from familial forms of human AD (5% of AD cases), they fail to replicate the complete neuropathology spectrum seen in patients. Nevertheless, AD animal models are crucial for developing new therapeutic strategies (Saraiva et al. 2016).

PD models are based on the administration of toxins that cause selective death of dopaminergic neurons (Saraiva et al. 2016). Two of the most promising models are the rotenone model and the combined paraquat/maneb model. Rotenone and paraquat are pesticides; maneb is a fungicide that has been linked to the development of parkinsonian symptoms in humans (Schapira and Jenner 2011; Thiruchelvam et al. 2000). PD neurotoxic models are essential for under-standing consequences of striatal dopamine loss and enable to develop current dopaminergic therapies (Bové et al. 2005; Schapira and Jenner 2011). Nume-rous genetic PD models have been developed using transgenes with mutations causing familial PD. Genetic models are mainly used for modeling familial PD but can also be used to study more common PD mechanisms. None of the current models recapitulates the complex and progressive pathology of human disease (Jagmag et al. 2016).

2.3. Nanomedicine

The use of nanoparticles has a surprisingly long history; already during Roman times gold nanoparticles were used by artisans to stain glass (Giljohann et al. 2010). The idea of using nanoparticles for medical purposes dates back more than a century ago, when German scientist Paul Ehrlich formulated a concept of

targeted delivery of drugs, that he called *Zauberkugeln* or magic bullets (Kreuter 2007).

Even today the nanomedicine is seen as the "the magic bullet" that could improve cancer therapy and ameliorate treatment of neurological disorders by developing noninvasive therapies that are more effective in reaching the target sites, have increased therapeutic efficacy, and cause less adverse side-effects (VanDyke et al. 2016; Hua et al. 2018). Multitude of nanoformulations of different composition, size, shape, and surface properties, have been designed for therapeutic, diagnostic and theranostic applications (Fig. 6), but only few of them have been approved for clinical use (Danhier 2016; Hua et al. 2018; L. Zhang et al. 2008).
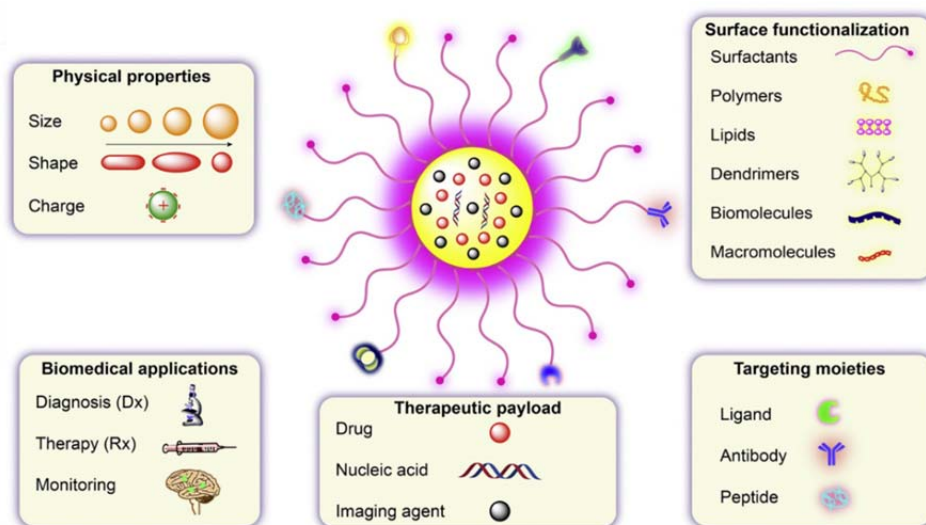
Figure 6: Design, physicochemical properties and biomedical applications of targeted nanoparticles. Adapted from Kevadiya et al. (2018).

2.3.1. Nanoparticle characteristics

The half-life of nanoparticles in the systemic circulation and how well they are able to accumulate in the target tissue is determined by their physicochemical properties. Very small particles, <5 nm, are not suitable for drug delivery, as they will be cleared quickly from the blood by kidneys and particles > 200 nm accumulate in the liver and spleen (Blanco, Shen, and Ferrari 2015; Ernsting et al. 2013). Nanoparticles with size between 8 nm and 100 nm are considered optimal for tumor targeting, as the circulation time is prolonged and they are still small enough to escape from the leaky vasculature present in tumors (Albanese, Tang, and Chan 2012). Bigger nanoparticles have longer half-life, but they would not be able to go through the fenestrations on the angiogenic blood vessels (Yue et al. 2013). Inside the tumor tissue, the correlation between

nanoparticle size and the penetration is reversed, with smaller nanoparticles able to accumulate deeper inside the tumor parenchyma, and bigger particles remaining close to the vasculature (Albanese, Tang, and Chan 2012). To take the advantage of the both phenomena, size-switchable nanoparticle systems have been developed that exploit the advantage of the longer circulation of larger particles and after extravasation particles shrink due to low pH or enzymatic cleavage, to penetrate more effectively (Ruan et al. 2015; Zhang et al. 2016).

The shape of nanoparticles has a strong effect on their distribution in the body and uptake by cells. Spherical nanoparticles are most often used in the preclinical studies, as it is relatively easy to synthesize them, but it has been shown that elongated nanoparticles have prolonged circulation and extravasate more effectively through the pores in tumor vessels (Geng et al. 2007; Stylianopoulos and Jain 2015). Targeted elongated particles have also stronger adsorption to their receptors; it has been shown that rod shape particles coated with transferrin receptor had seven times higher accumulation in the brain compared to spherical nanoparticles with the same targeting ligand (Kolhar et al. 2013).

The surface of nanoparticles is often coated with polyethylene glycol (PEG) to protect the particles from formation of protein corona, which would lead to aggregation and quick blood clearance by reticuloendothelial system (Jokerst et al. 2011). PEG is a water-soluble polymer that forms brush-like structure covering the particles. PEG has high hydration that enables to form water cloud around the particles protecting them from interactions with neighboring NPs, or with the plasma proteins. Nanoparticles with PEG coating have close to neutral surface charge independent of the molecules that have been PEGylated (Suk et al. 2016). Circulation time and delivery efficiency of the nanoparticles is strongly influenced by their zeta potential. Particles with neutral zeta potential have higher delivery efficiency compared to particles with negative or positive zeta potential (Wilhelm et al. 2016). Moreover, it has been shown that NPs with high zeta potential > 45 mV can damage the blood-brain barrier, and particles with low zeta potential are rapidly opsonized and cleared by macrophages (Honary and Zahir 2013; Lockman et al. 2004).

2.3.2. Silver nanoparticles

Silver nanoparticles (AgNPs) are used for various applications, including as antibacterial agents in medical device coatings, cosmetics, textiles and health-care products (Sukhanova et al. 2018). These nanosized metallic particles can possess very diverse physical, chemical and biological properties depending on their surface-to-volume ratio, shape, and surface chemistry, making them useful for various bio-applications such as antibacterial, antifungal, antiviral and anti-inflammatory agents (Zhang et al. 2016). The broad use of AgNPs has caused concerns regarding the possible risks for the human health and the environment.

Several studies have shown that the AgNPs are toxic by causing direct damage to cell membranes, by generation of active oxygen species, and by release Ag^+ ions (Sukhanova et al. 2018). Majority of these toxicity studies have been conducted using uncoated silver particles that can be oxidized and are able to release the ions. Coating the AgNPs with sodium citrate, polyvinylpyrrolidone, or polyethylene glycol molecules decreases their toxicity (Fahmy et al. 2019) .

AgNPs are well-suited for preclinical studies as the model payloads because these particles can be easily functionalized with targeting peptides and fluorescent dyes. AgNPs with surface-bound fluorophore have intense signals as the nanoparticles increase the fluorescence intensity of the dye by about an order of magnitude due to plasmonic enhancement. By using silver bio-compatible etchant to dissolve exposed AgNPs, it is possible to distinguish internalized particles from unbound and cell surface bound particles, allowing to study the cellular uptake of AgNPs (Braun et al. 2014).

2.3.3. Iron oxide nanoworms

Iron oxide nanoparticles are extensively used due to their magnetic properties that enables to exploit them for magnetic hyperthermia, magnetic separation and as contrast agent for MR imaging (Korchinski et al. 2015). As iron oxide NPs are reactive with oxidizing agents, the particles are usually coated with hydro-philic compounds (e.g. dextran) that do not affect the magnetic properties. Coated iron NPs are nontoxic and biocompatible and show prolonged systemic circulation (Ali et al. 2016). Dextran-coated ultrasmall superparamagnetic iron oxide ferumoxtran-10 nanoparticles used for MRI, have plasma half-life in humans up to 30 h (Arami et al. 2015).

Iron oxide nanoworms (IONWs) are approximately 100 nm strings of iron cores that are PEGylated and coated with dextran (Park et al. 2009). The elongated shape of IONWs extends their half-life in blood circulation and provides enhanced interaction between targeting ligands and their receptors. IONWs can be used for theranostic purposes, as their surface can be readily coated with targeting ligands and drugs, and their magnetic core is compatible with MR imaging (Park et al. 2009; Ruoslahti 2017). Peptide targeted cytotoxic IONWs loaded with proapoptotic peptide $_D$[KLAKLAK]$_2$ have been previously used to treat glioblastoma in orthotopic mouse models (Agemy et al. 2013).

2.4. Summary of the literature

Many people all over the world are diagnosed with age-related brain disorders, and as overall life expectancy is in rise, even more people will be affected by these pathologies. The drugs currently available for the treatment of AD and other neurodegenerative disorders do not slow down the progression of the diseases or cure the patients. Instead, they only temporarily alleviate the symptoms of neurodegeneration. To help the patients and to relieve the burden on health care system and society, early diagnosis methods and more efficient treatments need to be developed.

Treatment of CNS disorders is hampered by the presence of BBB – a highly selective protective barrier impermeable to most potential neuropharmaceuticals. Despite intense research the progress in development of new therapies for neurodegenerative disorders and brain tumors has been excruciatingly slow, mainly because large majority of the drug candidates have failed to reach the extravascular brain parenchyma. But most likely any effective treatment for neurodegenerative disorders would require therapeutic agent to be transported across the BBB, thereby the identification of efficient BBB targeting ligands are of utmost importance. Precision delivery of nanoscale carriers or drugs may allow for effective and site-specific transport of imaging agents, drugs, and other bioactive molecules across the BBB, to diagnose and treat brain tumors and neurodegenerative disorders.

3. AIMS OF THE STUDY

Brain parenchyma is shielded from systemic circulation by the BBB that allows penetration of only a limited number of agents with very specific characteristics. One strategy to improve delivery of drugs and nanoparticles across the barrier is to use homing peptides that interact with systemically accessible transport receptors in the brain. This doctoral thesis focused on the identification and pre-clinical validation of novel peptides, which could be used to target normal central nervous system and different neurological pathologies.

Validation of homing peptides is of critical importance for peptide development to establish whether the targeting takes place and on an adequate level. Targeting peptide validation typically involves *in vitro* and *in vivo* sample manipulation and is prone to artefacts. To improve the validation of homing peptides on cultured cells and *in vivo*, a highly sensitive and internally controlled AgNP-based cellular uptake/biodistribution quantification method was developed. This new method enables analysis of the tissues and cells with minimal prior sample processing.

More specifically the goals were:
1. Development of nanoparticle quantification system based on isotopically tagged AgNPs to study accessible affinity peptide receptors on cells (II)
2. Development of internally controlled AgNP quantification system for nano-particle homing studies (I)
3. Refinement of the AgNP quantification method for *in situ* analysis of tissues (I)
4. Targeting glioblastoma with nanoparticles functionalized with homing peptide (III)
5. Identification of novel peptides to target AD (IV).

4. MATERIALS AND METHODS

4.1. Peptides

Peptides (Table 2) were synthesized using Fmoc/t-Bu chemistry on a micro-wave-assisted automated peptide synthesizer (Liberty, CEM Corporation, NC, USA), purified by HPLC using 0.1% TFA in acetonitrile-water mixture to 90%–95% purity and validated by Q-TOF mass spectral analysis. Fluorescent peptides with blocked C-terminus were synthesized in-house by using 5(6)-carboxyfluorescein (FAM) with 6-aminohexanoic acid spacer attached to the N-terminus of the peptide, or ordered from a commercial supplier (TAG Copenhagen, Denmark).

Table 2: Previously identified peptides used in the *in vitro* and *in vivo* studies.

Peptide sequence	Identification	Target site and receptor	Reference	Publica-tion in thesis
RPARPAR	Prototypic CendR peptide	Lungs, heart, and angiogenic vasculature; receptor are NRP-1 and NRP-2	Teesalu et al. 2009	I-II
CGKRK	*In vivo* phage display on epidermal carcinogenesis mouse model	Angiogenic blood vessels and tumor cells; receptors are p32 and calreticulin	Hoffman et al. 2003	II
AKRGARSTA (LinTT1)	*In vitro* phage display on recombinant human p32 protein	Tumor lymphatics, tumor-associated macrophages, tumor endothelial cells, and tumor cells; receptor is p32	Paasonen et al. 2016	III
CAGALCY	*In vivo* phage display on healthy mice	Brain microvessels; receptor is unknown	Fan et al. 2007	V

4.2. Targeted nanoparticles

Three different nanoparticle platforms were used in the experiments presented in this thesis: AgNPs, IONWs and albumin-paclitaxel NPs (Fig. 7).

Silver nanoparticles
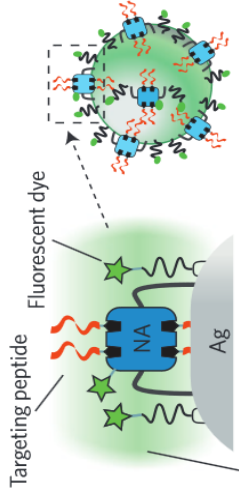
Iron oxide nanoworms

Albumin-paclitaxel nanoparticles

Targeting peptide   Fluorescent dye

- Dextran-coated iron oxide core
- 5 kDa PEG linker
- FAM-LinTT1

nab-Paclitaxel nanoparticle

Cross section
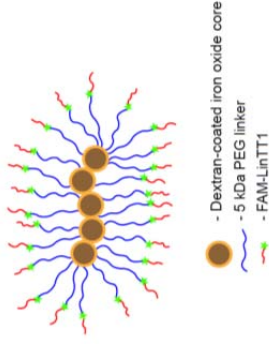
Paclitaxel

Albumin

Paclitaxel
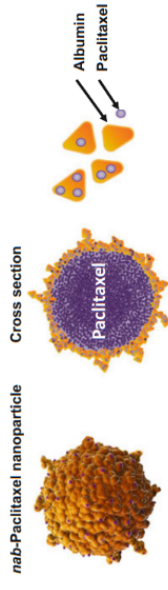
Figure 7: Nanoparticle platforms used in this thesis. Adapted from Braun et al., (2014); Säälik et al., (2019) and Desai (2016).

Ultraviolet-visible (UV-vis) absorption spectrum was analyzed with a Nanodrop 2000c spectrophotometer (Thermo Scientific Inc., Washington, USA) to quantify molarity of AgNPs. Dynamic Light Scattering (DLS; Zetasizer Nano ZS, Malvern Instruments, UK) was used to assess the polydispersity and hydrodynamic radius of the particles. Transmission electron microscopy (TEM; Tecnai 10, Philips, Netherlands) was used to characterize the morphology of the nanoparticles.

4.2.1. Synthesis of nanoparticles

4.2.1.1. Silver nanoparticles

Silver nanoparticles (AgNP) with four different compositions were used in the experiments: wtAg, Ag107, Ag109 and wtAg-Pd (Table 3). AgNP were synthesized in-house using Lee and Meisel citrate method or its modified version (Dadosh 2009; Lee and Meisel 1982). Synthesis of the particles was conducted using natural silver (composed of 51.8% Ag107 and 48.2% Ag109 isotopes) in case of wtAgNPs and wtAg-Pd, or by using isotopically pure silver (Ag107 or Ag109) in case of isotopic AgNPs. WtAg-Pd nanoparticles contained 1% naturally occurring Pd that was added in the form of $Pd(NO_3)_2$ at the end of synthesis process.

Synthesized particles had the Ag core size in the 20–70 nm range. Nanoparticles were functionalized with NeutrAvidin (NA) for biotinylated-peptide conjugation, and with lipoic acid-polyethylene glycol (1k)-NH_2 (PEG) molecules (Braun et al 2014). The terminal amines of PEG were used for coupling of CF555-N-hydroxysuccinimide-dye (NHS-dye). Nanoparticles with targeting ligand were prepared by attaching biotinylated peptides to the particles; in case of control particles the biotin binding pocket was blocked with free D-biotin.

Nanoparticles made of naturally occurring silver were used for optical imaging of NP distribution on tissue sections; fluorescence signal of CF555 dye was detected by confocal microscopy. Silver enhancement procedure that was conducted on tissue sections enabled to visualize silver grains using dark-field microscopy. Atomically distinct nanoparticles Ag107, Ag109 and wtAg-Pd were used for analysis of cells and tissue homogenates by ICP-MS. Ag107 and Ag109 particles were used in homing experiments where silver was quantified from tissue lysates by ICP-MS and tissue sections by laser ablation-ICP-MS.

Extracellular AgNPs can be "etched", or dissolved, using a mild biocompatible solution to differentiate between internalized and surface-bound exposed particles (Braun et al 2014). Etching solution was prepared fresh before each use from 0.2 M stock solutions of $Na_2S_2O_3$ and $K_3Fe(CN)_6$ stored in the dark. A working solution, 10 mM in each component diluted in PBS, was applied to cells for five minutes followed by PBS washes.

Table 3: Nanoparticles used in the experiments.

Nanoparticle type	Size	Synthesis protocol	Applications		
WtAgNP	20–60 nm	Ag-citrate (Lee and Meisel 1982)	*In vitro*	Confocal microscopy	Flow cytometry
			In vivo	Confocal microscopy	Silver enhancement and dark field microscopy
WtAgNP+1% Pd	25 nm	Tannic acid (Dadosh 2009)	*In vitro*	Confocal microscopy	ICP-MS
Ag107NP	25 nm	Tannic acid (Dadosh 2009)	*In vitro*	Confocal microscopy	ICP-MS
			In vivo	ICP-MS	LA-ICP-MS
Ag109NP	25 nm	Tannic acid (Dadosh 2009)	*In vitro*	Confocal microscopy	ICP-MS
			In vivo	ICP-MS	LA-ICP-MS
IONW	100 nm	(Fogal et al. 2015; Miao et al. 2014)	*In vitro*	Flow cytometry	
IONW	100 nm	(Fogal et al. 2015; Miao et al. 2014)	*In vivo*	Confocal microscopy	Pre-clinical therapy
Albumin-paclitaxel NP	130 nm		*In vivo*	Confocal microscopy	

4.2.1.2. Iron oxide nanoworms

NWs were synthesized as previously described (Fogal et al. 2015; Miao et al. 2014). Briefly, aminated NWs were PEGylated with maleimide-5k-PEG-NHS (JenKem Technology, TX, USA). Peptides were coupled to NWs through a thioether bond between the thiol group of a cysteine residue added to the N-terminus of the peptide and the maleimide on the functionalized particles.

4.2.1.3. Albumin-paclitaxel nanoparticles

Albumin-paclitaxel nanoparticles (Abraxane) were purchased from producer (Celgene). For peptide coupling, 5 mg of albumin-paclitaxel nanoparticles were dissolved in 1 mL of PBS (previously purged with nitrogen) and combined with 0.3 mg (0.6 μmols) of linker sulfosuccinimidyl 4-(N-maleimidomethyl)cyclo-hexane-1-carboxylate in 0.2 mL of PBS. The mixture was stirred for 30 min at RT and modified albumin-paclitaxel nanoparticles were purified using a NAP-10 column (GE Healthcare Life Sciences). 0.25 μmol of LinTT1 peptide with N-terminal extra cysteine residue dissolved in 0.2 mL of PBS was slowly added to the purified albumin-paclitaxel nanoparticles, the mixture was stirred for 1 h at RT and purified by gel permeation chromatography using Sepharose 4B columns (GE Healthcare Life Sciences).

4.2.2. Cell lines

Nine different tumor cell-lines derived from human or mouse tumors (Table 4) were used in the experiments. PPC-1 cells were obtained from the Ruoslahti laboratory at Sanford-Burnham-Prebys Medical Discovery Institute (SBPMDI), and M21 cells were a gift from David Cheresh at University of California San Diego (UCSD). U87-MG GBM and U251 cells were acquired from ATCC, and NCH421K cells from CLS Cell Lines Service GmbH (Eppelheim, Germany). WT-GBM and VEGF-KO GBM cells were a gift from Gabriele Bergers (Leuven, Belgium), P13 spheroids were a gift from Rolf Bjerkvig (Bergen, Norway), and 005 cells were established from murine GBM as previously described in Marumoto et al 2009.

Table 4: Cell-lines used in the *in vitro* and *in vivo* experiments.

Cell-line		Application	Publication in thesis
PPC1	Human prostate adenocarcinoma	*In vitro*	II
M21	Human melanoma	*In vitro*	II
U87-MG	Human glioblastoma	*In vitro* and *in vivo*	III
WT-GBM	Mouse glioblastoma	*In vitro* and *in vivo*	III
VEGF-KO-GBM	Mouse glioblastoma	*In vitro* and *in vivo*	III
005	Mouse glioblastoma	*In vivo*	III
NCH421k	Human glioblastoma	*In vitro* and *in vivo*	III
U251	Human glioblastoma	*In vitro*	IV
P13	Human glioblastoma	*In vivo*	IV

4.2.3. *In vitro* experiments

4.2.3.1. AgNP binding to immobilized proteins

His-tagged NRP-1 b1b2 domain (wt and mutant) were expressed and purified as described (Teesalu et al. 2009). 6× His-Tagged p32 was expressed in Rosetta-gami-2 cells (Novagen). The protein was purified by IMAC using HIS-select resin (Sigma) with an imidizole gradient from 20–300 mM and eluted fractions were analyzed on analytical SDS-PAGE. Sedimentation velocity assay was used to confirm the trimeric state of the recombinant p32 protein. AgNP binding experiments to magnetic beads coated with recombinant proteins were carried out with wtAgNPs. Ni-NTA magnetic agarose beads (Qiagen) in Tris buffer (50 mM Tris pH 7.4, 150 mM NaCl, 0.05% NP40, 5 mM imidazole) were loaded, as suggested by the manufacturer, with either the b1b2 binding domain of NRP-1, with p32, or with a b1b2 mutant, followed by multiple washes. NPs were incubated for one hour with the protein-loaded beads in Tris buffer with 1% BSA at room temperature with gentle agitation, followed by washes, and elution with high imidazole concentration buffer (PBS, 400 mM imidazole, 150 mM NaCl, 1% BSA, 0.05% NP40). The eluted samples were analyzed by UV-vis spectrophotometer (NanoDrop 2000c, Thermo Scientific). The spectrum and maximum absorbance at 400 nm were recorded for each sample.

4.2.3.2. Receptor-dependent binding and uptake of AgNPs

Receptor-dependent binding of AgNPs by two cancer cell-lines, M21 and PPC-1, was assessed by flow cytometry and uptake of AgNPs was determined by confocal microscopy. Both are well studied cell-lines with known receptors (Sugahara et al. 2009; Teesalu et al. 2009). PPC-1 cells express high levels of

NRP-1, whereas M21 cells lack the extracellular NRP-1 expression (Teesalu et al. 2009). Both cell lines have p32 protein exposed at the cell surface.

To study cellular uptake, three different types of wtAgNPs were prepared by conjugating biotinylated peptides: biotin-X-RPARPAR or biotin-X-SGKRK-NH_2, or by blocking the biotin binding pocket with free biotin. M21 and PPC1 cells were cultured in DMEM high glucose medium containing 100 IU/mL of penicillin, streptomycin, and 10% of fetal bovine serum (GE Healthcare, UK) in 5% CO_2 atmosphere.

For fluorescence confocal imaging the cells were washed twice with warm medium after which fresh medium with AgNP at 0.2 nM was added. The cells were incubated with NPs for one hour at 37 °C. After incubation the NP containing medium was removed, the cells were washed and fixed with -20 °C methanol for 60 sec. The cells were blocked (PBS, 1% BSA, 0.05% Tween-20) for 30 min at room temperature and co-stained with NRP-1 and p32 antibodies, and DAPI. The cells were imaged using fluorescence confocal microscopy (Zeiss LSM 510; Olympus FV1200MPE, Germany).

For flow cytometry experiments the cells were washed twice with warm medium, and fresh medium with AgNP at 0.2 nM was added. The cells were incubated with NPs for one hour at 37 °C. After incubation the AgNP containing medium was removed and the cells were washed with PBS. Cells were dissociated using Cell Dissociating Buffer (Gibco) and suspended in 300 µl PBS. Analysis was done using BD Accuri flow cytometer by monitoring the 555 channel FL2.

4.2.4. Animal experiments

Animal experimentation protocols were approved by Committee of Animal Experimentation of Estonian Ministry of Agriculture (Permit #48), by the Tel Aviv University Institutional Animal Care and Use Committee, and by the Institutional Animal Care and Use Committee of Sanford Burnham Prebys Medical Discovery Institute.

Athymic nude mice were purchased from Harlan and Balb/c mice were purchased from Charles River. Animal experiments were conducted using healthy mice or mouse models of various CNS disorders. Six different glioblastoma models (Table 5), two AD models, PD model and acute brain injury model were used in the experiments.

4.2.4.1. GBM tumor models

Cell culture reagents were from Gibco (USA) if not stated otherwise. WT-GBM and VEGF-KO-GBM cell lines (Blouw et al. 2003) were cultured in MEM with Earl's salts (Capricorn Scientific, Germany) supplemented with 100 IU/mL of penicillin/streptomycin, 1% sodium pyruvate, 0.01 M HEPES, 0.6% glucose (Applichem, USA) and 5% of fetal bovine serum (GE Healthcare, UK). NCH421k cells (Campos et al. 2010) were cultivated in neurobasal medium complemented with B27 neurobasal supplement (Thermo Fisher Scientific, USA), 100 IU/mL of penicillin/streptomycin, 0.4 mM Glutamax, 20 ng/ml basic FGF, 20 ng/ml EGF and 40 µg/ml of heparin (Sigma-Aldrich, USA). U87-MG cells were grown in DMEM (Lonza, Belgium) containing 100 IU/mL of penicillin, streptomycin, 10% fetal bovine serum, 1% sodium pyruvate and 1% non-essential amino acids (Sigma-Aldrich, USA). P13 spheroids (Fack et al. 2015) were grown in DMEM (Lonza, Belgium) containing 100 IU/mL of penicillin/ streptomycin, and 10% of fetal bovine serum (GE Healthcare, UK) as 3D culture on 0.75% agar coated flasks. All cells were cultured at 37°C in a humidified atmosphere containing 5% CO_2.

For induction of orthotopic GBM xenografts in nude mice, 7×10^5 (WT-GBM, VEGF-KO-GBM), 3×10^5 (NCH421k) cells, 3×10^5 (005) cells or 3×10^5 (P13) cells from dissociated spheroids were implanted intracranially in the right striatum of the brain (coordinates: 2 mm laterally and 2 mm posteriorly from bregma and at 2.5 mm depth). For induction of s.c. U87-MG tumors, 4×10^6 cells were injected under the skin of the right flank of nude mice. Intracranial tumors were allowed to develop for 6–7 (WT-GBM), 12–14 (VEGF-KO-GBM), ~30 (NCH421k), 10 (005) or ~35 (P13) days before performing experiments. U87-MG s.c. tumors were allowed to grow until tumors had reached ~ 1 cm^3.

Table 5: GBM tumor models used in the experiments.

Tumor model	Type	Culture conditions	Tumor location	Time of tumor formation	Characteristics
U87-MG	Cell-line xenograft	2D culture	Subcutaneous	~30 days	Poorly invasive and angiogenic
WT-GBM	Genetically engineered mouse model	2D culture	Orthotopic	~7 days	Angiogenic and poorly invasive
VEGF-KO-GBM	Genetically engineered mouse model	2D culture	Orthotopic	~14 days	Infiltrative
005	Genetically engineered mouse model	2D culture	Orthotopic	30–40 days	Invasive and angiogenic
NCH421k	Patient-derived xenograft	3D in neurobasal medium	Orthotopic	~21 days	Moderately invasive and slightly modified vasculature
P13	Patient-derived xenograft	3D in agar-coated flask	Orthotopic	30–40 days	Poorly invasive and angiogenic with areas of pseudo-palisading necrosis

4.2.4.2. Models of CNS disorders

Three transgenic mouse models of neurodegenerative disorders were used: AD models hApp-J20 and Tg2576, and PD model mTHY-1-α-synuclein. All the three transgenic mouse models were derived from C57BL/6 mice. The acute brain injury model was set up as previously described in Mann et al. 2016.

4.2.4.3. *In vivo* phage display

To find AD targeting peptides, CX7C (1e10 pfu) naïve phage library was injected intravenously to hAPP-J20 mice and allowed to circulate for 30 minutes. After circulation, the animals were anesthetized with 2.5% avertin and perfused intracardially with PBS. Hippocampus and control organs were collected and homogenized in LB-NP40 (1%). Bound phages were rescued by amplification in *E. coli* and their genomic DNA was sequenced by Ion Torrent next generation DNA sequencing system.

4.2.4.4. Peptide homing studies

To study AD peptide homing, mice were intravenously injected with 50 nmoles of peptide dissolved in PBS and allowed to circulate for 30 minutes. Mice were then anesthetized and perfused with PBS and all major organs were fixed in 4% paraformaldehyde at pH 7.4 overnight. The organs were washed with PBS and placed in graded sucrose solutions before embedding into optimal cutting temperature (OCT) medium. 10 μm thick sections were prepared by cryosectioning and subjected to immunostaining.

4.2.4.5. Homing of nanoparticles

To study homing of AgNPs, four different types of particles were prepared by attaching the following biotinylated peptides: biotin-X-RPARPAR-OH; biotin-X-RPARPAR-NH$_2$; biotin-X-CAGALCY (X = aminohexanoic acid), or by blocking the biotin binding pocket with free biotin. AgNPs at O.D.50 were suspended in 200 µl of PBS and injected intravenously to Balb/c mice. 1 h or 5 h after i.v. administration the mice were perfused intracardially with PBS. Organs were snap-frozen in liquid N$_2$ for cryosectioning.

For microscopic imaging, 10 μm cryosections were fixed in 4% paraformaldehyde in PBS and stained with DAPI. For silver enhancement, cryosections were fixed in MeOH (-20 °C for 60 s), washed in PBS, and treated with Silver Enhancement kit (Molecular Probes) for 30–40 min with fresh solution added every 13 min. The reaction was stopped in 75 mM Na$_2$S$_2$O$_3$ in water. The nuclei of cells were stained with DAPI, followed by dehydration of sections through graded ethanol series, xylene, and mounting in DPX mounting

medium. The signal in fluorescent confocal images and dark-field microphotographs was quantified with ImageJ freeware.

FAM-labeled NWs were injected intravenously (7.5 mg/kg Fe), and 1 or 5 h post i.v. administration the animals were perfused with DMEM-1% BSA. The organs were collected and snap-frozen in liquid nitrogen for cryosectioning. For confocal microscopy, the tissues were sectioned at 10 μm and stained with antibodies and DAPI.

Iron oxide nanoparticles (NWs) conjugated with DAG peptide (DAG-IONWs) were injected i.v. to 9-month-old hPPP-J20 mice and age-matched WT mice. NWs were allowed to circulate for 5 h before perfusion with PBS. The organs were collected and snap-frozen in liquid nitrogen for cryosectioning. NWs in tissue sections were stained with Prussian blue and the sections were counterstained with nuclear fast red.

4.2.4.6. ICP-MS experiments

Inductively coupled plasma mass spectrometry (ICP-MS) allows extremely high sensitivity analysis of elements and even enables discriminations of different isotopes of the same material (Agilent 2015). Two distinct ICP-mass spectrometry methods were applied for ratiometric analysis of cells and organs: ICP-MS analysis on cells and tissue extracts and laser ablation ICP-MS (LA-ICP-MS) on frozen tissue sections.

For ratiometric cell phenotyping, three atomically different AgNPs: Ag107, Ag109 and wtAg-Pd, and two different cell lines: M21 and PPC1 cells, were used. After incubating cells with AgNPs, the medium was removed, and cells were washed to remove the unbound particles. Cells were dissociated using non-enzymatic Cell Dissociation Buffer (Gibco), transferred to 1.5 mL tubes and disrupted with 2% SDS solution. The samples were analyzed using an Agilent 8800 QQQ ICP-MS.

For ratiometric ICP-MS-based biodistribution experiments, Ag107 and Ag109 isotopic nanoparticles were injected to healthy Balb/c mice. 200 μL of a mixture of peptide–AgNPs (prepared from Ag107) and control biotin-blocked AgNPs (prepared from Ag109) was administered i.v. and allowed to circulate for 1 or 5 hours. Animals were perfused with PBS and organs were collected and snap-frozen. Frozen tissue samples were thawed, digested and analyzed using Agilent 8800 ICP-MS.

For ratiometric LA-ICP-MS-based biodistribution studies, mice were injected i.v. with 200 μL of a mixture of peptide–AgNPs (prepared from Ag107) and control biotin-blocked AgNPs (prepared from Ag109). At indicated time points, the mice were perfused with PBS and the organs were collected, snap-frozen, sectioned at 30 μm on Superfrost+ slides, and air-dried. Determination of Ag107/109 ratio in tissue sections was performed using Cetac LSX-213 G2+ laser ablation system (Teledyne Cetac Technologies, USA) using a HelEx 2-volume ablation cell on Agilent 8800 ICP-MS system.

4.2.4.7. Experimental tumor therapy

For experimental therapy of mice bearing s.c. U87-MG tumors, 1×10^6 cells were injected under the skin of dorsal flank of 11–15-week old male nude mice. Tumor volume [calculated with the formula: V = (width × width × length)/2] and mouse weight was recorded every other day. When tumors reached 100–200 mm^3 in size, the mice were divided in 4 groups (n = 6) so that the total volume of tumors in all groups were equal. Treatment with intravenous FAM-LinTT1-NW, FAM-$_D$(KLAKLAK)$_2$-NW, or FAM-LinTT1- $_D$(KLAKLAK)$_2$-NWs (at 5 mg/kg Fe per injection), or 100 μl of PBS, was started on day 36 after tumor induction. Eight injections in total were performed on every other day. The study was terminated when the first tumor reached 1.5 cm^3. Mice were sacrificed by cardiac perfusion and tissues were snap-frozen for further analysis.

For experimental therapy of mice bearing orthotopic syngeneic 005 tumors, 3×10^5 cells were injected in the hippocampus (coordinates: 1.5 mm laterally and 2 mm posteriorly from bregma and at 2.3 mm depth) of 8–12 weeks old C57BL/6 female mice. Ten days after transplantation of tumor cells, mice were divided in 5 groups (n = 6) and treated intravenously with either FAM-NW, FAM-LinTT1-NW, FAM-$_D$(KLAKLAK)$_2$-NW, or FAM-LinTT1-$_D$(KLAKLAK)$_2$-NWs (at 5 mg/kg Fe per injection), or 100 ul of PBS. Mice were treated for 2 weeks, 7 injections in total performed on every other day. Mice showing symptoms of disease were sacrificed by perfusion and tissues collected for further analysis.

5. RESULTS

## 5.1. AgNP binding to immobilized receptor proteins

Affinity targeted nanoparticles need to bind to their receptors with high specificity. For proof-of-concept experiment, well-established peptide/receptor combinations were used. RPARPAR peptide binds to b1b2 domain of NRP-1 and p32 protein is the known receptor for CGKRK peptide. SGKRK was used instead of CGKRK as replacing the cysteine with a serine avoids potential peptide-dimer formation and cysteine is not required for the binding of the peptide (Agemy et al. 2011). NRP-1 b1b2 with mutated binding pocket that prevents RPARPAR peptide binding (Teesalu et al. 2009) was used as a negative control. Nanoparticles functionalized with RPARPAR peptide (R-AgNPs) bound to wild-type NRP-1 protein but not to mutant NRP-1, or to p32 (Fig. 8). SGKRK-AgNPs (K-AgNPs) bound to immobilized p32 and not to the other two proteins. In this assay, both peptide-guided AgNPs showed very low background binding.
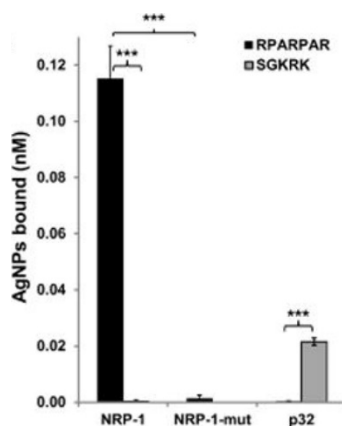
Figure 8: Cell free binding of peptide-AgNPs to recombinant receptor proteins. AgNP binding experiments to recombinant proteins were carried out with wtAgNPs. Ni-NTA magnetic agarose beads were loaded with either the b1b2 binding domain of NRP-1, with p32, or with a b1b2 mutant. NPs were incubated for 1 h with the protein loaded beads, followed by washes, and elution with high imidazole concentration buffer. The eluted samples were analyzed by UV-vis spectrophotometer. The spectrum and maximum absorbance at 400 nm were recorded for each sample. Data represent mean values $\pm$ SD (n=3); *** $p < 0.001$ by Student's t-test.

5.2. Receptor-dependent binding and uptake of nanoparticles by cultured tumor cells

NRP-1 and p32 are commonly present on the surface of cancer cells. Binding and internalization of peptide-functionalized AgNPs was tested using two tumor cell lines: PPC1 prostate carcinoma cells, which express both receptors, and M21 melanoma cells, which express only p32. To enable the detection by flow cytometry and fluorescence microscopy the AgNPs were labeled with CF555 fluorescent dye before adding the peptide. Flow cytometry-based assay showed that R-AgNPs bound specifically to NRP-1 expressing PPC1 cells ($66 \pm 1\%$ positive), but not to M21 cells that do not express NPR-1 (Fig. 9). As expected, both cell lines bound K-AgNPs ($7 \pm 1\%$ positive for M21 and $8 \pm 1\%$ for PPC-1 cells) because p32 is present on the surface of both cell lines. Control particles (B-AgNPs) showed only background binding in both cell lines.
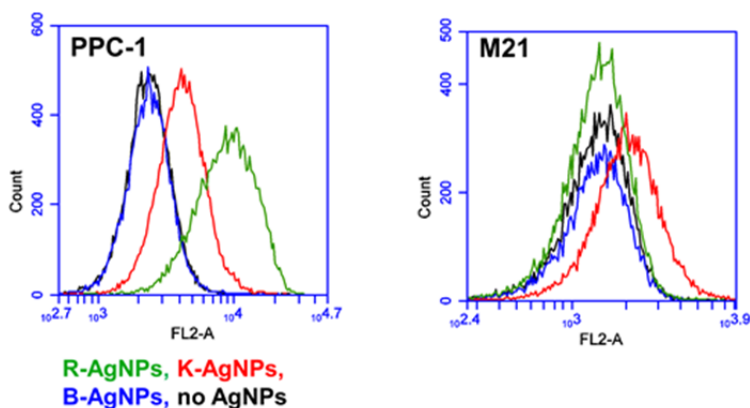
Figure 9: Receptor-dependent binding and uptake of nanoparticles in PPC-1 and M21 cells. For flow cytometry experiments, AgNPs were labeled with the fluorescent dye CF555. The AgNPs were tested individually for binding against two cancer cell lines: PPC-1 and M21. Cells were incubated for 1 h with R-, K-, or B-AgNPs at 0.2 nM. After incubation with AgNPs, the cells were washed, dissociated from the culture dish and analyzed for AgNP binding with a flow cytometer by monitoring the 555 channel: FL2. (n=3).

Next, the uptake of nanoparticles in M21 and PPC1 cells in co-culture was tested to assess whether the two cell lines can be phenotypically distinguished based on their nanoparticle uptake pattern (Fig. 10). R-AgNPs co-localized with NRP-1 on the surface and in endocytic vesicles of PPC-1 cells, whereas M21 cells did not display any signal from the R-AgNPs. In contrast, both cell lines bound K-AgNPs in agreement with the fact that both express p32. Control B-AgNPs showed only weak background signal in both cell lines. These results demonstrate that AgNP tropism could be accurately directed by attaching targeting peptide ligands to the NP surface.
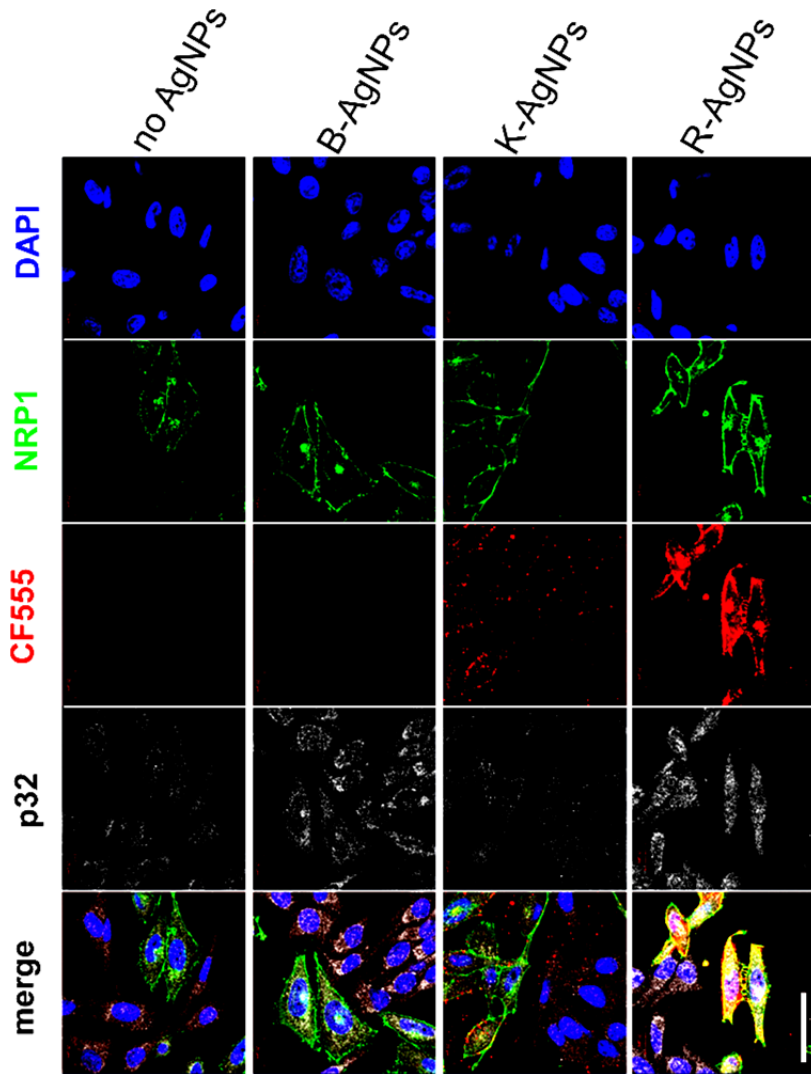
Figure 10: Receptor-dependent binding and uptake of nanoparticles by cultured PPC-1 and M21 cells. Fluorescence confocal microscopy of M21 and PPC-1 co-cultured cells incubated with R-, K-, or B-AgNPs at 0.2 nM. Attached cells were incubated with AgNPs for 1 h. The cells were stained with anti-NRP1-1 and anti-p32 antibodies and DAPI. AgNPs were labeled with CF555 fluorescent dye. The cells can be distinguished by the high amount of NRP-1 protein on the surface of PPC-1 cells and absence of NRP-1 in M21 cells. Note uptake of R-AgNPs in NRP-1-positive PPC-1 cells and binding of both PPC-1 and M21 cells by K-AgNPs. Scale bar = 50 μm.

5.3. Identification of Alzheimer's disease targeting peptide

To identify homing peptides for targeting AD, *in vivo* T7 phage screens on AD mouse model hAPP-J20 were conducted (Fig. 11a). T7 CX7C library was intravenously injected to transgenic mouse and age-matched wild-type mice in four different age groups: 3, 5, 7 and 9 months. Significant difference in phage counts recovered from AD brain compared to wt brain was seen only for 9-month-old age group, where AD brains with full-blown disease had four-fold higher phage titers than normal brains from wt mice (Fig. 11b).

Recovered phages were analyzed by high-throughput DNA sequencing to map the landscape of phage displayed peptides in AD and control brains in all the age groups. Data mining revealed a consensus motif (A/G)BB(N/Q) (where B is a basic amino acid) that was enriched in all the age groups of hAPP-J20 mice, but absent in the wt controls (Fig. 11c). One of the peptides from 9-month AD selected phage pool, CDAGRKQKC ("DAG"), was selected for subsequent studies as it agreed with the consensus sequence and contained the most commonly occurring amino acids in the adjacent positions.
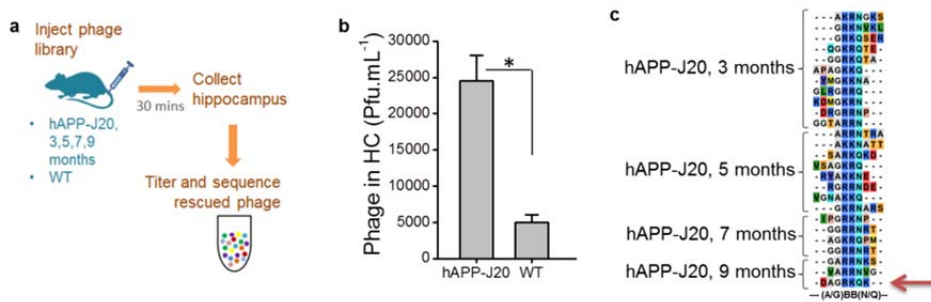
Figure 11: Identification of AD-homing DAG peptide by *in vivo* phage display. Schematic representation of phage screening done in transgenic hAPP-J20 mice. (a) A CX7C library (10^9 pfu) was injected intravenously in hAPP-J20 mice and wild-type (wt) littermate controls of different ages. After 30 minutes of circulation and perfusion to remove unbound phage, the hippocampus (HC) was excised, and phages were recovered and quantified. (b) The phage DNA was subjected to high-throughput sequencing, and the sequences present in the hAPP-J20 brains were compared to sequences from wt brains. (c) Analysis of the hAPP-J20-specific sequences revealed a consensus motif, (A/G)BB(N/Q) (where B is a basic amino acid). A cyclic 9-amino acid consensus peptide (red arrow) containing this motif (sequence CDAGRKQKC; abbreviated "DAG") was chemically synthesized.

### 5.3.1. DAG peptide homing to the AD lesions modeled in mice

To see whether the new cyclic DAG peptide is able to target AD lesions, synthetic fluorophore-labeled peptide was injected intravenously in hAPP-J20, Tg2576, and age-matched wt mice (Fig. 12). DAG peptide homed specifically to the brains of both AD models, whereas the brains from wt mice remained negative. In AD lesions, DAG accumulated in GFAP-positive activated astrocytes surrounding the Aβ plaques and blood vessels with adjoining glial cells (Fig. 12a). In the Tg2576 model, peptide showed co-localization with endothelial cells. Besides senile plaques, Aβ peptides are known to accumulate in small blood vessels in the AD brain; this phenomenon is particularly pronounced in aged Tg2576 mice (Fig. 12b) (Milner et al. 2014).
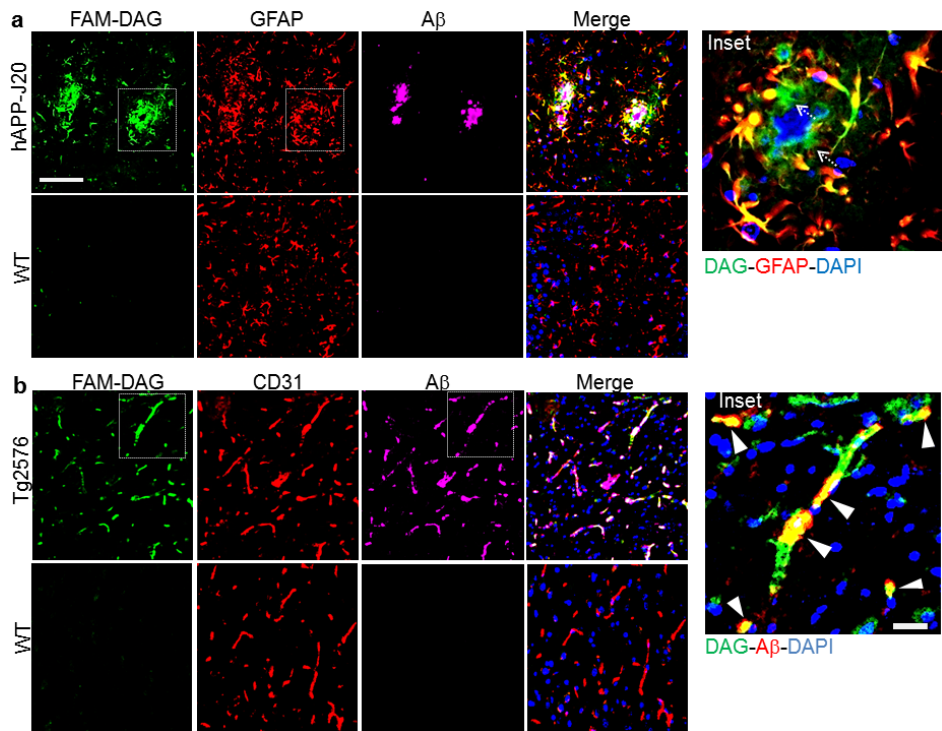
Figure 12: Homing of DAG peptide to the brains of AD model mice. (a) DAG targets activated astrocytes in AD mouse brain. FAM-DAG was intravenously injected to 9-month-old hAPP-J20 and wt mice and allowed to circulate for 30 minutes. The mice were perfused, and the brains were fixed, sectioned and stained for FAM in DAG (green), GFAP (red) and Aβ (magenta). The region shown is the hippocampus. The inset shows co-localization between DAG and GFAP, and also DAG⁺ and GFAP⁻ regions (arrows). (b) DAG targets vessels positive for Aβ in Tg mice. DAG was injected intravenously to 20-month-old Tg2576 wt mice, and processed as in panel a. The brain sections were stained for FAM (green), CD31 (red) and Aβ (magenta). The region shown is the cerebral cortex. The inset shows co-localization of DAG and Aβ (yellow, arrowheads). Scale bars, 50 μm (a and b), 20 μm (insets).

5.3.2. DAG homing to other models of neuroinflammation

Since DAG peptide in AD models showed co-localization with activated astrocytes, it was decided to test the homing in other models of neuroinflammation where reactive astrocytes are similarly present. DAG peptide showed high accumulation in P13 PDX glioblastoma, where it co-localized with GFAP-positive cells (Fig13a). For the brain injury model, DAG peptide homed to perilesional area containing activated astrocytes (Fig13b). Lastly, also in PD model DAG peptide showed preferential accumulation in GFAP-positive astrocytes (Fig13c). These experiments demonstrated that DAG targets activated astrocytes in both acute and chronic models of neuroinflammation.
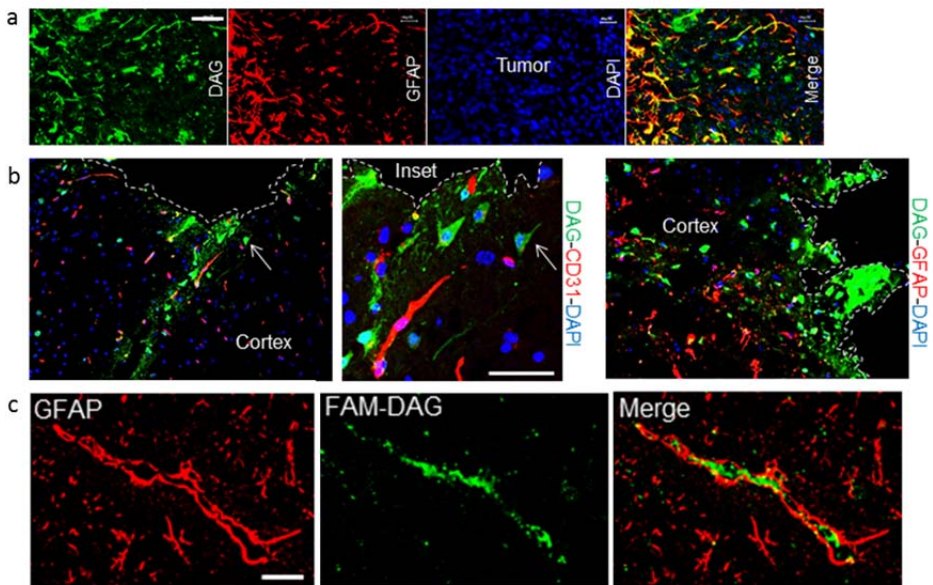

Figure 13: DAG accumulates in neuroinflammatory lesions of different etiologies.
(a) DAG homes to glioblastoma. FAM-DAG was i.v. injected in mice bearing an angiogenic glioblastoma derived from a patient (P13), and allowed to circulate for 30 minutes, after which the mice were intracardially perfused, the tumors were fixed, sectioned and immunostained for FAM (green), and GFAP (red). Scale bar, 40 μm. (b) DAG homes to acute brain injury. FAM-DAG was injected intravenously in mice with penetrating brain injury, processed as in panel a. Representative immunofluorescence images of brain sections from the injury area stained for FAM (green), and CD31 (red; left and middle panels) or GFAP (red; right panel) show stellate-shaped cells positive for DAG (see arrow). Scale bar, 40 μm. (c) DAG homes to the brain in a Parkinson's disease mouse model. FAM-labeled DAG or control peptide was intravenously injected to Parkinson's disease mice (mTHY-1-α-synuclein model, 1-year old) and processed as in panel a. Brain sections from DAG-injected mice were stained for FAM (green) and GFAP (red). DAG signal associates with activated astrocytes. Scale bar, 40 μm. *P<0.05.

5.4. Receptor-dependent homing of nanoparticles

5.4.1. Lung targeting in healthy mice

Systemically injected RPARPAR peptide homes to lung microvasculature in healthy animals (Teesalu et al. 2009). To test whether AgNPs functionalized with RPARPAR peptide target lungs as expected, polydisperse AgNPs particles with CF555 fluorescent label were used (Fig. 14). Wt-AgNPs were functionalized with either RPARPAR-OH or RPARPAR-NH_2 peptides. Amidated RPARPAR peptide is a control that does not bind to NRP-1 and thereby does not home to the lungs. Animals were injected with AgNPs and 5 hours after administration, the animals were perfused intracardially to remove unbound circulating particles. Fluorescence confocal imaging was used to study biodistribution of the AgNPs. Signal from the particles was quantified using ImageJ freeware.

RPARPAR-OH-AgNPs accumulated in lungs as expected, showing 7 times higher fluorescence signal compared to control particles (Fig. 14). This result was replicated by silver enhancement and imaging by dark-field microscopy (not shown).
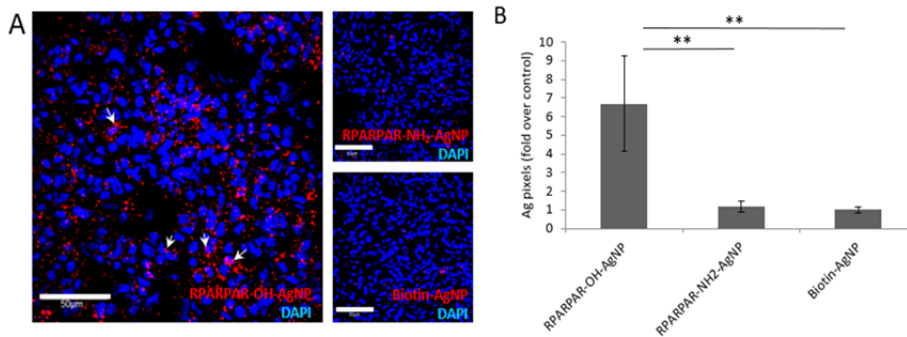
Figure 14: Systemic CF555-labeled RPARPAR-OH-AgNPs home to lung tissue.
CF555-labelled RPARPAR-OH-AgNPS and biotin-AgNPs in 200 µl PBS were intravenously injected to balb/c mice. After 5-h post i.v. administration, the animals were intracardially perfused with 15 ml PBS to wash out blood and to remove unbound AgNPs, and the organs of interest were snap-frozen. (A) Confocal imaging of lung cryosections from mice injected with CF555-AgNPs, 5 h post i.v. administration. Arrows point at areas of accumulation of CF555-positive RPARPAR-OH AgNPs. N=3; scale bars = 50µm. (B) Quantitation of the CF555 fluorescence in lung tissue sections. AgNP signal (red in panel A) expressed as percent of pixels with intensity above threshold. Five randomly chosen fields from 3 animals/group were analyzed. Data represent mean ± SD, ** $p < 0.01$.

5.4.2. Brain targeting in healthy mice

To verify that our AgNP platform is also suitable for targeting central nervous system, AgNPs functionalized with previously identified brain targeting peptide CAGALCY (Fan et al. 2007) were used. CAGALCY-AgNPs were injected intravenously and 5 h post administration biodistribution of AgNPs was assessed. CAGALCY-AgNPs accumulated in discrete areas in the brain parenchyma, quantitative analysis demonstrated ~9-fold increase of the fluorescence signal in the brain regions positive for these NPs than of control biotin-AgNPs (Fig. 15).
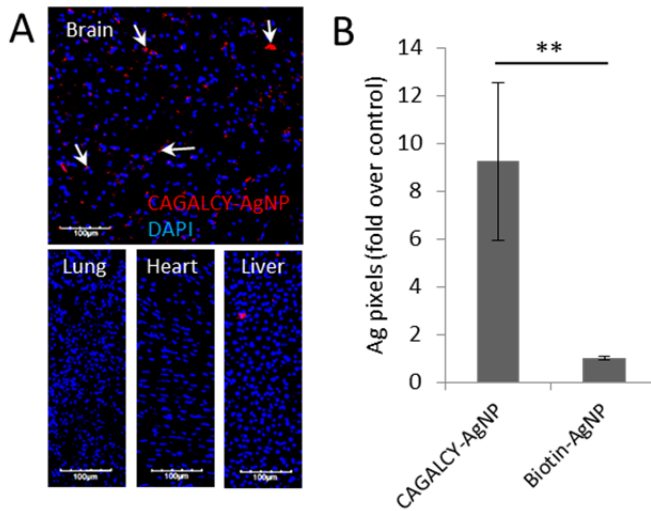

Figure 15: Biodistribution of systemically administered CAGALCY-AgNPs.
(A) Confocal imaging of tissues from mice injected i.v. with CAGALCY-functionalized AgNPs labeled with CF555 fluorescent dye, 5h post i.v. administration. Arrows point at areas of accumulation of CAGALCY AgNPs (red). Scale bars = 100μm. (B) Quantitation of CF555 fluorescence in tissue sections. Ag-positive pixels/field were plotted for each type of nanoparticle as fold over control. N=3; 5 fields were analyzed per tissue. Data represent mean ± SD, **p < 0.01.

5.4.3. DAG-mediated payload delivery to AD lesions

To test if previously identified DAG peptide could be used for site-specific delivery to AD lesions, iron oxide nanoworms (IONW) were used. DAG-coated IONWs were administered intravenously in 9-month old hAPP-J20 and wt mice, and 5 h post administration NW homing to different parts of brain was assessed (Fig. 16). NW accumulation was seen in the hippocampus and the cortex of AD mice but no nanoparticle signal was seen in wt control mice. This result demontrated the utility of DAG peptide to carry payload to AD brains.
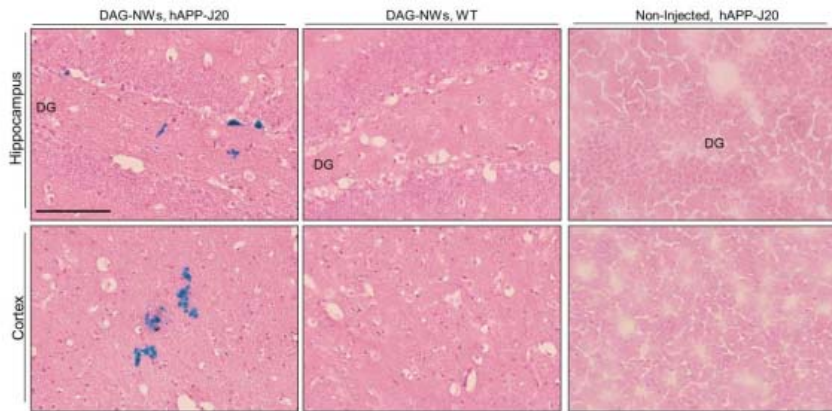
Figure 16: DAG-mediated delivery of nanoparticles to AD lesions. NWs conjugated with DAG (DAG-NWs) were injected i.v. into 9-month-old hAPP-J20 mice and allowed to circulate for 5 hours before perfusion (n=2). In the brain sections shown, NWs were visualized by Prussian blue staining and the sections were counterstained with nuclear fast red. Shown are representative sections with DAG-NWs in the hippocampus (top panel) and cortex (bottom panel). The controls include DAG-NWs injected into age-matched wt mice and non-injected hAPP-J20 mice. DG: dentate gyrus. Scale bar – 100 µm. DG: dentate gyrus.

5.4.4. p32-dependent precision targeting of glioblastoma

5.4.4.1. p32 expression in glioblastoma mouse models

Mitochondrial protein p32 is intracellular in normal cells, but in highly activated cells in tumors and atherosclerotic plaques, it is also exposed on the cell-surface. Extracellular presentation of the p32 has been detected both in tumor macrophages and in cancer cells (Fogal et al. 2008). It has been demonstrated that compared to the normal brain, malignant cells and tumor macrophages in lentivirally-induced 005 transgenic GBM model show upregulated cell surface expression of p32 (Agemy et al. 2013). To assess the relevance of p32 protein for GBM targeting, the distribution of total (Fig. 17a) and systemically accessible p32 (Fig. 17b) in a panel of four GBM models (orthotopic WT-GBM, VEGF-KO, NCH421k and subcutaneous U87-MG) was studied. Whereas in orthotopic tumors, the strongest signal was seen in the center of the tumor, in s.c.U87-MG tumors the p32 immunoreactivity was more pronounced at the tumor rim. To assess systemically accessible p32 rabbit polyclonal anti-p32 antibody was administered intravenously (Fig. 17b). In mice bearing WT-GBM, stronger signal was visible in the tumor periphery and for U87-MG the p32 antibody was predominantly seen at the rim of the tumor.

These results demonstrated upregulation of total p32 and presence of systemically accessible p32 in GBM models and suggested that p32 targeting peptides may be relevant for targeting glial tumors.
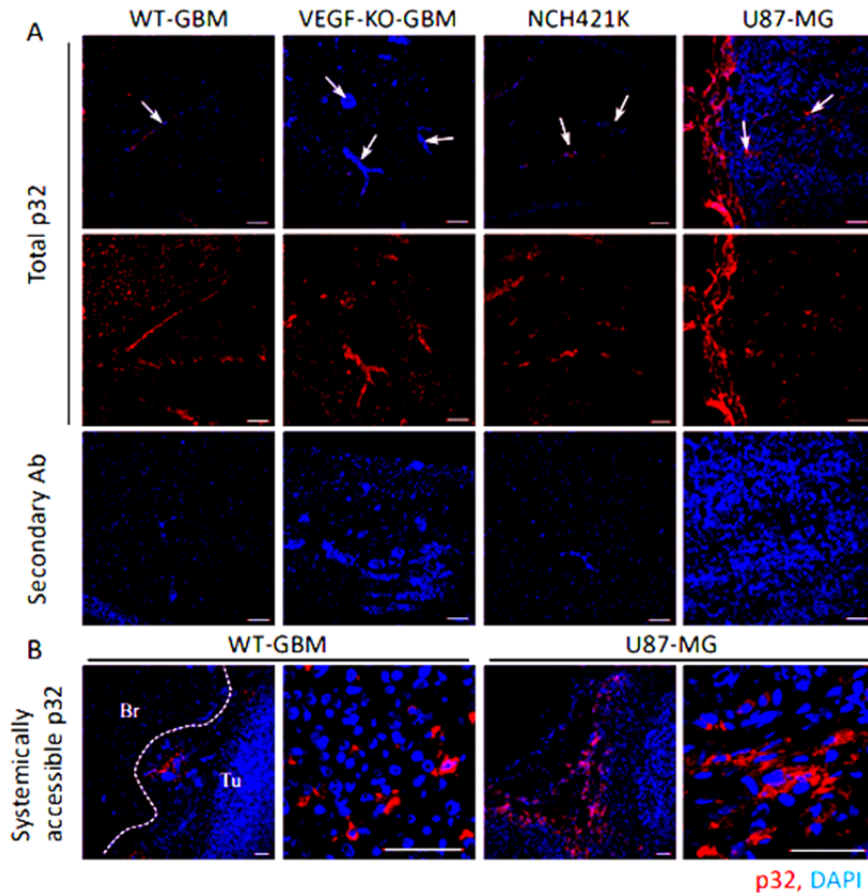
Figure 17: Expression of total and systemically accessible p32 in GBM models. (A) Mapping of total p32 in GBM tissue sections. Cryosections of orthotopic (WT-GBM, VEGF-KO- GBM, NCH421k) and subcutaneous tumors (U87) were stained with rabbit anti-p32 antibody and the nuclei were counterstained with DAPI. Arrows in the upper panel indicate p32-positive areas that colocalize with tumor nodules in GBM lesions. Middle panel – confocal planes with p32 staining only. Lower panel – staining with secondary antibody only. (B) Mapping of systemically accessible p32. Mice bearing orthotopic WT-GBM or subcutaneous U87 tumor were injected i.v. with 200 µg of anti-P32 antibody and let circulate for 20 minutes. Cryosections from tumors were stained by secondary anti-rabbit Alexa 546 antibody to visualize the tissue-retained anti-p32 antibody. Br – brain, Tu – tumor. Scale bars: 100 µm and 50 µm in low and high magnification fields, respectively.

5.4.4.2. LinTT1-guided NWs home to GBM tumors

Elevated expression of total p32 and presence of extracellular p32 on GBM tumors demonstrated feasibility of targeting p32 in brain tumors. LinTT1 is a tumor homing peptide that was identified from *in vitro* phage display on immobilized p32 protein (Paasonen et al. 2016). LinTT1 is a tumor penetrating peptide that contains a cryptic CendR motif. After binding to p32 cell surface proteases cleave the peptide exposing C-terminal RPAR peptide that interacts with NRP-1, leading to vascular leakage and tissue penetration (Sugahara et al. 2009; Teesalu et al. 2009) LinTT1 peptide targets tumor endothelial cells, macrophages, tumor lymphatics and tumor cells (Paasonen et al. 2016).

FAM-LinTT1 or FAM alone was conjugated to iron oxide nanoworms. Functionalized NWs were administered in mice with phenotypically diverse GBM xenograft tumors. Peptide-guided NWs were accumulating in all the different tumors, whereas control particles demonstrated only background signal (Fig. 18). Increased uptake of peptide-guided NWs was seen only for malignant tissue; in control organs, including the brain, the fluorescent signal of LinTT1-NWs was at the same level with non-guided NWs.
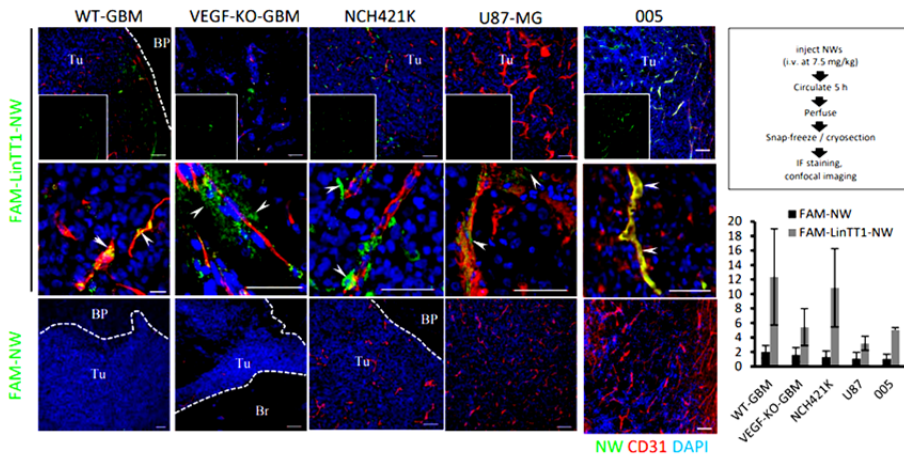
Figure 18: Systemic FAM-LinTT1-iron oxide nanoworms home to mouse and human GBM tumors implanted in nude mice. Mice bearing GBM xenografts of mouse (005, WT-GBM, VEGF-KO-GBM – intracranial) or of human origin (NCH421k – intracranial, U87-MG – subcutaneous) were injected intravenously with 7.5 mg/kg FAM-LinTT1-NW or FAM-NW, and allowed to circulate for 5 h followed by cardiac perfusion of the animals. Cryosections from subcutaneous tumor or coronal cryo-sections from brain with GBM were stained by anti-FAM (NWs), anti-CD31 (blood vessels), and DAPI and visualized by confocal microscopy. Tu – tumor, BP – brain parenchyma. Insets show the FAM channel alone. Arrowheads indicate LinTT1-NW signal. Scale bars – 100 µm in low magnification panels; 50 µm in high magnification panel. FAM-LinTT1-NW and FAM-NW signal intensity in GBM tissue was quantified from 6–9 confocal images and analyzed by ImageJ. Statistical analysis was performed by one-way ANOVA. Error bars: standard deviation.

5.4.4.3. LinTT1 guided Abraxane homes to GBM

To demonstrate that GBM homing by LinTT1 guided NPs is not dependent on nanoparticle platform, LinTT1 peptide was conjugated to nanoformulated paclitaxel-albumin. Mice bearing WT-GBM tumors were administered FAM-LinTT1-Abraxane or control FAM-Abraxane particles without the peptide. Fluorescence signal of LinTT1-Abraxane was detected in tumor blood vessels and tumor parenchyma, whereas non-guided Abraxane showed no accumulation in the GBM tissue (Fig. 19).
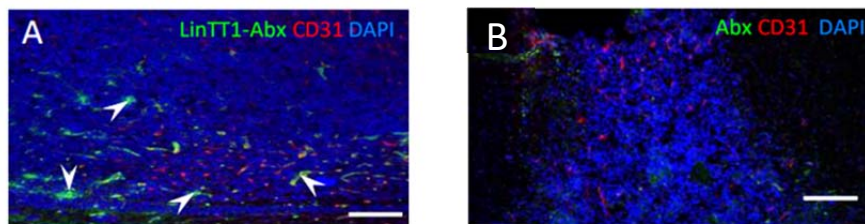
Figure 19: LinTT1-guided Abraxane home to GBM lesions. Systemic LinTT1-functionalized Abraxane nanoparticles home to WT-GBM glioma. Mice bearing ortho-topic WT-GBM glioma were injected intravenously with 0.5 mg of FAM-labeled LinTT1-Abraxane conjugate (A) or FAM-Abraxane (B), after 5h animals were per-fused, and tissue snap-frozen for microscopy. Coronal cryosections from PFA-fixed brain with tumor were stained with anti-FAM (green, FAM-LinTT1-abraxane or FAM-Abraxane) and anti-CD31 (red, blood vessels) antibodies, nuclei were counterstained with DAPI (blue), and sections were imaged by confocal microscopy. Tumor is seen as an area of high nuclear density. Scale bar: 100 μm.

5.5. ICP-MS-based quantification of AgNPs

5.5.1. Phenotyping of cells using isotopically barcoded AgNPs

As shown before with co-culture of PPC1 cells and M21 cells, binding of targeted nanoparticles can be used to phenotypically distinguish cells (Fig. 10). To audit targeting peptide receptors on cells a highly sensitive tool based on isotopic AgNPs and ICP-MS quantification was developed. AgNPs were prepared from >99% pure silver isotopes (Ag107 or Ag109), or from wtAg-Pd particles that contained naturally occurring wild-type silver (wtAg), made up of 51.8% Ag107 and 48.2% Ag109 isotopes, doped with 1% Pd. Cells were incubated with a mixture of homing peptide-functionalized isotopically bar-coded AgNPs, uptake of particles was quantified by ICP-MS (Fig. 20).
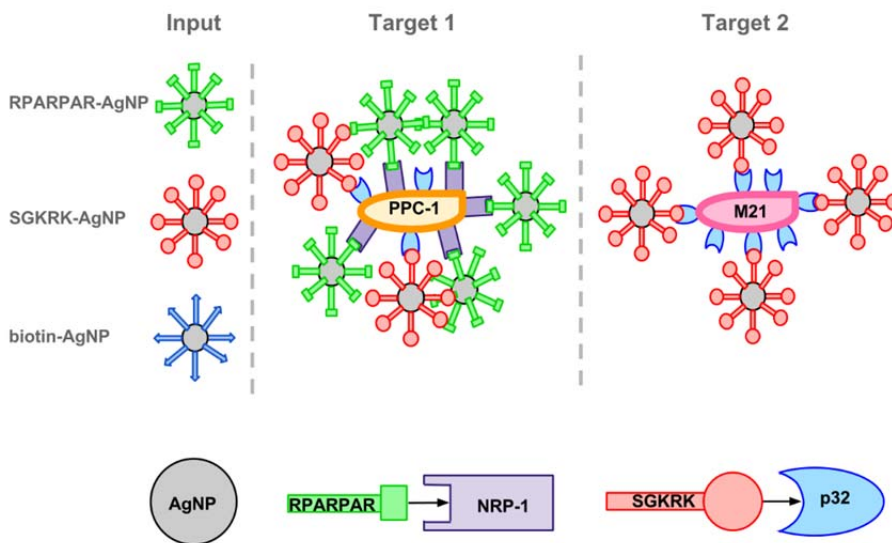
Figure 20: The principle of multiplexed ratiometric AgNP-based test system. The triplex system shown here is based on two targeting peptides: RPARPAR and SGKRK, and two biological targets: NRP-1 and p32. M21 cells express cell surface p32, whereas PPC-1 cells expose both p32 and NRP-1 on the cell surface. Control biotin-AgNPs do not bind to either cell line and serve as a negative control. When an input of three different AgNPs is applied to the cells, their cell binding and uptake pattern will correlate with availability of accessible cell surface receptor.

To make sure that composition of NP core does not affect the functionality of targeted AgNPs, all the three isotopically-tagged AgNPs were functionalized with RPARPAR peptide and cells were incubated with the particles. Independent of core type, all RPARPAR functionalized AgNPs bound specifically to PPC1 cells and not to M21 cells. ICP-MS was able to correctly identify different Ag isotopes and Pd doping (Fig. 21a).

As a next step, isotopic AgNPs were functionalized with SGKRK and RPARPAR peptides and biotin-AgNPs were used as non-targeted control. Three types of AgNPs were mixed and applied to M21 and PPC1 cells. Uptake of AgNPs was quantified, after removing unbound and extracellular AgNPs by etching and washing (Fig. 21b). $75 \pm 5\%$ of AgNPs internalized by PPC1 cells were RPARPAR particles and the remaining $25 \pm 5\%$ were SGKRK particles. M21 cells were preferentially internalizing SGKRK particles ($89 \pm 9\%$) and only a small amount of RPARPAR particles ($11 \pm 1\%$). The amount of biotin-AgNPs remained under detection limit, low background binding expected based on previous experiments was further reduced by etching of the extracellular particles. These results demonstrated the potential of multiplexing isotopic particles for assessing simultaneously the presence of multiple receptors on cultured cells.
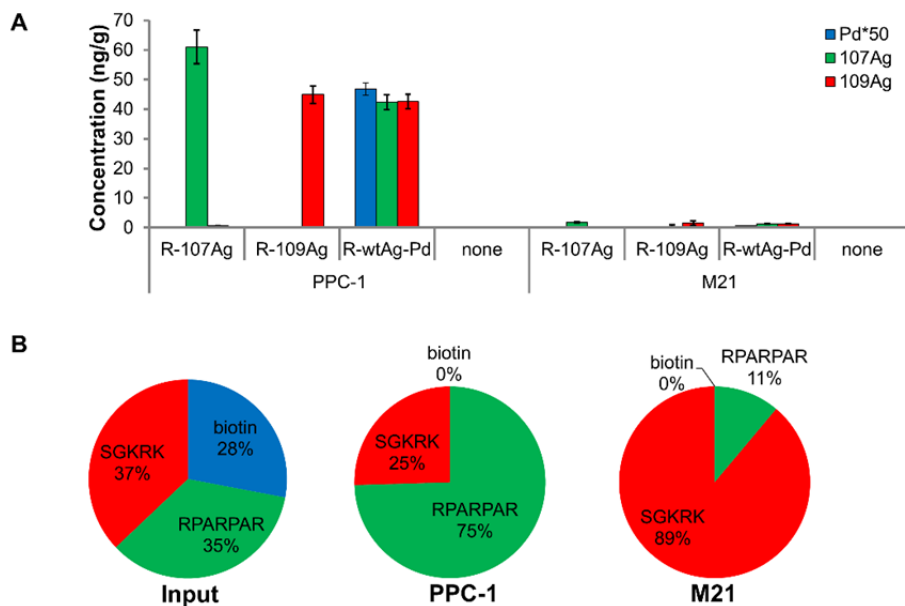
Figure 21. Isotopic multiplexing of peptide-AgNPs after incubation with M21 and PPC-1 cells. A) Three isotope-tagged RPARPAR-coupled silver cores were incubated with PPC-1 or M21 cells for 1 hour and total bound AgNPs were quantified by ICP-MS. Each of the three silver cores functionalized with RPARPAR peptide showed robust PPC-1 binding and low M21 binding. The Pd concentration is multiplied by 50 to visualize more clearly; the R-wt-Ag-Pd sample's Pd content of 0.94 ± 0.04 ng/g is 100 times above the detection limit. Data represent mean values $\pm$ SD (n=3). B) Cells incubated with isotopically coded AgNPs (R-107AgNPs, K-109AgNPs, B-wtAg-Pd), followed by etching to remove the extracellular nanoparticles and quantification of the internalized nanoparticles by ICP-MS. PPC-1 cells demonstrated preferential uptake of R-AgNPs and M21 cells took up mainly K-AgNPs (n=3).

5.5.2. Application of ratiometric ICP-MS for
AgNP *in vivo* homing studies

Cell phenotyping with isotopically barcoded AgNPs suggested applications of the same technology for *in vivo* homing studies. For proof of concept animal experiments with Ag107NPs and Ag109NPs were used. Ag107NPs were functionalized with targeting peptides and Ag109NPs were blocked with biotin. To determine ratio of Ag107/109 from tissue extracts ICP-MS was used that provides information on the average representation of the isotopic particles in the tissue (Fig. 22a). LA-ICP-MS analysis of frozen tissue sections was used to study spatial distribution of AgNPs in tissues (Fig. 22b).
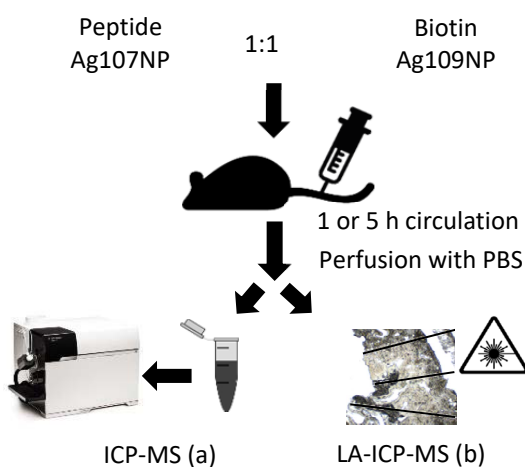
Figure 22: ICP-MS-based ratiometric analysis of homing experiments with isotopically-barcoded AgNPs. Balb/c mice were injected in tail vein with an equimolar mix of peptide-AgNPs (Ag107) and biotin-AgNPs (Ag109) in 200 µl PBS. 1 h or 5 h post i.v. administration, the animals were perfused with 15 ml PBS to remove free plasma AgNPs, and the organs of interest were snap-frozen. Tissues were subjected to HNO_3/H_2O_2 extraction protocol for ICP-MS or cryosectioned for Laser Ablation ICP-MS (LA-ICP-MS).

5.5.2.1. ICP-MS analysis of whole organs

To study biodistribution of targeted and non-targeted isotopic AgNPs in healthy animals, Ag107 particles were functionalized with either lung-homing RPARPAR or brain-homing CAGALCY peptide. Equal amount of targeted Ag107-AgNPs and control biotin-AgNPs were i.v. injected in healthy animals. Preferential accumulation of RPARPAR-AgNPs was detected in lungs, ~9 fold higher amount of targeted particles were found in lungs at the one hour time point, after five hours the ratio over control particles had been reduced to ~5 (Fig. 23a), which agreed well with the results from confocal imaging (Fig. 15b). CAGALCY-AgNPs were overrepresented in the brain but the difference was lower, than seen by optical imaging, this phenomenon was likely caused by heterogeneous homing pattern of CAGALCY and averaging of the whole brain extract (Fig. 23b).
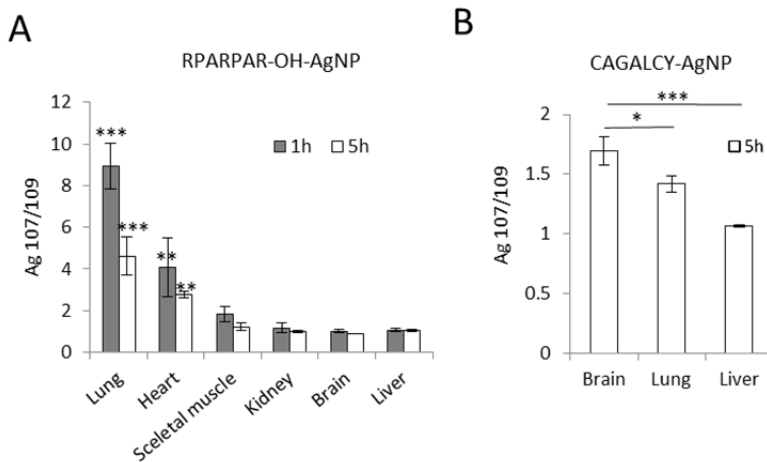
Figure 23: ICP-MS analysis of tissue distribution of homing peptide-functionalized AgNPs. (A) ICP-MS analysis of tissue distribution of RPARPAR-OH-AgNPs after 1 or 5 h post i.v. administration. Data represent mean values ± SD (n=3). *** $p < 0.001$, ** $p < 0.01$, * $p < 0.05$. (B) ICP-MS-based analysis of tissue distribution of CAGALCY AgNPs. Balb/c mice were intravenously injected with an equimolar mixture of targeted CAGALCY AgNPs and biotin-AgNPs. 5-h post i.v. administration the animals were intracardially perfused with PBS, and the extracts of organs were subjected to ICP-MS to for relative quantitation of silver isotopes. Data represent mean ± SD (n=3), *** $p < 0.001$, ** $p < 0.01$, * $p < 0.05$.

5.5.2.2. LA-ICP-MS based analysis of spatial homing

5.5.2.2.1. *In situ* analysis of of RPARPAR-AgNPs in the lungs

Homing pattern of targeted nanoparticles can be very heterogeneous and if averaged, the difference compared to non-targeted payloads is strongly diminished. To study heterogeneous accumulation in tissues, LA-ICP-MS based spatial analysis of cryosections was used. Heterogeneous homing of RPARPAR-AgNPs in the lungs was observed, more particles were accumulating in regions close to pulmonary vasculature and bronchioli with Ag107/109 ratio over 8 (Fig. 24a). When Ag107/109 ratio from multiple ablation paths was averaged, the resulting Ag107/109 value from lungs was similar to the value obtained from tissue extract: ~6.1 with LA-ICP-MS vs ~5 with ICP-MS. In contrast, the ratio of Ag107/109 in the liver, a control organ, was ~1 with both analysis methods.
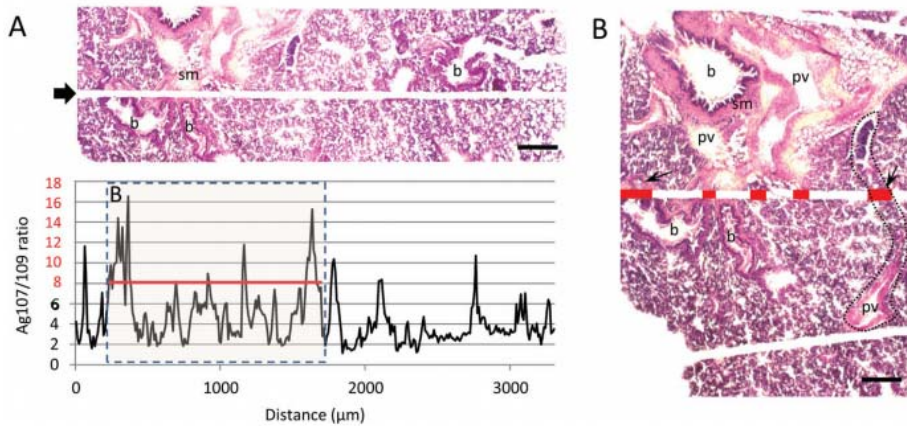
Figure 24: Ratiometric LA-ICP-MS profiling in lung cryosections. (A) Balb/c mice were injected i.v. with 200 μL of a mixture of RPARPAR-OH-Ag107NPs and control biotin-Ag109NPs. At 5 h time point mice were perfused, and organs collected. Tissues were snap-frozen, sectioned at 30 μm, and laser ablation line scans using 40 μm spot were performed. Hematoxylin–eosin staining of a lung cryosections used for LA-ICP-MS. The laser ablation path is indicated by arrow. Note the microanatomical heterogeneity of the lung section. The region of the graph indicated by the dashed box and pink shading correspond to the inset showing the laser ablation path in panel B. (B) Areas along the ablation path with Ag107/109 > 9 are indicated in red. Elevated Ag107/109 ratios are associated with vascular and bronchial structures. Data are representative of 16 laser ablation paths. Scale bars: (A) 200 μm; (B) 100 μm. b: bronchiole, sm: smooth muscle, pv: pulmonary vessel.

5.5.2.2.2. *In situ* analysis of of CAGALCY-AgNPs in the brain

To study heterogeneous accumulation of CAGALCY AgNPs in brain tissue LA-ICP-MS-based spatial analysis of cryosections was used. Mice injected with a mixture of CAGALCY and control AgNPs demonstrated overrepresentation of CAGALCY AgNPs in several areas in the brain, such as fibrillary tracts and pontine microvessels (Fig. 25). In these areas, the ratio of Ag107/109 was remarkably higher, between 15 and 30, compared to result from ICP-MS where ratio remained under 2.

These results demonstrate the importance of tissue heterogeneity in the homing of targeted NPs to tissue. Spatial distribution analysis provides valuable information to validate new affinity ligands and study targeted therapies.
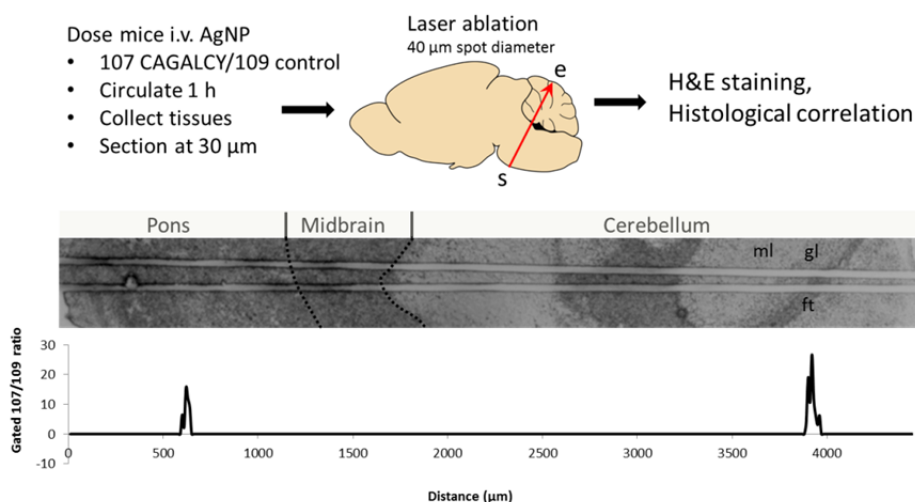
**Figure 25: Ratiometric LA-ICP-MS profiling on brain cryosections.** Balb/c mice were injected i.v. with 200 µL of a mixture of CAGALCY-AgNPs (prepared from Ag107) and control biotin-AgNPs (prepared from Ag109). At 5 h time point, tissues were snap-frozen, sectioned at 30 µm, and laser ablation line scans using 40 µm spot were performed. ft: fibrillary tract, ml: molecular layer, gl: granular layer.

5.5.2.2.3. Spatial distribution analysis of LinTT1-AgNPs in GBM lesions

To study accumulation of LinTT1-AgNPs in GBM tissue, Ag109 isotopic particles were functionalized with linTT1 peptide and injected in equal amount with biotin-Ag107-NPs to s.c. U87-MG tumor bearing animals. Spatial analysis of tissues demonstrated elevated ratios of Ag109/107 (up to 30) in tumor areas rich in tumor vessels (Fig. 26) whereas isotopic ratio in liver was homogeneous all over the tissue.
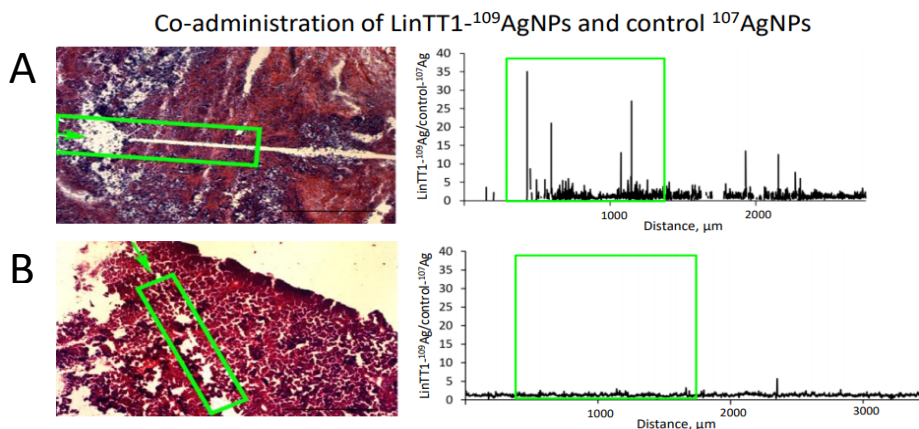
Figure 26: Lin-TT1-targeted silver nanoparticles home to GBM lesions. (A, B) Profiling of LinTT1-coupled AgNPs in U87-MG tumor by laser ablation ion-coupled mass spectrometry (ICP-MS). Mice bearing s.c. U87-MG tumor were injected i.v. with equimolar ratio of neutravidin-coated Ag109 nanoparticles coupled to biotinylated linTT1, and Ag107 nanoparticles coupled to biotin only. Mice were subjected to cardiac perfusion after 5 h of circulation of the particles, and tissue sections from snap-frozen organs were applied for laser ablation ICP-MS and subsequent staining with H&E. Left panel – tissue sections of H&E-stained tumor and liver from mouse bearing U87-MG subcutaneous tumor. Right panel: ratio of Ag109/107 isotopes detected from the laser ablation line shown in the left panel. Areas from the representative tissues and the respective areas on silver ratio profile are depicted with green boxes on both panels. Note the uniform ratio of Ag109/107 in the liver. Scale bar in H&E stained tissue sections: 500 μm.

5.6. LinTT1-guided experimental therapy of GBM tumors

To evaluate the effect of linTT1 functionalization on anti-GBM activity of therapeutic NWs two different tumor models were used: s.c. U87-MG and orthotopic 005. Nanoworms were loaded with amphipilic proapoptotic $_D$(KLAKLAK)$_2$ peptide that destabilizes mitochondrial membranes leading to apoptosis. $_D$(KLAKLAK)$_2$ has been used in several experimental studies (Agemy et al. 2011; Hunt et al. 2017). In mice with s.c. U87-MG tumors, treatment with LinTT1-$_D$(KLAKLAK)$_2$-NWs suppressed tumor progression and tumor size at the end of treatment was significantly reduced compared to PBS group (Fig. 27). In mice with orthotopic 005 tumors, LinTT1-$_D$(KLAKLAK)$_2$-NWs delayed the tumor progression and improved survival of the animals (Fig. 28).
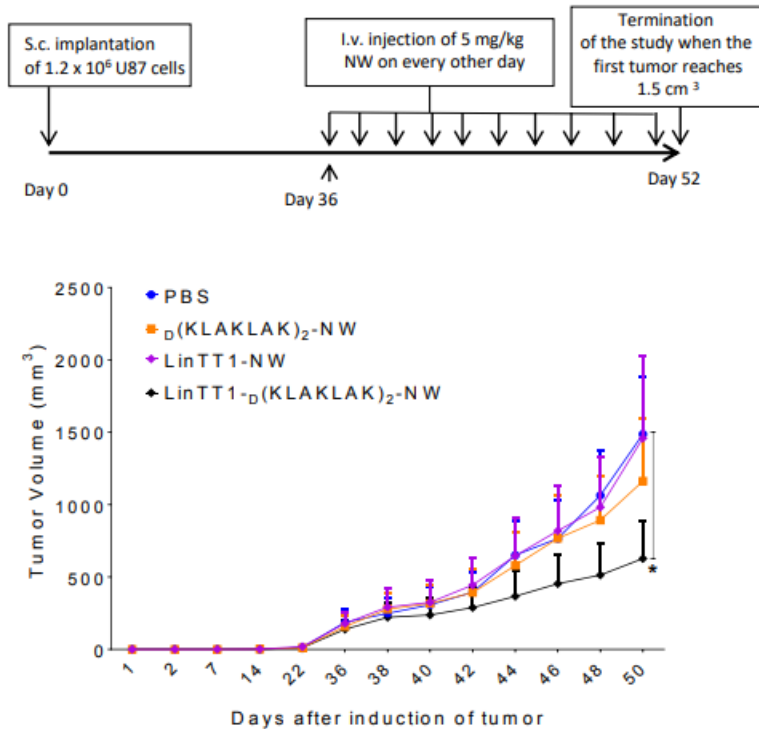
Figure 27: Experimental therapy of U87-MG subcutaneous tumor-bearing mice with LinTT1-$_D$(KLAKLAK)$_2$-NW inhibits the tumor growth.
The treatment of U87-MG-bearing mice with LinTT1-D(KLAKLAK)$_2$-NW and control agents [$_D$(KLAKLAK)$_2$-NW, LinTT1-$_D$(KLAKLAK)$_2$-NWs, and PBS] was started on day 36 after tumor induction. The therapy consisted of 8 intravenous injections of NWs (5 mg/kg Fe in 100 µl) every other day. Tumor size was recorded daily, and the study was terminated when the first tumor reached 1.5 cm^3, the maximum size allowed by the animal care committee. * – $p < 0.01$. Error bars – standard deviation.
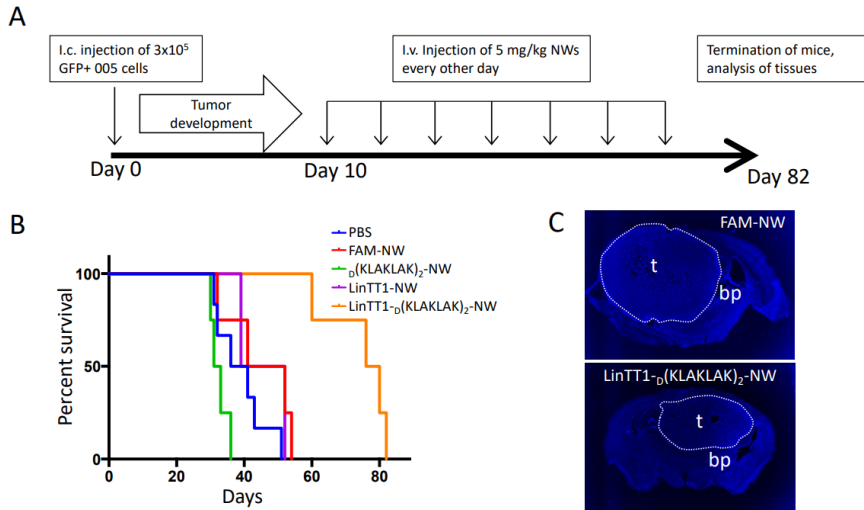
Figure 28: Experimental therapy of 005 GBM with LinTT1-$_D$(KLAKLAK)$_2$-NW inhibits the tumor growth. (A) – Starting on day 10 post tumor induction, the 005-bearing mice received 7 i.v. injections of 5 mg/kg of LinTT1-$_D$(KLAKLAK)$_2$-NW, or control compounds [$_D$(KLAKLAK)$_2$-NW, LinTT1- $_D$(KLAKLAK)$_2$-NWs, and PBS] every other day. (B) – Body weight and motor functions of mice were monitored daily and the animals were sacrificed when they reached the limits allowed by the animal ethics committee, and the survival data were expressed as Kaplan-Meyer plots. (C) – Representative images DAPI-counterstained (blue) sections of orthotopic GBM (indicated by dotted line) collected on day 82 from mice treated with FAM-$_D$(KLAKLAK)$_2$-NW and FAM-LinTT1- $_D$(KLAKLAK)$_2$-NWs. t: tumor, bp: brain parenchyma.

6. DISCUSSION

6.1. Significance

The identification of new affinity ligands to target CNS is important for the development of novel strategies to diagnose and treat nervous system disorders – as most brain disorders have no effective cure. Brain is a difficult organ to target as it is shielded by different protective barriers against invading pathogens and neurotoxic molecules. These barriers also prevent access to the brain of over 90% of potential neuropharmaceuticals. Nanoparticles are considered one of the most promising strategies to deliver drugs to the CNS. Several NP formulations have been reported to successfully reach the brain tissue, mainly when modified with surfactants or affinity ligands (De la Torre and Ceña 2018). Functionalizing nanoparticles with brain targeting ligands could enable therapeutics and imaging agents to effectively cross the blood-brain barrier and reach to disease sites in the brain. Targeted therapies have improved sensitivity and reduced off-target side effects compared to untargeted nanomedicines and conventional drug formulations. To develop novel targeted nanomedicines with a high potential to reach to clinical settings, it is important to make the right decisions over key features, like NP size, shape, coating and affinity ligands. Making these decisions is often difficult due to the lack of quantitative assays to evaluate *in vivo* homing of nanoparticles.

6.2. Main findings

The current study focused on identification and characterization of brain-homing peptides that could be used to deliver cargo to brain tissue and target various nervous system disorders. To improve validation process of novel affinity ligands a highly sensitive ICP-MS-based internally controlled system was developed that enables silver nanoparticle quantification from cell and tissue lysates, and *in situ* analysis of tissue sections. It was demonstrated that previously described tumor homing peptide linTT1 increases selectivity of nanoparticles to malignant brain tumors and improves therapeutic efficacy of NPs functionalized with proapoptotic peptide. In addition, a novel homing peptide was identified, that recognizes cerebrovascular changes in Alzheimer`s disease models and homes to activated astrocytes also in other models of neurological disorders.

6.2.1. ICP-MS-based ratiometric system for quantitative and internally controlled receptor profiling

Novel targeting ligands identified by screening combinatorial libraries, e.g. phage display peptide library, need to be validated. Assessment of expression and accessibility of the target receptors on the cell surface can be conducted by assessing binding and internalization of peptide-nanoparticles in the cells. A multiplex ultrasensitive ICP-MS-based assay was developed to quantitate nanoparticles prepared from pure silver isotopes and palladium. In proof of concept experiments, isotopically-barcoded AgNPs were functionalized with two different homing peptides (RPARPAR and GKRK) and used in internalization studies using cell lines with different homing peptide receptor expression. Amount of internalized particles was quantified by ICP-MS. It was established, that uptake of peptide-functionalized particles was dependent on the expression of the relevant receptors on the cell surface and was not affected by the exact composition of the nanoparticles. This highly sensitive method enables to measure relative ratios of internalized differentially functionalized nanoparticles and thereby provides information on the expression and availability of the relevant receptors.

6.2.2. Ratiometric *in vivo* comparison of AgNPs is a highly sensitive internally controlled assay for homing studies

Isotopically barcoded AgNPs can be used for simultaneous evaluation of the affinity targeting ligands in the same animal to minimize artefacts due to inter-animal variability. Quantitative biodistribution studies using multiplexed nanoparticles would facilitate optimization of affinity ligands to target disease sites or specific organs. Firstly, *in vivo* homing of AgNPs functionalized with non-pathogenic organ homing peptides RPARPAR (selective for lungs in normal mice) and CAGALCY (brain microvessels) was evaluated. Equimolar amount of peptide-guided Ag107 and control Ag109 particles was injected intravenously in the animals. Ag107/109 ratio was determined from tissue extracts by ICP-MS and from cryosections by LA-ICP-MS. Both methods showed overrepresentation of RPARPAR-NPs in the lung and CAGALCY-NPs in the brain, but LA-ICP-MS provided additional information about the homing within the tissue. Later, the LA-ICP-MS method was also used to study linTT1-AgNP homing to GBM lesions, showing accumulation of functionalized particles in tumor areas rich in blood vessels.

Several internally controlled multiplexing approaches have been reported in the literature (Dahlman et al. 2017; Kunjachan et al. 2014), but they possess several disadvantages compared to ICP-MS based quantification. DNA-barcoded NPs have high sensitivity and can be used across a wide dynamic range, but for several reasons: these particles cannot be readily distinguished on tissue sections for spatial mapping, barcodes need to be protected from degradation,

and barcode sequences can affect PCR amplification, or NP behavior (Dahlman et al. 2017). NPs with different fluorophores allow noninvasive longitudinal homing studies, but optical imaging is not quantitative (Kunjachan et al. 2014).

6.2.3. LinTT1 peptide guided nanoparticles accumulate in GBM lesions

Precision delivery of anticancer drugs could potentially improve the prognosis of GBM patients. Currently, there are only two approved anticancer compounds, temozolomide and nitrosourea, that are able to cross the BBB and reach to the cerebral tissue. Temozolomide, the standard chemotherapeutic drug of GBM, has only modest anticancer effect and it fails to penetrate the GBM lesions (Chamberlain 2010). Affinity targeted delivery of anticancer compounds could increase the concentration of drugs at disease site and enable to deliver drugs that do not readily cross the BBB.

A novel tumor penetrating peptide, linTT1, was evaluated as an affinity ligand on five phenotypically diverse GBM tumor models. Functionalization with linTT1 peptide increased accumulation of nanoparticles at tumor site in all the tested models. LinTT1-NWs accumulated preferentially in stromal cell populations: in endothelial cells and in tumor associated macrophages (TAM). Experimental therapy with linTT1 guided proapoptotic iron NPs inhibited tumor growth and markedly improved survival of the mice compared to control groups. Increased amounts of TAMs have been found in stroma of various human malignancies (Chanmee et al. 2014). TAMs are the main cell population promoting tumor growth and drug resistance (Yang and Zhang 2017). Targeting TAMs could be a potential strategy to treat tumors that are unresponsive to conventional anticancer therapies. Thus, linTT1 could be used to develop targeted therapies to selectively kill or reprogram TAMs, and thereby improve the prognosis of cancer patients. Furthermore, elevated expression of p32 is associated with worse prognosis in GBM patients and knockdown of p32 has been demonstrated to slow the progression of tumor growth (Laakkonen et al. 2004; Yenugonda et al. 2017). Future studies will show whether peptidic p32 targeting ligands possess intrinsic antitumor activity and act in synergy with payload drugs promoting their therapeutic efficacy.

6.2.4. AD peptide targets activated astrocytes in AD and other models of neuroinflammation

AD is the most common age-related progressive neurodegenerative disorder with no effective cure. Detailed mechanistic understanding of the pathogenesis of AD is still missing (Du, Wang, and Geng 2018). Changes in the brain vasculature that lead to disruption of BBB have been reported in AD animal models as well as in patients with late-stage AD. Morphological and functional

changes in the vessels could contribute to neuronal dysfunction and neuro-degeneration (De la Torre 2002; Zlokovic 2011). *In vivo* phage display screens on AD animal model were conducted to identify peptides that bind to molecular changes in the vasculature associated with AD. The novel peptide, DAG, bound selectively to activated astrocytes present in early stages of AD and in other models of neuroinflammation. DAG receptor was identified using affinity chromatography separation; and found to be connective tissue growth factor (CTGF), a matricellular protein with elevated expression in various types of brain injuries and in small blood vessels in the brains of human AD patients (Conrad et al. 2009; Spliet et al. 2003; Ueberham et al. 2003).

DAG peptide accumulation was also seen in GBM lesions, in patient-derived GBM model (P13). It is worth noting that P13 model has been reported to have elevated CTGF expression (Bougnaud et al. 2016). P13 tumors are angiogenic with areas of pseudopalisading necrosis, features characteristic of clinical GBM. Our results suggest the potential uses for DAG peptide as a targeting ligand for improving imaging of neurological disorders, especially early AD and for delivery of drugs to brain for the treatment of neuroinflammatory conditions.

6.3. Future directions

Precision nanomedicine is a rapidly developing field with potential to overcome challenges associated with diagnosis and treatment of brain disorders. Nano-scale systems can potentially improve imaging and treatment of neurodegene-rative disorders and brain tumors. Nanomedicines conjugated with targeting ligands provide platforms for selective delivery of drugs and imaging agents to the CNS. Encapsulating drugs into affinity guided nanocarriers protects the drugs from degradation, increases their circulation time, enables crossing the BBB and provides controlled release at the disease site. Targeted therapies increase local drug concentration and protect peripheral system and surrounding brain tissue from toxicities.

7. CONCLUSIONS

1. ICP-MS-based quantification of peptide-coated isotopically tagged AgNPs can be used to determine peptide receptor phenotype of cultured cells.
2. Internally controlled ICP-MS-based AgNP quantification system makes it possible to study homing of targeted NPs and compare specificity of different homing peptides in the same animal.
3. LA-ICP-MS based AgNP quantification method allows internally controlled mapping of peptide-AgNP distribution within the tissue.
4. LinTT1 peptide guided NPs accumulate in GBM lesions and exert therapeutic activity in case the particles carry anticancer compounds.
5. Phage display screens on AD model led to the discovery of homing peptide, DAG, which recognizes connective tissue growth factor (CTGF) in Alzheimer's brains. DAG peptide homes to the brain also in GBM, PD and traumatic brain injury animal models.

8. SUMMARY IN ESTONIAN

Kullerpeptiidide kasutamine ajuhaiguste ravis

Ühiskonna keskmise eluea suurenemise tulemusel kasvab vananemisega seotud kesknärvisüsteemi haiguste, näiteks Alzheimeri ja Parkinsoni tõve, sagedus. Nende haiguste puhul puudub tõhus ravi haiguse kulu peatamiseks või patsientide terveks ravimiseks. Neurodegeneratiivsed haigused pole iseenesest letaalsed, kuid haiguse progresseeruv kulg muudab patsiendid kõrvalabist sõltuvaks. Seevastu ajukasvajad on väga kehva prognoosiga – hoolimata ravist ei ületa agressiivsemate ajukasvajate korral patsiendide elulemus 1,5 aastat.

Kesknärvisüsteemi haiguste ravi on keeruline, kuna seda kaitsevad erinevad füüsilised ja funktsionaalsed barjäärid, mille eesmärgiks on takistada patogeenide, toksiinide ja vererakkude sisenemist ajukoesse. Olulisimad nendest mehhanismidest on vere-aju barjäär ning vere-tserebrospinaalvedeliku barjäär, millest vaid väga kindlate omadustega molekulid on võimelised läbi tungima. Enamikele molekulidele ning ka 99% ravimitele on need tõkked läbipääsmatud.

Vananemisega seotud neuroloogiliste haiguste ravi parandamiseks on oluline parendada nende haiguste diagnoosimist. Selleks on vaja identifitseerida ja valideerida molekulaarseid markereid, mis võimaldavad haigusi diagnoosida varasemas staadiumis. Eelistatult juba enne kliiniliste sümptomite avaldumist. Järgmine oluline samm neuroloogiliste haiguste ravis on leida molekulaarsed transportsüsteemid, mille abil saaks ravimeid viia läbi kaitsva barjääri, et need jõuaksid haigusest haaratud koeni. Üks strateegia, mis võiks parandada ajuhaiguste ravi, on nanotehnoloogia rakendamine. Vere-aju barjääri läbivad kullermolekulid on võimalik kinnitada ravimitega laaditud nanoosakeste pinnale. Sel viisil oleks võimalik ajukoesse transportida ka ravimeid, mis on koekultuuri süsteemis näidanud efektiivsust kasvajarakkude hävitamisel või neuronite kaitsmisel, kuid vereringesse süstituna ei suuda iseseisvalt aju kaitsvaid tõkkeid läbida.

Käesoleva prekliinilise töö eesmärgiks oli leida peptiidid, mis akumuleeruvad ajus ning mida saab rakendada kullermolekulidena kontrastainete ja/või ravimite transportimiseks. Parimate kullermolekulide välja valimiseks töötasime välja väga täpse kvantitatiivse metoodika, mis võimaldab erinevaid kullerpeptiide raku- ja loomkatsetes omavahel võrrelda.

Uurimistöö eesmärgid

1. Töötada välja kvantitatiivne meetod, mis võimaldab võrrelda kullerpeptiididega funktsionaliseeritud nanoosakeste võimet rakku siseneda;
2. Töötada välja kvantitatiivne meetod, mis võimaldab võrrelda süsteemselt manustatud kullerpeptiididega nanoosakeste võimet sihtmärkkoes akumuleeruda;
3. Kohandada kvantitatiivne meetod sobivaks koelõikude analüüsimiseks;
4. Hinnata kullerpeptiididega kaetud nanoosakeste võimet siseneda ajukasvaja koesse ning võimendada nanoravimite efektiivsust;
5. Identifitseerida Alzheimeri tõve spetsiifiliste molekulaarsete markerite suhtes selektiivsed kullerpeptiidid.

Materjal ja metoodika

Käesolevas uurimistöös oli kasutusel kokku üheksa erinevat kasvajarakuliini, millest kolm pärinesid hiirtelt ja ülejäänud kuus inimestelt. Loomkatsetes kasutati Balb/c hiiri ja atüümseid karvutuid hiiri. Kokku kasutati kuut erinevat multiformse glioblastoomi mudelit, kahte Alzheimeri tõve mudelit, ühte Parkinsoni tõve mudelit ning ühte traumaatilise ajukahjustuse loommudelit. Kõik loomkatsed olid kooskõlastatud vastavalt Eesti Põllumajandusministeeriumi, Tel Avivi ülikooli ja Sanford Burnham Prebyse meditsiiniuuringute instituudi vastava komisjoni poolt. Töös kasutati erinevaid varasemalt kirjeldatud kullerpeptiide (RPARPAR, CGKRK, CAGALCY, linTT1), mis kinnitati nanoosakeste pinnale. Nanoosakestest kasutati kahe erineva suurusega hõbeosakesi, raudoksiidi osakesi ja albumiin-paklitakseel nanoosakesi (Abraxane). Hõbe- ja raudosakesed sünteesiti vastavalt varem kirjeldatud protokollidele, Abraxane'i osakesed soetati valmiskujul. Peptiidid kinnitati hõbeosakestele biotiin-neutravidiin interaktsiooni abil ning raudoksiidi ja Abraxane'i osakestele NHS-PEG-maleimiidlinkeri abil. Nanoosakeste seondumist retseptorvalgule analüüsiti spektrofotomeetriat kasutades. Seondumiskatsed kasvajarakkudele viidi läbi kasutades voolutsütomeetriat, konfokaalmikroskoopiat ja induktiiv-sidestatud plasma mass-spektromeetriat (ICP-MS). Alzheimeri tõve (AD) peptiidi koejaotumise uurimiseks kasutati AD, Parkinsoni tõve, P13 ajukasvaja ja traumaatilise ajukahjustuse loommudeleid, hiirtele süstiti FAM märgisega peptiidi ja hiljem värviti ajude ja kontrollkudede koelõike antikehadega ning koed visualiseeriti konfokaalmikroskoopia abil. Hõbeosakeste biojaotumise uurimiseks süstiti peptiidiga osakesed ja kontrollosakesed tervetesse loomadesse ning hiljem teostati immunohistokeemilised värvingud ja visualiseeriti konfokaalmikroskoopia abil koelõigud. Kvantitatiivse analüüsimeetodi väljatöötamiseks süstiti tervetele loomadele peptiidiga osakeste ja kontrollosakeste segu ning postmortaalselt eemaldatud koed jagati kaheks: üks osa külmutati ning teine osa kudedest lüüsiti. Kudede lüsaate analüüsiti ICP-mass-spektromeetriaga ning külmutatud koest tehti lõigud, mida analüüsiti laser-ablatsioon ICP-

mass-spektromeetria abil. Kasvajaspetsiifilise peptiidiga nanoosakeste biojaotumise kvantitatiivseks analüüsiks indutseeriti hiirtele kas ortotoopsed või nahaalused kasvajad ning loomadele süstiti peptiidiga raudoksiidi ja Abraxane'i osakesi. Pärast ohverdamist tehti kudedest krüolõigud, mida värviti sobivate antikehadega ning visualiseeriti konfokaalmikroskoopia abil. Kasvajaspetsiifilise peptiidiga nanoosakeste biojaotumise kvantitatiivseks analüüsiks süstiti nahaaluste kasvajatega loomadele peptiidiga osakeste ja kontrollosakeste segu, koed külmutati ning tehti krüolõigud, mida kuivatati vaakumis ning seejärel analüüsiti laser-ablatsioon ICP-MS analüsaatoriga. Hindamaks kullerpeptiidi spetsiifilisust kasvajakoe suhtes ja proapoptootilise peptiidiga nanoosakeste efektiivsust kasvajarakkude hävitamisel viidi läbi ravikatse kahe erineva GBM loommudeliga. Selleks tekitati hiirtel ortotoopsed ja nahaalused kasvajad ja kui kasvajad olid saavutanud vajaliku suuruse, süstiti nanoosakesi sabaveeni ning katse lõpus võrreldi kasvajate suurust ja koehistoloogiat kontrollosakestega süstitud loomade kasvajatega.

Uurimistöö peamised tulemused ja järeldused

1. Töötati välja hõbedananoosakeste platvormil põhinev süsteem, mis võimaldab kvantiseerida erinevate peptiididega nanoosakeste võimet rakkudesse siseneda. Metoodika võimaldab hinnata nanoosakeste rakku sisenemiseks vajalike retseptorite ekspressioonitaset ja ligipääsetavust. Lisaks võimaldab see metoodika fenotüpiseerida segukultuurina kasvavaid rakke tänu varieeruvale retseptorite ekspressioonimustrile erinevatel rakuliinidel.

2. *In vitro* analüüsi süsteem kohandati sobivaks *in vivo* katsete jaoks nii, et see võimaldab võrrelda erinevate kullerpeptiididega nanoosakeste võimet sihtmärkkoes akumuleeruda. Välja töötatud analüüsimeetodi abil saab mitme erineva peptiidiga nanoosakesi testida seguna samas loomas, lisades meetodile nn sisemise kontrolli ning vähendades kõrvalekallete esinemise tõenäosust.

3. Laser-ablatsioon ICP-MS abil on võimalik sihtmärkkoe külmlõikudel kullerpeptiidiga nanoosakeste biojaotumist kvantitatiivselt analüüsida.

4. LinTT1 kasvajaspetsiifilise peptiidiga nanoosakesed akumuleerusid kasvajakoes kõigi viie testitud GBM mudeli puhul sõltumata nanoosakeste tüübist. LinTT1 nanoosakeste peamiseks sihtmärgiks olid kasvaja veresooned ja kasvajaseoselised makrofaagid. LinTT1 peptiidi ja proapoptootilise peptiidiga raudoksiidi nanoosakesed olid eksperimentaalteraapia katses võrreldes kontrollosakestega efektiivsed, pidurdades tuumorite kasvu ning pikendes loomade elulemust.

5. *In vivo* faagidisplei AD mudelil viis sidekoe kasvufaktor CTGFga seonduva DAG peptiidi avastamiseni, ning me näitasime, et DAG peptiid akumuleerub hiirtes glioblastoomi mudelites.

9. REFERENCES

Adams, G.P., Schier, R., McCall, A.M., Simmons, H.H., Horak, E.M., Alpaugh, R.K., Marks, J.D., and Weiner, L.M. (2001). High affinity restricts the localization and tumor penetration of single-chain Fv antibody molecules. Cancer Research *61*, 4750–4755.

Agemy, L., Friedmann-Morvinski, D., Kotamraju, V.R., Roth, L., Sugahara, K.N., Girard, O.M., Mattrey, R.F., Verma, I.M., and Ruoslahti, E. (2011). Targeted nanoparticle enhanced proapoptotic peptide as potential therapy for glioblastoma. Proceedings of the National Academy of Sciences of the United States of America *108*, 17450–17455.

Agemy, L., Kotamraju, V.R., Friedmann-Morvinski, D., Sharma, S., Sugahara, K.N., and Ruoslahti, E. (2013). Proapoptotic peptide-mediated cancer therapy targeted to cell surface p32. Molecular Therapy *21*, 2195–2204.

Agilent (2015). Agilent 8800 ICP-QQQ Application Handbook, 2nd edition, Agilent.

Aird, W.C. (2012). Endothelial cell heterogeneity. Cold Spring Harbor Perspectives in Medicine *2*.

Albanese, A., Tang, P.S., and Chan, W.C.W. (2012). The Effect of Nanoparticle Size, Shape, and Surface Chemistry on Biological Systems. Annual Review of Biomedical Engineering *14*, 1–16. Teja, A.S., and Koh, P.Y. (2009). Synthesis, properties, and applications of magnetic iron oxide nanoparticles. Progress in Crystal Growth and Characterization of Materials *55*, 22–45.

Alshaer, W., Hillaireau, H., and Fattal, E. (2018). Aptamer-guided nanomedicines for anticancer drug delivery. Advanced Drug Delivery Reviews *134*, 122–137.

alzforum.org/research-models/j20-pdgf-appswind Accessed: 2020.01.10

Andrieu, J., Re, F., Russo, L., and Nicotra, F. (2019). Phage-displayed peptides targeting specific tissues and organs. Journal of Drug Targeting *27*, 555–565.

Arami, H., Khandhar, A., Liggitt, D., and Krishnan, K.M. (2015). In vivo delivery, pharmacokinetics, biodistribution and toxicity of iron oxide nanoparticles. Chemical Society Reviews *44*, 8576–8607.

Argyriou, A.A., and Kalofonos, H.P. (2009). Molecularly targeted therapies for malignant gliomas. Molecular Medicine *15*, 115–122.

Assi, H., Candolfi, M., Baker, G., Mineharu, Y., Lowenstein, P.R., and Castro, M.G. (2012). Gene therapy for brain tumors: Basic developments and clinical implementation. Neuroscience Letters *527*, 71–77.

Barenholz, Y. (2012). Doxil® – The first FDA-approved nano-drug: Lessons learned. Journal of Controlled Release *160*, 117–134.

Bartanusz, V., Jezova, D., Alajajian, B., and Digicaylioglu, M. (2011). The blood-spinal cord barrier: Morphology and clinical implications. Annals of Neurology *70*, 194–206.

Bateman, R.J., Aisen, P.S., De Strooper, B., Fox, N.C., Lemere, C.A., Ringman, J.M., Salloway, S., Sperling, R.A., Windisch, M., and Xiong, C. (2011). Autosomal-dominant Alzheimer's disease: A review and proposal for the prevention of Alzheimer's disease. Alzheimer's Research and Therapy *2*.

Bates, A., and Power, C.A. (2019). David vs. Goliath: The Structure, Function, and Clinical Prospects of Antibody Fragments. Antibodies *8*, 28.

Bertrand, N., Wu, J., Xu, X., Kamaly, N., and Farokhzad, O.C. (2014). Cancer nanotechnology: The impact of passive and active targeting in the era of modern cancer biology. Advanced Drug Delivery Reviews *66*, 2–25.

Bjerkvig, R., Tonnesen, A., Laerum, O.D., and Backlund, E.O. (1990). Multicenter tumor spheroids from human gliomas maintained in organ culture. Journal of Neuro-surgery *72*, 463–475.

Blanco, E., Shen, H., and Ferrari, M. (2015). Principles of nanoparticle design for over-coming biological barriers to drug delivery. Nature Biotechnology *33*, 941–951.

Blouw, B., Song, H., Tihan, T., Bosze, J., Ferrara, N., Gerber, H.P., Johnson, R.S., and Bergers, G. (2003). The hypoxic response of tumors is dependent on their micro-environment. Cancer Cell *4*, 133–146.

Bobo, D., Robinson, K.J., Islam, J., Thurecht, K.J., and Corrie, S.R. (2016). Nano-particle-Based Medicines: A Review of FDA-Approved Materials and Clinical Trials to Date. Pharmaceutical Research *33*, 2373–2387.

Bougnaud, S., Golebiewska, A., Oudin, A., Keunen, O., Harter, P.N., Mäder, L., Azuaje, F., Fritah, S., Stieber, D., Kaoma, T., et al. (2016). Molecular crosstalk between tumour and brain parenchyma instructs histopathological features in glio-blastoma. Oncotarget *7*, 31955–31971.

Bové, J., Prou, D., Perier, C., and Przedborski, S. (2005). Toxin-induced models of Parkinson's disease. NeuroRx *2*, 484–494.

Braun, G.B., Friman, T., Pang, H.B., Pallaoro, A., De Mendoza, T.H., Willmore, A.M.A., Kotamraju, V.R., Mann, A.P., She, Z.G., Sugahara, K.N., et al. (2014). Etchable plasmonic nanoparticle probes to image and quantify cellular internaliza-tion. Nature Materials *13*, 904–911.

Campbell, J.E., and Cohall, D. (2017). Pharmacodynamics-A Pharmacognosy Perspec-tive. In Pharmacognosy: Fundamentals, Applications and Strategy, (Elsevier Inc.), pp. 513–525.

Campos, B., Wan, F., Farhadi, M., Ernst, A., Zeppernick, F., Tagscherer, K.E., Ahmadi, R., Lohr, J., Dictus, C., Gdynia, G., et al. (2010). Differentiation therapy exerts anti-tumor effects on stem-like glioma cells. Clinical Cancer Research *16*, 2715–2728.

Casi, G., and Neri, D. (2015). Antibody-Drug Conjugates and Small Molecule-Drug Conjugates: Opportunities and Challenges for the Development of Selective Anti-cancer Cytotoxic Agents. Journal of Medicinal Chemistry *58*, 8751–8761.

Chamberlain, M.C. (2010). Temozolomide: Therapeutic limitations in the treatment of adult high-grade gliomas. Expert Review of Neurotherapeutics *10*, 1537–1544.

Chanmee, T., Ontong, P., Konno, K., and Itano, N. (2014). Tumor-associated macro-phages as major players in the tumor microenvironment. Cancers *6*, 1670–1690.

Chen, F., and Cai, W. (2014). Tumor vasculature targeting: A generally applicable approach for functionalized nanomaterials. Small *10*, 1887–1893.

Chen, J., Sun, J., Han, W., Chen, J., Wang, W., Cheng, G., Lin, J., Ma, N., Chen, H., Ou, L., et al. (2018). Computer-aided design of short peptide ligands targeting tumor necrosis factor-alpha for adsorbent applications. Journal of Materials Chemistry B *6*, 4368–4379.

Chen, Y., Li, T., Li, J., Cheng, S., Wang, J., Verma, C., Zhao, Y., and Wu, C. (2017). Stabilization of peptides against proteolysis through disulfide-bridged conjugation with synthetic aromatics. Organic and Biomolecular Chemistry *15*, 1921–1929.

Cheng, C.Y., Ou, K.L., Huang, W.T., Chen, J.K., Chang, J.Y., and Yang, C.H. (2013). Gadolinium-based CuInS2/ZnS nanoprobe for dual-modality magnetic resonance/ optical imaging. ACS Applied Materials and Interfaces *5*, 4389–4400.

Cipolla MJ. (2009). Barriers of the CNS. In The Cerebral Circulation., p. 9.

Clinicaltrials.gov Accessed: 2020.01.10

Conrad, S., Schluesener, H.J., Adibzahdeh, M., and Schwab, J.M. (2005). Spinal cord injury induction of lesional expression of profibrotic and angiogenic connective tissue growth factor confined to reactive astrocytes, invading fibroblasts and endothelial cells. Journal of Neurosurgery. Spine *2*, 319–326.

Coppiello, G., Collantes, M., Sirerol-Piquer, M.S., Vandenwijngaert, S., Schoors, S., Swinnen, M., Vandersmissen, I., Herijgers, P., Topal, B., Van Loon, J., et al. (2015). Meox2/Tcf15 heterodimers program the heart capillary endothelium for cardiac fatty acid uptake. Circulation *131*, 815–826.

Cummings, J., Mintzer, J., Brodaty, H., Sano, M., Banerjee, S., Devanand, D.P., Gauthier, S., Howard, R., Lanctôt, K., Lyketsos, C.G., et al. (2015). Agitation in cognitive disorders: International Psychogeriatric Association provisional consensus clinical and research definition. International Psychogeriatrics *27*, 7–17.

D'Agata, F., Ruffinatti, F.A., Boschi, S., Stura, I., Rainero, I., Abollino, O., Cavalli, R., and Guiot, C. (2018). Magnetic nanoparticles in the central nervous system: Targeting principles, applications and safety issues. Molecules *23*.

Dadosh, T. (2009). Synthesis of uniform silver nanoparticles with a controllable size. Materials Letters *63*, 2236–2238.

Dahlman, J.E., Kauffman, K.J., Xing, Y., Shaw, T.E., Mir, F.F., Dlott, C.C., Langer, R., Anderson, D.G., and Wang, E.T. (2017). Barcoded nanoparticles for high throughput in vivo discovery of targeted therapeutics. Proceedings of the National Academy of Sciences of the United States of America *114*, 2060–2065.

Van Dam, D., and De Deyn, P.P. (2011). Animal models in the drug discovery pipeline for Alzheimer's disease. British Journal of Pharmacology *164*, 1285–1300.

Danhier, F. (2016). To exploit the tumor microenvironment: Since the EPR effect fails in the clinic, what is the future of nanomedicine? Journal of Controlled Release *244*, 108–121.

Demeule, M., Currie, J.C., Bertrand, Y., Ché, C., Nguyen, T., Régina, A., Gabathuler, R., Castaigne, J.P., and Béliveau, R. (2008). Involvement of the low-density lipoprotein receptor-related protein in the transcytosis of the brain delivery vector Angiopep-2. Journal of Neurochemistry *106*, 1534–1544.

Deng, X., Wang, L., You, X., Dai, P., and Zeng, Y. (2018). Advances in the T7 phage display system (Review). Molecular Medicine Reports *17*, 714–720.

Dhermain, F.G., Hau, P., Lanfermann, H., Jacobs, A.H., and van den Bent, M.J. (2010). Advanced MRI and PET imaging for assessment of treatment response in patients with gliomas. The Lancet Neurology *9*, 906–920.

Du, X., Wang, X., and Geng, M. (2018). Alzheimer's disease hypothesis and related therapies. Translational Neurodegeneration *7*.

Dzamba, D., Harantova, L., Butenko, O., and Anderova, M. (2016). Glial Cells – The Key Elements of Alzheimers Disease. Current Alzheimer Research *13*, 894–911.

Ehrlich, P. (2013). Über die Beziehungen von chemischer Constitution, Vertheilung und pharmakologischer Wirkung. In The Collected Papers of Paul Ehrlich, (Elsevier), pp. 570–595.

Engelhardt, B., and Sorokin, L. (2009). The blood-brain and the blood-cerebrospinal fluid barriers: Function and dysfunction. Seminars in Immunopathology *31*, 497–511.

Ernsting, M.J., Murakami, M., Roy, A., and Li, S.D. (2013). Factors controlling the pharmacokinetics, biodistribution and intratumoral penetration of nanoparticles. Journal of Controlled Release *172*, 782–794.

Fack, F., Espedal, H., Keunen, O., Golebiewska, A., Obad, N., Harter, P.N., Mittelbronn, M., Bähr, O., Weyerbrock, A., Stuhr, L., et al. (2015). Bevacizumab treatment induces metabolic adaptation toward anaerobic metabolism in glioblastomas. Acta Neuropathologica *129*, 115–131.

Fahmy, H.M., Mosleh, A.M., Elghany, A.A., Shams-Eldin, E., Abu Serea, E.S., Ali, S.A., and Shalan, A.E. (2019). Coated silver nanoparticles: Synthesis, cytotoxicity, and optical properties. RSC Advances *9*, 20118–20136.

Fan, X., Venegas, R., Fey, R., Van Der Heyde, H., Bernard, M.A., Lazarides, E., and Woods, C.M. (2007). An in vivo approach to structure activity relationship analysis of peptide ligands. Pharmaceutical Research *24*, 868–879.

Fogal, V., Babic, I., Chao, Y., Pastorino, S., Mukthavaram, R., Jiang, P., Cho, Y.J., Pingle, S.C., Crawford, J.R., Piccioni, D.E., et al. (2015). Mitochondrial p32 is upregulated in Myc expressing brain cancers and mediates glutamine addiction. Oncotarget *6*, 1157–1170.

Fogal, V., Zhang, L., Krajewski, S., and Ruoslahti, E. (2008). Mitochondrial/cell-surface protein p32/gC1qR as a molecular target in tumor cells and tumor stroma. Cancer Research *68*, 7210–7218.

Gabathuler, R. (2010). Approaches to transport therapeutic drugs across the blood-brain barrier to treat brain diseases. Neurobiology of Disease *37*, 48–57.

Gao, H. (2016). Progress and perspectives on targeting nanoparticles for brain drug delivery. Acta Pharmaceutica Sinica B *6*, 268–286.

Geng, Y., Dalhaimer, P., Cai, S., Tsai, R., Tewari, M., Minko, T., and Discher, D.E. (2007). Shape effects of filaments versus spherical particles in flow and drug delivery. Nature Nanotechnology *2*, 249–255.

Ghosh, D., Peng, X., Leal, J., and Mohanty, R.P. (2018). Peptides as drug delivery vehicles across biological barriers. Journal of Pharmaceutical Investigation *48*, 89–111.

Giljohann, D. A., Seferos, D. S., Daniel, W. L., Massich, M. D., Patel, P. C., & Mirkin, C. A. (2010, April 26). Gold nanoparticles for biology and medicine. *Angewandte Chemie – International Edition*. https://doi.org/10.1002/anie.200904359

Golde, T.E., Eckman, C.B., and Younkin, S.G. (2000). Biochemical detection of Aβ isoforms: Implications for pathogenesis, diagnosis, and treatment of Alzheimer's disease. Biochimica et Biophysica Acta – Molecular Basis of Disease *1502*, 172–187.

Hane, F.T., Robinson, M., Lee, B.Y., Bai, O., Leonenko, Z., and Albert, M.S. (2017). Recent Progress in Alzheimer's Disease Research, Part 3: Diagnosis and Treatment. Journal of Alzheimer's Disease *57*, 645–665.

Harris, L., Batist, G., Belt, R., Rovira, D., Navari, R., Azarnia, N., Welles, L., Winer, E., Garrett, T., Blayney, D., et al. (2002). Liposome-encapsulated doxorubicin compared with conventional doxorubicin in a randomized multicenter trial as first-line therapy of metastatic breast carcinoma. Cancer *94*, 25–36.

Hawkins, B.T., and Davis, T.P. (2005). The blood-brain barrier/neurovascular unit in health and disease. Pharmacological Reviews *57*, 173–185.

Hoffman, J.A., Giraudo, E., Singh, M., Zhang, L., Inoue, M., Porkka, K., Hanahan, D., and Ruoslahti, E. (2003). Progressive vascular changes in a transgenic mouse model of squamous cell carcinoma. Cancer Cell *4*, 383–391.

Honary, S., and Zahir, F. (2013). Effect of zeta potential on the properties of nano-drug delivery systems – A review (Part 1). Tropical Journal of Pharmaceutical Research *12*, 255–264.

Hua, S., de Matos, M.B.C., Metselaar, J.M., and Storm, G. (2018). Current trends and challenges in the clinical translation of nanoparticulate nanomedicines: Pathways for translational development and commercialization. Frontiers in Pharmacology *9*.

Hunt, H., Simón-Gracia, L., Tobi, A., Teesalu, T., Kotamraju, V.R., Sharma, S., Sugahara, K.N., Ruoslahti, E., Teesalu, T., Nigul, M., et al. (2017). Targeting of p32 in peritoneal carcinomatosis with intraperitoneal linTT1 peptide-guided pro-apoptotic nanoparticles. Journal of Controlled Release *260*, 142–153.

Huszthy, P.C., Daphu, I., Niclou, S.P., Stieber, D., Nigro, J.M., Sakariassen, P.O., Miletic, H., Thorsen, F., and Bjerkvig, R. (2012). In vivo models of primary brain tumors: Pitfalls and perspectives. Neuro-Oncology *14*, 979–993.

Jaffer, H., Morris, V.B., Stewart, D., and Labhasetwar, V. (2011). Advances in stroke therapy. Drug Delivery and Translational Research *1*, 409–419.

Jagmag, S.A., Tripathi, N., Shukla, S.D., Maiti, S., and Khurana, S. (2016). Evaluation of models of Parkinson's disease. Frontiers in Neuroscience *9*.

Jokerst, J.V., Lobovkina, T., Zare, R.N., and Gambhir, S.S. (2011). Nanoparticle PEGylation for imaging and therapy. Nanomedicine *6*, 715–728.

Kevadiya, B.D., Ottemann, B.M., Thomas, M.B., Mukadam, I., Nigam, S., McMillan, J.E., Gorantla, S., Bronich, T.K., Edagwa, B., and Gendelman, H.E. (2018). Neuro-theranostics as personalized medicines. Advanced Drug Delivery Reviews.

Kijima, N., & Kanemura, Y. (2017). Mouse Models of Glioblastoma. In *Glioblastoma* (pp. 131–139). Codon Publications. https://doi.org/10.15586/codon.glioblastoma.2017.ch7

Kolhar, P., Anselmo, A.C., Gupta, V., Pant, K., Prabhakarpandian, B., Ruoslahti, E., and Mitragotri, S. (2013). Using shape effects to target antibody-coated nanoparticles to lung and brain endothelium. Proceedings of the National Academy of Sciences of the United States of America *110*, 10753–10758.

Korchinski, D.J., Taha, M., Yang, R., Nathoo, N., and Dunn, J.F. (2015). Iron Oxide as an Mri Contrast Agent for Cell Tracking: Supplementary Issue. Magnetic Resonance Insights *8s1*, MRI.S23557.

Kreuter, J. (2007). Nanoparticles-a historical perspective. International Journal of Pharmaceutics *331*, 1–10.

Krumpe, L.R.H., Atkinson, A.J., Smythers, G.W., Kandel, A., Schumacher, K.M., McMahon, J.B., Makowski, L., and Mori, T. (2006). T7 lytic phage-displayed peptide libraries exhibit less sequence bias than M13 filamentous phage-displayed peptide libraries. Proteomics *6*, 4210–4222.

Kue, C.S., Kamkaew, A., Burgess, K., Kiew, L.V., Chung, L.Y., and Lee, H.B. (2016). Small Molecules for Active Targeting in Cancer. Medicinal Research Reviews *36*, 494–575.

Kunjachan, S., Pola, R., Gremse, F., Theek, B., Ehling, J., Moeckel, D., Hermanns-Sachweh, B., Pechar, M., Ulbrich, K., Hennink, W.E., et al. (2014). Passive versus active tumor targeting using RGD- and NGR-modified polymeric nanomedicines. Nano Letters *14*, 972–981.

De la Torre, C., and Ceña, V. (2018). The delivery challenge in neurodegenerative disorders: The nanoparticles role in alzheimer's disease therapeutics and diagnostics. Pharmaceutics *10*.

De la Torre, J.C. (2002). Alzheimer disease as a vascular disorder: Nosological evidence. Stroke *33*, 1152–1162.

Laakkonen, P., Åkerman, M.E., Biliran, H., Yang, M., Ferrer, F., Karpanen, T., Hoffman, R.M., and Ruoslahti, E. (2004). Antitumor activity of a homing peptide that

targets tumor lymphatics and tumor cells. Proceedings of the National Academy of Sciences of the United States of America *101*, 9381–9386.

Lajoie, J.M., and Shusta, E.V. (2015). Targeting Receptor-Mediated Transport for Delivery of Biologics Across the Blood-Brain Barrier. Annual Review of Pharmacology and Toxicology *55*, 613–631.

Lam, K.S., Salmon, S.E., Hersh, E.M., Hruby, V.J., Kazmierskit, W.M., and Knappt, R.J. (1991). A new type of synthetic peptide library for identifying ligand-binding activity. Nature *354*, 82–84.

Laterra, J., Keep, R., Betz, L.A., and Goldstein, G.W. (1999). Cerebrospinal Fluid—Brain interface. In Basic Neurochemistry: Molecular, Cellular and Medical Aspects

Lee, J.H., Engler, J.A., Collawn, J.F., and Moore, B.A. (2001). Receptor mediated uptake of peptides that bind the human transferrin receptor. European Journal of Biochemistry *268*, 2004–2012.

Lee, P.C., and Meisel, D. (1982). Adsorption and surface-enhanced Raman of dyes on silver and gold sols. Journal of Physical Chemistry *86*, 3391–3395.

Lenting, K., Verhaak, R., ter Laan, M., Wesseling, P., and Leenders, W. (2017). Glioma: experimental models and reality. Acta Neuropathologica *133*, 263–282.

Levi, M.S., and Brimble, M.A., (2004). A review of neuroprotective agents. Current Medicinal Chemistry *11*, 2383–2397.

Li, J., Feng, L., and Jiang, X. (2015). In vivo phage display screen for peptide sequences that cross the blood-cerebrospinal-fluid barrier. Amino Acids *47*, 401–405.

Liu, R., Li, X., Xiao, W., and Lam, K.S. (2017). Tumor-targeting peptides from combinatorial libraries. Advanced Drug Delivery Reviews *110–111*, 13–37.

Lockman, P.R., Koziara, J.M., Mumper, R.J., and Allen, D. (2004). Nanoparticle surface charges alter blood-brain barrier integrity and permeability. Journal of Drug Targeting *12*, 635–641.

Lopci, E., Nanni, C., Rampin, L., Rubello, D., and Fanti, S. (2008). Clinical applications of 68Ga-DOTANOC in neuroendocrine tumours. Minerva Endocrinologica *33*, 277–281.

Louis, D.N., Perry, A., Reifenberger, G., von Deimling, A., Figarella-Branger, D., Cavenee, W.K., Ohgaki, H., Wiestler, O.D., Kleihues, P., and Ellison, D.W. (2016). The 2016 World Health Organization Classification of Tumors of the Central Nervous System: a summary. Acta Neuropathologica *131*, 803–820.

Maeda, H., Nakamura, H., and Fang, J. (2013). The EPR effect for macromolecular drug delivery to solid tumors: Improvement of tumor uptake, lowering of systemic toxicity, and distinct tumor imaging in vivo. Advanced Drug Delivery Reviews *65*, 71–79.

Mahesparan, R., Read, T.A., Lund-Johansen, M., Skaftnesmo, K.O., Bjerkvig, R., and Engebraaten, O. (2003). Expression of extracellular matrix components in a highly infiltrative in vivo glioma model. Acta Neuropathologica *105*, 49–57.

Malcor, J.D., Payrot, N., David, M., Faucon, A., Abouzid, K., Jacquot, G., Floquet, N., Debarbieux, F., Rougon, G., Martinez, J., et al. (2012). Chemical optimization of new ligands of the low-density lipoprotein receptor as potential vectors for central nervous system targeting. Journal of Medicinal Chemistry *55*, 2227–2241.

Mann, A.P., Scodeller, P., Hussain, S., Joo, J., Kwon, E., Braun, G.B., Mölder, T., She, Z.G., Kotamraju, V.R., Ranscht, B., et al. (2016). A peptide for targeted, systemic delivery of imaging and therapeutic compounds into acute brain injuries. Nature Communications *7*.

Marumoto, T., Tashiro, A., Friedmann-Morvinski, D., Scadeng, M., Soda, Y., Gage, F.H., Verma, I.M. (2009) Development of a novel mouse glioma model using lentiviral vectors, Nature Medicine 15, 110–116.

Mi, P., Cabral, H., and Kataoka, K. (2019). Ligand-Installed Nanocarriers toward Precision Therapy. Advanced Materials 1902604.

Miao, D., Jiang, M., Liu, Z., Gu, G., Hu, Q., Kang, T., Song, Q., Yao, L., Li, W., Gao, X., et al. (2014). Co-administration of dual-targeting nanoparticles with penetration enhancement peptide for antiglioblastoma therapy. Molecular Pharmaceutics *11*, 90–101.

Milner, E., Zhou, M.L., Johnson, A.W., Vellimana, A.K., Greenberg, J.K., Holtzman, D.M., Han, B.H., and Zipfel, G.J. (2014). Cerebral amyloid angiopathy increases susceptibility to infarction after focal cerebral ischemia in Tg2576 mice. Stroke *45*, 3064–3069.

Ningaraj, N.S., Rao, M., Hashizume, K., Asotra, K., and Black, K.L. (2002). Regulation of blood-brain tumor barrier permeability by calcium-activated potassium channels. Journal of Pharmacology and Experimental Therapeutics *301*, 838–851.

Ningaraj, N.S. (2006). Drug delivery to brain tumours: Challenges and progress. Expert Opinion on Drug Delivery *3*, 499–509.

VanDyke D., Kyriacopulos P., Yassini B., Wright A., Burkhart E., Jacek S., Pratt M., Peterson C.R., Rai P. (2016). Nanoparticle Based Combination Treatments for Targeting Multiple Hallmarks of Cancer. International Journal of Nano Studies & Technology 1–18.

Paasonen, L., Sharma, S., Braun, G.B., Kotamraju, V.R., Chung, T.D.Y., She, Z.G., Sugahara, K.N., Yliperttula, M., Wu, B., Pellecchia, M., et al. (2016). New p32/gC1qR Ligands for Targeted Tumor Drug Delivery. ChemBioChem *17*, 570–575.

Pan, W., Banks, W.A., and Kastin, A.J. (1997). Permeability of the blood-brain and blood-spinal cord barriers to interferons. Journal of Neuroimmunology *76*, 105–111.

Pardridge, W.M. (2005). The blood-brain barrier: Bottleneck in brain drug development. NeuroRx *2*, 3–14.

Pardridge, W.M. (1986). Receptor-mediated peptide transport through the blood-brain barrier. Endocrine Reviews *7*, 314–330.

Pardridge, W.M. (2005). The blood-brain barrier: Bottleneck in brain drug development. NeuroRx *2*, 3–14.

Park, J.H., Von Maltzahn, G., Zhang, L., Derfus, A.M., Simberg, D., Harris, T.J., Ruoslahti, E., Bhatia, S.N., and Sailor, M.J. (2009). Systematic surface engineering of magnetic nanoworms for in vivo tumor targeting. Small *5*, 694–700.

Parsons, D.W., Jones, S., Zhang, X., Lin, J.C.H., Leary, R.J., Angenendt, P., Mankoo, P., Carter, H., Siu, I.M., Gallia, G.L., et al. (2008). An integrated genomic analysis of human glioblastoma multiforme. Science *321*, 1807–1812.

Pasqualini, R., and Ruoslahti, E. (1996). Organ targeting in vivo using phage display peptide libraries. Nature *380*, 364–366.

Pereira, R.L., Nascimento, I.C., Santos, A.P., Ogusuku, I.E.Y., Lameu, C., Mayer, G., and Ulrich, H. (2018). Aptamers: Novelty tools for cancer biology. Oncotarget *9*, 26934–26953.

De La Torre, J.C. (2014). Phase 3 trials of solanezumab and bapineuzumab for Alzheimer's disease [2]. New England Journal of Medicine *370*, 1459–1460.

Potente, M., and Mäkinen, T. (2017). Vascular heterogeneity and specialization in development and disease. Nature Reviews Molecular Cell Biology *18*, 477–494.

Ross, C., Taylor, M., Fullwood, N., and Allsop, D. (2018). Liposome delivery systems for the treatment of Alzheimer's disease. International Journal of Nanomedicine *13*, 8507–8522.

Ruan, S., Cao, X., Cun, X., Hu, G., Zhou, Y., Zhang, Y., Lu, L., He, Q., and Gao, H. (2015). Matrix metalloproteinase-sensitive size-shrinkable nanoparticles for deep tumor penetration and pH triggered doxorubicin release. Biomaterials *60*, 100–110.

Ruoslahti, E. (2004). Vascular zip codes in angiogenesis and metastasis. In Biochemical Society Transactions, pp. 397–402.

Ruoslahti, E. (2012). Peptides as targeting elements and tissue penetration devices for nanoparticles. Advanced Materials *24*, 3747–3756.

Ruoslahti, E. (2017). Tumor penetrating peptides for improved drug delivery. Advanced Drug Delivery Reviews *110–111*, 3–12.

Saraiva, C., Praça, C., Ferreira, R., Santos, T., Ferreira, L., and Bernardino, L. (2016). Nanoparticle-mediated brain drug delivery: Overcoming blood-brain barrier to treat neurodegenerative diseases. Journal of Controlled Release *235*, 34–47.

Schapira, A.H., and Jenner, P. (2011). Etiology and pathogenesis of Parkinson's disease. Movement Disorders *26*, 1049–1055.

Schlageter, K.E., Molnar, P., Lapin, G.D., and Groothuis, D.R. (1999). Microvessel organization and structure in experimental brain tumors: Microvessel populations with distinctive structural and functional properties. Microvascular Research *58*, 312–328.

Sharma, R., Kim, S.Y., Sharma, A., Zhang, Z., Kambhampati, S.P., Kannan, S., and Kannan, R.M. (2017). Activated Microglia Targeting Dendrimer-Minocycline Conjugate as Therapeutics for Neuroinflammation. Bioconjugate Chemistry *28*, 2874–2886.

Singhal, A., Morris, V.B., Labhasetwar, V., and Ghorpade, A. (2013). Nanoparticle-mediated catalase delivery protects human neurons from oxidative stress. Cell Death and Disease *4*.

Smith, G.P., and Petrenko, V.A. (1997). Phage display. Chemical Reviews *97*, 391–410.

Spliet, W.G.M., Aronica, E., Ramkema, M., Aten, J., and Troost, D. (2003). Increased expression of connective tissue growth factor in amyotrophic lateral sclerosis human spinal cord. Acta Neuropathologica *106*, 449–457.

Stupp, R., Mason, W.P., Van Den Bent, M.J., Weller, M., Fisher, B., Taphoorn, M.J.B., Belanger, K., Brandes, A.A., Marosi, C., Bogdahn, U., et al. (2005). Radiotherapy plus concomitant and adjuvant temozolomide for glioblastoma. New England Journal of Medicine *352*, 987–996.

Stylianopoulos, T., and Jain, R.K. (2015). Design considerations for nanotherapeutics in oncology. Nanomedicine: Nanotechnology, Biology, and Medicine *11*, 1893–1907.

Sugahara, K.N., Teesalu, T., Karmali, P.P., Kotamraju, V.R., Agemy, L., Girard, O.M., Hanahan, D., Mattrey, R.F., and Ruoslahti, E. (2009). Tissue-Penetrating Delivery of Compounds and Nanoparticles into Tumors. Cancer Cell *16*, 510–520.

Suk, J.S., Xu, Q., Kim, N., Hanes, J., and Ensign, L.M. (2016). PEGylation as a strategy for improving nanoparticle-based drug and gene delivery. Advanced Drug Delivery Reviews *99*, 28–51.

Sukhanova, A., Bozrova, S., Sokolov, P., Berestovoy, M., Karaulov, A., and Nabiev, I. (2018). Dependence of Nanoparticle Toxicity on Their Physical and Chemical Properties. Nanoscale Research Letters *13*.

Tan, Y., Tian, T., Liu, W., Zhu, Z., and J. Yang, C. (2016). Advance in phage display technology for bioanalysis. Biotechnology Journal *11*, 732–745.

Tan, Y., Tian, T., Liu, W., Zhu, Z., and J. Yang, C. (2016). Advance in phage display technology for bioanalysis. Biotechnology Journal *11*, 732–745.

Tang, M., Taghibiglou, C., and Liu, J. (2017). The Mechanisms of Action of Curcumin in Alzheimer's Disease. Journal of Alzheimer's Disease *58*, 1003–1016.

Tang, X.N., and Yenari, M.A. (2010). Hypothermia as a cytoprotective strategy in ischemic tissue injury. Ageing Research Reviews *9*, 61–68.

Teesalu, T., Sugahara, K.N., Kotamraju, V.R., and Ruoslahti, E. (2009). C-end rule peptides mediate neuropilin-1-dependent cell, vascular, and tissue penetration. Proceedings of the National Academy of Sciences of the United States of America *106*, 16157–16162.

Teesalu, T., Sugahara, K.N., and Ruoslahti, E. (2012). Mapping of vascular ZIP codes by phage display. In Methods in Enzymology, (Academic Press Inc.), pp. 35–56.

Van Tellingen, O., Yetkin-Arik, B., De Gooijer, M.C., Wesseling, P., Wurdinger, T., and De Vries, H.E. (2015). Overcoming the blood-brain tumor barrier for effective glioblastoma treatment. Drug Resistance Updates *19*, 1–12.

Tentler, J.J., Tan, A.C., Weekes, C.D., Jimeno, A., Leong, S., Pitts, T.M., Arcaroli, J.J., Messersmith, W.A., and Eckhardt, S.G. (2012). Patient-derived tumour xenografts as models for oncology drug development. Nature Reviews Clinical Oncology *9*, 338–350.

Thiruchelvam, M., Richfield, E.K., Baggs, R.B., Tank, A.W., and Cory-Slechta, D.A. (2000). The nigrostriatal dopaminergic system as a preferential target of repeated exposures to combined paraquat and maneb: Implications for Parkinson's disease. Journal of Neuroscience *20*, 9207–9214.

Ueberham, U., Ueberham, E., Gruschka, H., and Arendt, T. (2003). Connective tissue growth factor in Alzheimer's disease. Neuroscience *116*, 1–6.

Urich, E., Schmucki, R., Ruderisch, N., Kitas, E., Certa, U., Jacobsen, H., Schweitzer, C., Bergadano, A., Ebeling, M., Loetscher, H., et al. (2015). Cargo Delivery into the Brain by in vivo identified Transport Peptides. Scientific Reports *5*.

Ventola, C.L. (2017). Progress in nanomedicine: Approved and investigational nanodrugs. P and T *42*, 742–755.

Vieira, D.B., and Gamarra, L.F. (2016). Getting into the brain: Liposome-based strategies for effective drug delivery across the blood–brain barrier. International Journal of Nanomedicine *11*, 5381–5414.

Wilhelm, S., Tavares, A.J., Dai, Q., Ohta, S., Audet, J., Dvorak, H.F., and Chan, W.C.W. (2016). Analysis of nanoparticle delivery to tumours. Nature Reviews Materials *1*.

De Witt Hamer, P.C., Van Tilborg, A.A.G., Eijk, P.P., Sminia, P., Troost, D., Van Noorden, C.J.F., Ylstra, B., and Leenstra, S. (2008). The genomic profile of human malignant glioma is altered early in primary cell culture and preserved in spheroids. Oncogene *27*, 2091–2096.

Wolburg, H., Noell, S., Mack, A., Wolburg-Buchholz, K., and Fallier-Becker, P. (2009). Brain endothelial cells and the glio-vascular complex. Cell and Tissue Research *335*, 75–96.

Wolburg, H., Noell, S., Fallier-Becker, P., MacK, A.F., and Wolburg-Buchholz, K. (2012). The disturbed blood-brain barrier in human glioblastoma. Molecular Aspects of Medicine *33*, 579–589.

Xu, Q., and Lam, K.S. (2003). Protein and Chemical Microarrays – Powerful Tools for Proteomics. Journal of Biomedicine and Biotechnology *2003*, 257–266.

Yang, L., and Zhang, Y. (2017). Tumor-associated macrophages: from basic research to clinical application. Journal of Hematology & Oncology *10*, 58.

Yenugonda, V., Nomura, N., Kouznetsova, V., Tsigelny, I., Fogal, V., Nurmemmedov, E., Kesari, S., and Babic, I. (2017). A novel small molecule inhibitor of p32 mitochondrial protein overexpressed in glioma. Journal of Translational Medicine *15*.

Yip, S., Miao, J., Cahill, D.P., Iafrate, A.J., Aldape, K., Nutt, C.L., and Louis, D.N. (2009). MSH6 mutations arise in glioblastomas during temozolomide therapy and mediate temozolomide resistance. Clinical Cancer Research *15*, 4622–4629.

Zarebkohan, A., Najafi, F., Moghimi, H.R., Hemmati, M., Deevband, M.R., and Kazemi, B. (2015). Synthesis and characterization of a PAMAM dendrimer nanocarrier functionalized by SRL peptide for targeted gene delivery to the brain. European Journal of Pharmaceutical Sciences *78*, 19–30.

Zhang, C.C., Li, S.H., Zhang, C.F., and Liu, Y. (2016). Size Switchable Supramolecular Nanoparticle Based on Azobenzene Derivative within Anionic Pillar[5]arene. Scientific Reports *6*.

Zhang, L., Gu, F.X., Chan, J.M., Wang, A.Z., Langer, R.S., and Farokhzad, O.C. (2008). Nanoparticles in medicine: Therapeutic applications and developments. Clinical Pharmacology and Therapeutics *83*, 761–769.

Zhang, X.F., Liu, Z.G., Shen, W., and Gurunathan, S. (2016). Silver nanoparticles: Synthesis, characterization, properties, applications, and therapeutic approaches. International Journal of Molecular Sciences *17*.

Zhao, Z., Nelson, A.R., Betsholtz, C., and Zlokovic, B.V. (2015). Establishment and Dysfunction of the Blood-Brain Barrier. Cell *163*, 1064–1078.

Zlokovic, B.V. (2011). Neurovascular pathways to neurodegeneration in Alzheimer's disease and other disorders. Nature Reviews Neuroscience *12*.

ACKNOWLEDGEMENTS

PUBLICATIONS

CURRICULUM VITAE

Name: Kadri Toome
Date of birth: September 29, 1984
Citizenship: Estonian
Contact: Cancer Biology Group, Institute of Biomedicine and
                 Translational Medicine,
                 University of Tartu, Ravila 14b 50411, Tartu
Phone: +372 737 4268
E-mail: kadri.toome@gmail.com

Education:
1991–2003   Kadrina Secondary School
2003–2006   University of Tartu, Faculty of Science and Technology, Gene
                technology, BSc
2006–2008   University of Tartu, Faculty of Science and Technology,
                Biotechnology and biomedicine, MSc
2012–   University of Tartu, Faculty of Medicine, PhD

Professional employment:
2007–2008   Asper Biotech Ltd., Laboratory specialist
2008–2014   Asper Biotech Ltd., Project manager
2012–2019   University of Tartu, Cancer Biology Group, Institute of
                Biomedicine and Translational Medicine, Laboratory specialist
2016–   Tartu University Hospital, United Laboratories,
                Clinical Genetics Center, Laboratory specialist

Professional organization:
Member of the Estonian Society of Medical Genetics

Special courses:
2014   EMBO Young Investigator PhD Course, Heidelberg, Germany

List of publications:
1. Säälik P, Lingasamy P, **Toome K**, Mastandrea I, Rousso-Noori L, Tobi A, Simón-Gracia L, Hunt H, Paiste P, Kotamraju VR, Bergers G, Asser T, Rätsep T, Ruoslahti E, Bjerkvig R, Friedmann-Morvinski D, Teesalu T. (2019) Peptide-guided nanoparticles for glioblastoma targeting., *J Control Release*
2. Mann AP, Scodeller P, Hussain S, Braun GB, Mölder T, **Toome K**, Ambasudhan R, Teesalu T, Lipton SA, Ruoslahti E. (2017) Identification of a peptide recognizing cerebrovascular changes in mouse models of Alzheimer's disease. *Nat Commun*, 8, 1403

3. **Toome K**, Willmore AA, Paiste P, Tobi A, Sugahara KN, Kirsimäe K, Ruoslahti E, Braun GB, Teesalu T. (2017) Ratiometric in vivo auditioning of targeted silver nanoparticles., *Nanoscale*, 9, 10094–10100.

4. Willmore AM, Simón-Gracia L, **Toome K**, Paiste P, Kotamraju VR, Mölder T, Sugahara KN, Ruoslahti E, Braun GB, Teesalu T. (2016) Targeted silver nanoparticles for ratiometric cell phenotyping. *Nanoscale*, 8:9096–9101.

5. Dymerska, D., Kurzawski, G., Suchy, J., Roomere, H., **Toome, K**., Metspalu, A., Janavičius, R., Elsakov, P., Irmejs, A., Berzina, D., Miklaševičs, E., Gardovskis, J., Rebane, E., Kelve, M. et al. (2014). Lynch syndrome mutations shared by the Baltic States and Poland. *Clinical Genetics*, 86 (2), 190−193.

6. Scheler O, Kaplinski L, Glynn B, Palta P, Parkel S, **Toome K**, Maher M, Barry T, Remm M, Kurg A. (2011) Detection of NASBA amplified bacterial tmRNA molecules on SLICSel designed microarray probes. *BMC Biotechnol*, 11, 17.

7. Kaplinski L, Scheler O, Parkel S, Palta P, **Toome K**, Kurg A, Remm M. (2010) Detection of tmRNA molecules on microarrays at low temperatures using helper oligonucleotides. *BMC Biotechnol*, 10, 34.

8. Scheler O, Glynn B, Parkel S, Palta P, **Toome K**, Kaplinski L, Remm M, Maher M, Kurg A. (2009) Fluorescent labeling of NASBA amplified tmRNA molecules for microarray applications. *BMC Biotechnol*, 9, 45.

ELULOOKIRJELDUS

Nimi: Kadri Toome
Sünniaeg: 29. september 1984
Kodakondsus: Eesti
Kontaktandmed: Vähibioloogia töögrupp, Bio- ja Siirdemeditsiini instituut, Tartu Ülikool, Ravila 14b 50411, Tartu
Telefon: +372 737 4268
E-mail: kadri.toome@gmail.com

Hariduskäik:
1991–2003   Kadrina Keskkool
2003–2006   Tartu Ülikool, Geenitehnoloogia, BSc
2006–2008   Tartu Ülikool, Biotehnoloogia ja biomeditsiin, MSc
2012–   Tartu Ülikool, arstiteaduse doktoriõpe

Teenistuskäik:
2007–2008   Asper Biotech Ltd., Laborispetsialist
2008–2014   Asper Biotech Ltd., Projektijuht
2012–2019   University of Tartu, Laborispetsialist
2016–   Tartu Ülikooli Kliinikum, Ühendlabor, Kliinilise geneetika keskus, Laborispetsialist

Erialaorganisatsioonid:
Eesti Meditsiinigeneetika Seltsi liige

Erialane enesetäiendus:
2014   *EMBO Young Investigator PhD Course*, Heidelberg, Saksamaa

List of publications:
1. Säälik P, Lingasamy P, **Toome K**, Mastandrea I, Rousso-Noori L, Tobi A, Simón-Gracia L, Hunt H, Paiste P, Kotamraju VR, Bergers G, Asser T, Rätsep T, Ruoslahti E, Bjerkvig R, Friedmann-Morvinski D, Teesalu T. (2019) Peptide-guided nanoparticles for glioblastoma targeting., *J Control Release*
2. Mann AP, Scodeller P, Hussain S, Braun GB, Mölder T, **Toome K**, Ambasudhan R, Teesalu T, Lipton SA, Ruoslahti E. (2017) Identification of a peptide recognizing cerebrovascular changes in mouse models of Alzheimer's disease., *Nat Commun*, 8, 1403
3. **Toome K**, Willmore AA, Paiste P, Tobi A, Sugahara KN, Kirsimäe K, Ruoslahti E, Braun GB, Teesalu T. (2017) Ratiometric in vivo auditioning of targeted silver nanoparticles., *Nanoscale*, 9, 10094–10100.
4. Willmore AM, Simón-Gracia L, **Toome K**, Paiste P, Kotamraju VR, Mölder T, Sugahara KN, Ruoslahti E, Braun GB, Teesalu T. (2016)

Targeted silver nanoparticles for ratiometric cell phenotyping., *Nanoscale*, 8:9096–9101.

5. Dymerska, D., Kurzawski, G., Suchy, J., Roomere, H., **Toome, K**., Metspalu, A., Janavičius, R., Elsakov, P., Irmejs, A., Berzina, D., Miklaševičs, E., Gardovskis, J., Rebane, E., Kelve, M. et al. (2014). Lynch syndrome mutations shared by the Baltic States and Poland. *Clinical Genetics*, 86 (2), 190−193.

6. Scheler O, Kaplinski L, Glynn B, Palta P, Parkel S, **Toome K**, Maher M, Barry T, Remm M, Kurg A. (2011) Detection of NASBA amplified bacterial tmRNA molecules on SLICSel designed microarray probes. *BMC Biotechnol*, 11, 17.

7. Kaplinski L, Scheler O, Parkel S, Palta P, **Toome K**, Kurg A, Remm M. (2010) Detection of tmRNA molecules on microarrays at low temperatures using helper oligonucleotides. *BMC Biotechnol*, 10, 34.

8. Scheler O, Glynn B, Parkel S, Palta P, **Toome K**, Kaplinski L, Remm M, Maher M, Kurg A. (2009) Fluorescent labeling of NASBA amplified tmRNA molecules for microarray applications. *BMC Biotechnol*, 9, 45.

DISSERTATIONES MEDICINAE
UNIVERSITATIS TARTUENSIS

1. **Heidi-Ingrid Maaroos**. The natural course of gastric ulcer in connection with chronic gastritis and *Helicobacter pylori*. Tartu, 1991.
2. **Mihkel Zilmer**. Na-pump in normal and tumorous brain tissues: Structural, functional and tumorigenesis aspects. Tartu, 1991.
3. **Eero Vasar**. Role of cholecystokinin receptors in the regulation of behaviour and in the action of haloperidol and diazepam. Tartu, 1992.
4. **Tiina Talvik**. Hypoxic-ischaemic brain damage in neonates (clinical, biochemical and brain computed tomographical investigation). Tartu, 1992.
5. **Ants Peetsalu**. Vagotomy in duodenal ulcer disease: A study of gastric acidity, serum pepsinogen I, gastric mucosal histology and *Helicobacter pylori*. Tartu, 1992.
6. **Marika Mikelsaar**. Evaluation of the gastrointestinal microbial ecosystem in health and disease. Tartu, 1992.
7. **Hele Everaus**. Immuno-hormonal interactions in chronic lymphocytic leukaemia and multiple myeloma. Tartu, 1993.
8. **Ruth Mikelsaar**. Etiological factors of diseases in genetically consulted children and newborn screening: dissertation for the commencement of the degree of doctor of medical sciences. Tartu, 1993.
9. **Agu Tamm**. On metabolic action of intestinal microflora: clinical aspects. Tartu, 1993.
10. **Katrin Gross**. Multiple sclerosis in South-Estonia (epidemiological and computed tomographical investigations). Tartu, 1993.
11. **Oivi Uibo**. Childhood coeliac disease in Estonia: occurrence, screening, diagnosis and clinical characterization. Tartu, 1994.
12. **Viiu Tuulik**. The functional disorders of central nervous system of chemistry workers. Tartu, 1994.
13. **Margus Viigimaa**. Primary haemostasis, antiaggregative and anticoagulant treatment of acute myocardial infarction. Tartu, 1994.
14. **Rein Kolk**. Atrial versus ventricular pacing in patients with sick sinus syndrome. Tartu, 1994.
15. **Toomas Podar**. Incidence of childhood onset type 1 diabetes mellitus in Estonia. Tartu, 1994.
16. **Kiira Subi**. The laboratory surveillance of the acute respiratory viral infections in Estonia. Tartu, 1995.
17. **Irja Lutsar**. Infections of the central nervous system in children (epidemiologic, diagnostic and therapeutic aspects, long term outcome). Tartu, 1995.
18. **Aavo Lang**. The role of dopamine, 5-hydroxytryptamine, sigma and NMDA receptors in the action of antipsychotic drugs. Tartu, 1995.
19. **Andrus Arak**. Factors influencing the survival of patients after radical surgery for gastric cancer. Tartu, 1996.

20. **Tõnis Karki**. Quantitative composition of the human lactoflora and method for its examination. Tartu, 1996.
21. **Reet Mändar**. Vaginal microflora during pregnancy and its transmission to newborn. Tartu, 1996.
22. **Triin Remmel**. Primary biliary cirrhosis in Estonia: epidemiology, clinical characterization and prognostication of the course of the disease. Tartu, 1996.
23. **Toomas Kivastik**. Mechanisms of drug addiction: focus on positive reinforcing properties of morphine. Tartu, 1996.
24. **Paavo Pokk**. Stress due to sleep deprivation: focus on $GABA_A$ receptor-chloride ionophore complex. Tartu, 1996.
25. **Kristina Allikmets**. Renin system activity in essential hypertension. Associations with atherothrombogenic cardiovascular risk factors and with the efficacy of calcium antagonist treatment. Tartu, 1996.
26. **Triin Parik**. Oxidative stress in essential hypertension: Associations with metabolic disturbances and the effects of calcium antagonist treatment. Tartu, 1996.
27. **Svetlana Päi**. Factors promoting heterogeneity of the course of rheumatoid arthritis. Tartu, 1997.
28. **Maarike Sallo**. Studies on habitual physical activity and aerobic fitness in 4 to 10 years old children. Tartu, 1997.
29. **Paul Naaber**. *Clostridium difficile* infection and intestinal microbial ecology. Tartu, 1997.
30. **Rein Pähkla**. Studies in pinoline pharmacology. Tartu, 1997.
31. **Andrus Juhan Voitk**. Outpatient laparoscopic cholecystectomy. Tartu, 1997.
32. **Joel Starkopf**. Oxidative stress and ischaemia-reperfusion of the heart. Tartu, 1997.
33. **Janika Kõrv**. Incidence, case-fatality and outcome of stroke. Tartu, 1998.
34. **Ülla Linnamägi**. Changes in local cerebral blood flow and lipid peroxidation following lead exposure in experiment. Tartu, 1998.
35. **Ave Minajeva**. Sarcoplasmic reticulum function: comparison of atrial and ventricular myocardium. Tartu, 1998.
36. **Oleg Milenin**. Reconstruction of cervical part of esophagus by revascularised ileal autografts in dogs. A new complex multistage method. Tartu, 1998.
37. **Sergei Pakriev**. Prevalence of depression, harmful use of alcohol and alcohol dependence among rural population in Udmurtia. Tartu, 1998.
38. **Allen Kaasik**. Thyroid hormone control over β-adrenergic signalling system in rat atria. Tartu, 1998.
39. **Vallo Matto**. Pharmacological studies on anxiogenic and antiaggressive properties of antidepressants. Tartu, 1998.
40. **Maire Vasar**. Allergic diseases and bronchial hyperreactivity in Estonian children in relation to environmental influences. Tartu, 1998.
41. **Kaja Julge**. Humoral immune responses to allergens in early childhood. Tartu, 1998.

42. **Heli Grünberg**. The cardiovascular risk of Estonian schoolchildren. A cross-sectional study of 9-, 12- and 15-year-old children. Tartu, 1998.
43. **Epp Sepp**. Formation of intestinal microbial ecosystem in children. Tartu, 1998.
44. **Mai Ots**. Characteristics of the progression of human and experimental glomerulopathies. Tartu, 1998.
45. **Tiina Ristimäe**. Heart rate variability in patients with coronary artery disease. Tartu, 1998.
46. **Leho Kõiv**. Reaction of the sympatho-adrenal and hypothalamo-pituitary-adrenocortical system in the acute stage of head injury. Tartu, 1998.
47. **Bela Adojaan**. Immune and genetic factors of childhood onset IDDM in Estonia. An epidemiological study. Tartu, 1999.
48. **Jakov Shlik**. Psychophysiological effects of cholecystokinin in humans. Tartu, 1999.
49. **Kai Kisand**. Autoantibodies against dehydrogenases of α-ketoacids. Tartu, 1999.
50. **Toomas Marandi**. Drug treatment of depression in Estonia. Tartu, 1999.
51. **Ants Kask**. Behavioural studies on neuropeptide Y. Tartu, 1999.
52. **Ello-Rahel Karelson**. Modulation of adenylate cyclase activity in the rat hippocampus by neuropeptide galanin and its chimeric analogs. Tartu, 1999.
53. **Tanel Laisaar**. Treatment of pleural empyema — special reference to intrapleural therapy with streptokinase and surgical treatment modalities. Tartu, 1999.
54. **Eve Pihl**. Cardiovascular risk factors in middle-aged former athletes. Tartu, 1999.
55. **Katrin Õunap**. Phenylketonuria in Estonia: incidence, newborn screening, diagnosis, clinical characterization and genotype/phenotype correlation. Tartu, 1999.
56. **Siiri Kõljalg**. *Acinetobacter* – an important nosocomial pathogen. Tartu, 1999.
57. **Helle Karro**. Reproductive health and pregnancy outcome in Estonia: association with different factors. Tartu, 1999.
58. **Heili Varendi**. Behavioral effects observed in human newborns during exposure to naturally occurring odors. Tartu, 1999.
59. **Anneli Beilmann**. Epidemiology of epilepsy in children and adolescents in Estonia. Prevalence, incidence, and clinical characteristics. Tartu, 1999.
60. **Vallo Volke**. Pharmacological and biochemical studies on nitric oxide in the regulation of behaviour. Tartu, 1999.
61. **Pilvi Ilves**. Hypoxic-ischaemic encephalopathy in asphyxiated term infants. A prospective clinical, biochemical, ultrasonographical study. Tartu, 1999.
62. **Anti Kalda**. Oxygen-glucose deprivation-induced neuronal death and its pharmacological prevention in cerebellar granule cells. Tartu, 1999.
63. **Eve-Irene Lepist**. Oral peptide prodrugs – studies on stability and absorption. Tartu, 2000.

64. **Jana Kivastik**. Lung function in Estonian schoolchildren: relationship with anthropometric indices and respiratory symptomas, reference values for dynamic spirometry. Tartu, 2000.

65. **Karin Kull**. Inflammatory bowel disease: an immunogenetic study. Tartu, 2000.

66. **Kaire Innos**. Epidemiological resources in Estonia: data sources, their quality and feasibility of cohort studies. Tartu, 2000.

67. **Tamara Vorobjova**. Immune response to *Helicobacter pylori* and its association with dynamics of chronic gastritis and epithelial cell turnover in antrum and corpus. Tartu, 2001.

68. **Ruth Kalda**. Structure and outcome of family practice quality in the changing health care system of Estonia. Tartu, 2001.

69. **Annika Krüüner**. *Mycobacterium tuberculosis* – spread and drug resistance in Estonia. Tartu, 2001.

70. **Marlit Veldi**. Obstructive Sleep Apnoea: Computerized Endopharyngeal Myotonometry of the Soft Palate and Lingual Musculature. Tartu, 2001.

71. **Anneli Uusküla**. Epidemiology of sexually transmitted diseases in Estonia in 1990–2000. Tartu, 2001.

72. **Ade Kallas**. Characterization of antibodies to coagulation factor VIII. Tartu, 2002.

73. **Heidi Annuk**. Selection of medicinal plants and intestinal lactobacilli as antimicrobil components for functional foods. Tartu, 2002.

74. **Aet Lukmann**. Early rehabilitation of patients with ischaemic heart disease after surgical revascularization of the myocardium: assessment of health-related quality of life, cardiopulmonary reserve and oxidative stress. A clinical study. Tartu, 2002.

75. **Maigi Eisen**. Pathogenesis of Contact Dermatitis: participation of Oxidative Stress. A clinical – biochemical study. Tartu, 2002.

76. **Piret Hussar**. Histology of the post-traumatic bone repair in rats. Elaboration and use of a new standardized experimental model – bicortical perforation of tibia compared to internal fracture and resection osteotomy. Tartu, 2002.

77. **Tõnu Rätsep**. Aneurysmal subarachnoid haemorrhage: Noninvasive monitoring of cerebral haemodynamics. Tartu, 2002.

78. **Marju Herodes**. Quality of life of people with epilepsy in Estonia. Tartu, 2003.

79. **Katre Maasalu**. Changes in bone quality due to age and genetic disorders and their clinical expressions in Estonia. Tartu, 2003.

80. **Toomas Sillakivi**. Perforated peptic ulcer in Estonia: epidemiology, risk factors and relations with *Helicobacter pylori*. Tartu, 2003.

81. **Leena Puksa**. Late responses in motor nerve conduction studies. F and A waves in normal subjects and patients with neuropathies. Tartu, 2003.

82. **Krista Lõivukene**. *Helicobacter pylori* in gastric microbial ecology and its antimicrobial susceptibility pattern. Tartu, 2003.

83. **Helgi Kolk**. Dyspepsia and *Helicobacter pylori* infection: the diagnostic value of symptoms, treatment and follow-up of patients referred for upper gastrointestinal endoscopy by family physicians. Tartu, 2003.

84. **Helena Soomer**. Validation of identification and age estimation methods in forensic odontology. Tartu, 2003.

85. **Kersti Oselin**. Studies on the human MDR1, MRP1, and MRP2 ABC transporters: functional relevance of the genetic polymorphisms in the *MDR1* and *MRP1* gene. Tartu, 2003.

86. **Jaan Soplepmann**. Peptic ulcer haemorrhage in Estonia: epidemiology, prognostic factors, treatment and outcome. Tartu, 2003.

87. **Margot Peetsalu**. Long-term follow-up after vagotomy in duodenal ulcer disease: recurrent ulcer, changes in the function, morphology and *Helicobacter pylori* colonisation of the gastric mucosa. Tartu, 2003.

88. **Kersti Klaamas**. Humoral immune response to *Helicobacter pylori* a study of host-dependent and microbial factors. Tartu, 2003.

89. **Pille Taba**. Epidemiology of Parkinson's disease in Tartu, Estonia. Prevalence, incidence, clinical characteristics, and pharmacoepidemiology. Tartu, 2003.

90. **Alar Veraksitš**. Characterization of behavioural and biochemical phenotype of cholecystokinin-2 receptor deficient mice: changes in the function of the dopamine and endopioidergic system. Tartu, 2003.

91. **Ingrid Kalev**. CC-chemokine receptor 5 (CCR5) gene polymorphism in Estonians and in patients with Type I and Type II diabetes mellitus. Tartu, 2003.

92. **Lumme Kadaja**. Molecular approach to the regulation of mitochondrial function in oxidative muscle cells. Tartu, 2003.

93. **Aive Liigant**. Epidemiology of primary central nervous system tumours in Estonia from 1986 to 1996. Clinical characteristics, incidence, survival and prognostic factors. Tartu, 2004.

94. **Andres, Kulla**. Molecular characteristics of mesenchymal stroma in human astrocytic gliomas. Tartu, 2004.

95. **Mari Järvelaid**. Health damaging risk behaviours in adolescence. Tartu, 2004.

96. **Ülle Pechter**. Progression prevention strategies in chronic renal failure and hypertension. An experimental and clinical study. Tartu, 2004.

97. **Gunnar Tasa**. Polymorphic glutathione S-transferases – biology and role in modifying genetic susceptibility to senile cataract and primary open angle glaucoma. Tartu, 2004.

98. **Tuuli Käämbre**. Intracellular energetic unit: structural and functional aspects. Tartu, 2004.

99. **Vitali Vassiljev**. Influence of nitric oxide syntase inhibitors on the effects of ethanol after acute and chronic ethanol administration and withdrawal. Tartu, 2004.

100. **Aune Rehema**. Assessment of nonhaem ferrous iron and glutathione redox ratio as markers of pathogeneticity of oxidative stress in different clinical groups. Tartu, 2004.

101. **Evelin Seppet**. Interaction of mitochondria and ATPases in oxidative muscle cells in normal and pathological conditions. Tartu, 2004.

102. **Eduard Maron**. Serotonin function in panic disorder: from clinical experiments to brain imaging and genetics. Tartu, 2004.

103. **Marje Oona**. *Helicobacter pylori* infection in children: epidemiological and therapeutic aspects. Tartu, 2004.

104. **Kersti Kokk**. Regulation of active and passive molecular transport in the testis. Tartu, 2005.

105. **Vladimir Järv**. Cross-sectional imaging for pretreatment evaluation and follow-up of pelvic malignant tumours. Tartu, 2005.

106. **Andre Õun**. Epidemiology of adult epilepsy in Tartu, Estonia. Incidence, prevalence and medical treatment. Tartu, 2005.

107. **Piibe Muda**. Homocysteine and hypertension: associations between homocysteine and essential hypertension in treated and untreated hypertensive patients with and without coronary artery disease. Tartu, 2005.

108. **Külli Kingo**. The interleukin-10 family cytokines gene polymorphisms in plaque psoriasis. Tartu, 2005.

109. **Mati Merila**. Anatomy and clinical relevance of the glenohumeral joint capsule and ligaments. Tartu, 2005.

110. **Epp Songisepp**. Evaluation of technological and functional properties of the new probiotic *Lactobacillus fermentum* ME-3. Tartu, 2005.

111. **Tiia Ainla**. Acute myocardial infarction in Estonia: clinical characteristics, management and outcome. Tartu, 2005.

112. **Andres Sell**. Determining the minimum local anaesthetic requirements for hip replacement surgery under spinal anaesthesia – a study employing a spinal catheter. Tartu, 2005.

113. **Tiia Tamme**. Epidemiology of odontogenic tumours in Estonia. Pathogenesis and clinical behaviour of ameloblastoma. Tartu, 2005.

114. **Triine Annus**. Allergy in Estonian schoolchildren: time trends and characteristics. Tartu, 2005.

115. **Tiia Voor**. Microorganisms in infancy and development of allergy: comparison of Estonian and Swedish children. Tartu, 2005.

116. **Priit Kasenõmm**. Indicators for tonsillectomy in adults with recurrent tonsillitis – clinical, microbiological and pathomorphological investigations. Tartu, 2005.

117. **Eva Zusinaite**. Hepatitis C virus: genotype identification and interactions between viral proteases. Tartu, 2005.

118. **Piret Kõll**. Oral lactoflora in chronic periodontitis and periodontal health. Tartu, 2006.

119. **Tiina Stelmach**. Epidemiology of cerebral palsy and unfavourable neurodevelopmental outcome in child population of Tartu city and county, Estonia Prevalence, clinical features and risk factors. Tartu, 2006.

120. **Katrin Pudersell**. Tropane alkaloid production and riboflavine excretion in the field and tissue cultures of henbane (*Hyoscyamus niger* L.). Tartu, 2006.
121. **Külli Jaako**. Studies on the role of neurogenesis in brain plasticity. Tartu, 2006.
122. **Aare Märtson**. Lower limb lengthening: experimental studies of bone regeneration and long-term clinical results. Tartu, 2006.
123. **Heli Tähepõld**. Patient consultation in family medicine. Tartu, 2006.
124. **Stanislav Liskmann**. Peri-implant disease: pathogenesis, diagnosis and treatment in view of both inflammation and oxidative stress profiling. Tartu, 2006.
125. **Ruth Rudissaar**. Neuropharmacology of atypical antipsychotics and an animal model of psychosis. Tartu, 2006.
126. **Helena Andreson**. Diversity of *Helicobacter pylori* genotypes in Estonian patients with chronic inflammatory gastric diseases. Tartu, 2006.
127. **Katrin Pruus**. Mechanism of action of antidepressants: aspects of sero-toninergic system and its interaction with glutamate. Tartu, 2006.
128. **Priit Põder**. Clinical and experimental investigation: relationship of ischaemia/reperfusion injury with oxidative stress in abdominal aortic aneurysm repair and in extracranial brain artery endarterectomy and possi-bilities of protection against ischaemia using a glutathione analogue in a rat model of global brain ischaemia. Tartu, 2006.
129. **Marika Tammaru**. Patient-reported outcome measurement in rheumatoid arthritis. Tartu, 2006.
130. **Tiia Reimand**. Down syndrome in Estonia. Tartu, 2006.
131. **Diva Eensoo**. Risk-taking in traffic and Markers of Risk-Taking Beha-viour in Schoolchildren and Car Drivers. Tartu, 2007.
132. **Riina Vibo**. The third stroke registry in Tartu, Estonia from 2001 to 2003: incidence, case-fatality, risk factors and long-term outcome. Tartu, 2007.
133. **Chris Pruunsild**. Juvenile idiopathic arthritis in children in Estonia. Tartu, 2007.
134. **Eve Õiglane-Šlik**. Angelman and Prader-Willi syndromes in Estonia. Tartu, 2007.
135. **Kadri Haller**. Antibodies to follicle stimulating hormone. Significance in female infertility. Tartu, 2007.
136. **Pille Ööpik**. Management of depression in family medicine. Tartu, 2007.
137. **Jaak Kals**. Endothelial function and arterial stiffness in patients with atherosclerosis and in healthy subjects. Tartu, 2007.
138. **Priit Kampus**. Impact of inflammation, oxidative stress and age on arterial stiffness and carotid artery intima-media thickness. Tartu, 2007.
139. **Margus Punab**. Male fertility and its risk factors in Estonia. Tartu, 2007.
140. **Alar Toom**. Heterotopic ossification after total hip arthroplasty: clinical and pathogenetic investigation. Tartu, 2007.

141. **Lea Pehme**. Epidemiology of tuberculosis in Estonia 1991–2003 with special regard to extrapulmonary tuberculosis and delay in diagnosis of pulmonary tuberculosis. Tartu, 2007.

142. **Juri Karjagin**. The pharmacokinetics of metronidazole and meropenem in septic shock. Tartu, 2007.

143. **Inga Talvik**. Inflicted traumatic brain injury shaken baby syndrome in Estonia – epidemiology and outcome. Tartu, 2007.

144. **Tarvo Rajasalu**. Autoimmune diabetes: an immunological study of type 1 diabetes in humans and in a model of experimental diabetes (in RIP-B7.1 mice). Tartu, 2007.

145. **Inga Karu**. Ischaemia-reperfusion injury of the heart during coronary surgery: a clinical study investigating the effect of hyperoxia. Tartu, 2007.

146. **Peeter Padrik**. Renal cell carcinoma: Changes in natural history and treatment of metastatic disease. Tartu, 2007.

147. **Neve Vendt**. Iron deficiency and iron deficiency anaemia in infants aged 9 to 12 months in Estonia. Tartu, 2008.

148. **Lenne-Triin Heidmets**. The effects of neurotoxins on brain plasticity: focus on neural Cell Adhesion Molecule. Tartu, 2008.

149. **Paul Korrovits**. Asymptomatic inflammatory prostatitis: prevalence, etiological factors, diagnostic tools. Tartu, 2008.

150. **Annika Reintam**. Gastrointestinal failure in intensive care patients. Tartu, 2008.

151. **Kristiina Roots**. Cationic regulation of Na-pump in the normal, Alzheimer's and CCK_2 receptor-deficient brain. Tartu, 2008.

152. **Helen Puusepp**. The genetic causes of mental retardation in Estonia: fragile X syndrome and creatine transporter defect. Tartu, 2009.

153. **Kristiina Rull**. Human chorionic gonadotropin beta genes and recurrent miscarriage: expression and variation study. Tartu, 2009.

154. **Margus Eimre**. Organization of energy transfer and feedback regulation in oxidative muscle cells. Tartu, 2009.

155. **Maire Link**. Transcription factors FoxP3 and AIRE: autoantibody associations. Tartu, 2009.

156. **Kai Haldre**. Sexual health and behaviour of young women in Estonia. Tartu, 2009.

157. **Kaur Liivak**. Classical form of congenital adrenal hyperplasia due to 21-hydroxylase deficiency in Estonia: incidence, genotype and phenotype with special attention to short-term growth and 24-hour blood pressure. Tartu, 2009.

158. **Kersti Ehrlich**. Antioxidative glutathione analogues (UPF peptides) – molecular design, structure-activity relationships and testing the protective properties. Tartu, 2009.

159. **Anneli Rätsep**. Type 2 diabetes care in family medicine. Tartu, 2009.

160. **Silver Türk**. Etiopathogenetic aspects of chronic prostatitis: role of mycoplasmas, coryneform bacteria and oxidative stress. Tartu, 2009.

161. **Kaire Heilman**. Risk markers for cardiovascular disease and low bone mineral density in children with type 1 diabetes. Tartu, 2009.
162. **Kristi Rüütel**. HIV-epidemic in Estonia: injecting drug use and quality of life of people living with HIV. Tartu, 2009.
163. **Triin Eller**. Immune markers in major depression and in antidepressive treatment. Tartu, 2009.
164. **Siim Suutre**. The role of TGF-β isoforms and osteoprogenitor cells in the pathogenesis of heterotopic ossification. An experimental and clinical study of hip arthroplasty. Tartu, 2010.
165. **Kai Kliiman**. Highly drug-resistant tuberculosis in Estonia: Risk factors and predictors of poor treatment outcome. Tartu, 2010.
166. **Inga Villa**. Cardiovascular health-related nutrition, physical activity and fitness in Estonia. Tartu, 2010.
167. **Tõnis Org**. Molecular function of the first PHD finger domain of Auto-immune Regulator protein. Tartu, 2010.
168. **Tuuli Metsvaht**. Optimal antibacterial therapy of neonates at risk of early onset sepsis. Tartu, 2010.
169. **Jaanus Kahu**. Kidney transplantation: Studies on donor risk factors and mycophenolate mofetil. Tartu, 2010.
170. **Koit Reimand**. Autoimmunity in reproductive failure: A study on associated autoantibodies and autoantigens. Tartu, 2010.
171. **Mart Kull**. Impact of vitamin D and hypolactasia on bone mineral density: a population based study in Estonia. Tartu, 2010.
172. **Rael Laugesaar**. Stroke in children – epidemiology and risk factors. Tartu, 2010.
173. **Mark Braschinsky**. Epidemiology and quality of life issues of hereditary spastic paraplegia in Estonia and implemention of genetic analysis in everyday neurologic practice. Tartu, 2010.
174. **Kadri Suija**. Major depression in family medicine: associated factors, recurrence and possible intervention. Tartu, 2010.
175. **Jarno Habicht**. Health care utilisation in Estonia: socioeconomic determinants and financial burden of out-of-pocket payments. Tartu, 2010.
176. **Kristi Abram**. The prevalence and risk factors of rosacea. Subjective disease perception of rosacea patients. Tartu, 2010.
177. **Malle Kuum**. Mitochondrial and endoplasmic reticulum cation fluxes: Novel roles in cellular physiology. Tartu, 2010.
178. **Rita Teek**. The genetic causes of early onset hearing loss in Estonian children. Tartu, 2010.
179. **Daisy Volmer**. The development of community pharmacy services in Estonia – public and professional perceptions 1993–2006. Tartu, 2010.
180. **Jelena Lissitsina**. Cytogenetic causes in male infertility. Tartu, 2011.
181. **Delia Lepik**. Comparison of gunshot injuries caused from Tokarev, Makarov and Glock 19 pistols at different firing distances. Tartu, 2011.
182. **Ene-Renate Pähkla**. Factors related to the efficiency of treatment of advanced periodontitis. Tartu, 2011.

183. **Maarja Krass**. L-Arginine pathways and antidepressant action. Tartu, 2011.
184. **Taavi Lai**. Population health measures to support evidence-based health policy in Estonia. Tartu, 2011.
185. **Tiit Salum**. Similarity and difference of temperature-dependence of the brain sodium pump in normal, different neuropathological, and aberrant conditions and its possible reasons. Tartu, 2011.
186. **Tõnu Vooder**. Molecular differences and similarities between histological subtypes of non-small cell lung cancer. Tartu, 2011.
187. **Jelena Štšepetova**. The characterisation of intestinal lactic acid bacteria using bacteriological, biochemical and molecular approaches. Tartu, 2011.
188. **Radko Avi**. Natural polymorphisms and transmitted drug resistance in Estonian HIV-1 CRF06_cpx and its recombinant viruses. Tartu, 2011, 116 p.
189. **Edward Laane**. Multiparameter flow cytometry in haematological malignancies. Tartu, 2011, 152 p.
190. **Triin Jagomägi**. A study of the genetic etiology of nonsyndromic cleft lip and palate. Tartu, 2011, 158 p.
191. **Ivo Laidmäe**. Fibrin glue of fish (*Salmo salar*) origin: immunological study and development of new pharmaceutical preparation. Tartu, 2012, 150 p.
192. **Ülle Parm**. Early mucosal colonisation and its role in prediction of invasive infection in neonates at risk of early onset sepsis. Tartu, 2012, 168 p.
193. **Kaupo Teesalu**. Autoantibodies against desmin and transglutaminase 2 in celiac disease: diagnostic and functional significance. Tartu, 2012, 142 p.
194. **Maksim Zagura**. Biochemical, functional and structural profiling of arterial damage in atherosclerosis. Tartu, 2012, 162 p.
195. **Vivian Kont**. Autoimmune regulator: characterization of thymic gene regulation and promoter methylation. Tartu, 2012, 134 p.
196. **Pirje Hütt**. Functional properties, persistence, safety and efficacy of potential probiotic lactobacilli. Tartu, 2012, 246 p.
197. **Innar Tõru**. Serotonergic modulation of CCK-4- induced panic. Tartu, 2012, 132 p.
198. **Sigrid Vorobjov**. Drug use, related risk behaviour and harm reduction interventions utilization among injecting drug users in Estonia: implications for drug policy. Tartu, 2012, 120 p.
199. **Martin Serg**. Therapeutic aspects of central haemodynamics, arterial stiffness and oxidative stress in hypertension. Tartu, 2012, 156 p.
200. **Jaanika Kumm**. Molecular markers of articular tissues in early knee osteoarthritis: a population-based longitudinal study in middle-aged subjects. Tartu, 2012, 159 p.
201. **Kertu Rünkorg**. Functional changes of dopamine, endopioid and endocannabinoid systems in CCK2 receptor deficient mice. Tartu, 2012, 125 p.
202. **Mai Blöndal**. Changes in the baseline characteristics, management and outcomes of acute myocardial infarction in Estonia. Tartu, 2012, 127 p.

203. **Jana Lass**. Epidemiological and clinical aspects of medicines use in children in Estonia. Tartu, 2012, 170 p.

204. **Kai Truusalu**. Probiotic lactobacilli in experimental persistent *Salmonella* infection. Tartu, 2013, 139 p.

205. **Oksana Jagur**. Temporomandibular joint diagnostic imaging in relation to pain and bone characteristics. Long-term results of arthroscopic treatment. Tartu, 2013, 126 p.

206. **Katrin Sikk**. Manganese-ephedrone intoxication – pathogenesis of neurological damage and clinical symptomatology. Tartu, 2013, 125 p.

207. **Kai Blöndal**. Tuberculosis in Estonia with special emphasis on drug-resistant tuberculosis: Notification rate, disease recurrence and mortality. Tartu, 2013, 151 p.

208. **Marju Puurand**. Oxidative phosphorylation in different diseases of gastric mucosa. Tartu, 2013, 123 p.

209. **Aili Tagoma**. Immune activation in female infertility: Significance of autoantibodies and inflammatory mediators. Tartu, 2013, 135 p.

210. **Liis Sabre**. Epidemiology of traumatic spinal cord injury in Estonia. Brain activation in the acute phase of traumatic spinal cord injury. Tartu, 2013, 135 p.

211. **Merit Lamp**. Genetic susceptibility factors in endometriosis. Tartu, 2013, 125 p.

212. **Erik Salum**. Beneficial effects of vitamin D and angiotensin II receptor blocker on arterial damage. Tartu, 2013, 167 p.

213. **Maire Karelson**. Vitiligo: clinical aspects, quality of life and the role of melanocortin system in pathogenesis. Tartu, 2013, 153 p.

214. **Kuldar Kaljurand**. Prevalence of exfoliation syndrome in Estonia and its clinical significance. Tartu, 2013, 113 p.

215. **Raido Paasma**. Clinical study of methanol poisoning: handling large outbreaks, treatment with antidotes, and long-term outcomes. Tartu, 2013, 96 p.

216. **Anne Kleinberg**. Major depression in Estonia: prevalence, associated factors, and use of health services. Tartu, 2013, 129 p.

217. **Triin Eglit**. Obesity, impaired glucose regulation, metabolic syndrome and their associations with high-molecular-weight adiponectin levels. Tartu, 2014, 115 p.

218. **Kristo Ausmees**. Reproductive function in middle-aged males: Associations with prostate, lifestyle and couple infertility status. Tartu, 2014, 125 p.

219. **Kristi Huik**. The influence of host genetic factors on the susceptibility to HIV and HCV infections among intravenous drug users. Tartu, 2014, 144 p.

220. **Liina Tserel**. Epigenetic profiles of monocytes, monocyte-derived macrophages and dendritic cells. Tartu, 2014, 143 p.

221. **Irina Kerna**. The contribution of *ADAM12* and *CILP* genes to the development of knee osteoarthritis. Tartu, 2014, 152 p.

222. **Ingrid Liiv**. Autoimmune regulator protein interaction with DNA-dependent protein kinase and its role in apoptosis. Tartu, 2014, 143 p.
223. **Liivi Maddison**. Tissue perfusion and metabolism during intra-abdominal hypertension. Tartu, 2014, 103 p.
224. **Krista Ress**. Childhood coeliac disease in Estonia, prevalence in atopic dermatitis and immunological characterisation of coexistence. Tartu, 2014, 124 p.
225. **Kai Muru**. Prenatal screening strategies, long-term outcome of children with marked changes in maternal screening tests and the most common syndromic heart anomalies in Estonia. Tartu, 2014, 189 p.
226. **Kaja Rahu**. Morbidity and mortality among Baltic Chernobyl cleanup workers: a register-based cohort study. Tartu, 2014, 155 p.
227. **Klari Noormets**. The development of diabetes mellitus, fertility and energy metabolism disturbances in a Wfs1-deficient mouse model of Wolfram syndrome. Tartu, 2014, 132 p.
228. **Liis Toome**. Very low gestational age infants in Estonia. Tartu, 2014, 183 p.
229. **Ceith Nikkolo**. Impact of different mesh parameters on chronic pain and foreign body feeling after open inguinal hernia repair. Tartu, 2014, 132 p.
230. **Vadim Brjalin**. Chronic hepatitis C: predictors of treatment response in Estonian patients. Tartu, 2014, 122 p.
231. **Vahur Metsna**. Anterior knee pain in patients following total knee arthroplasty: the prevalence, correlation with patellar cartilage impairment and aspects of patellofemoral congruence. Tartu, 2014, 130 p.
232. **Marju Kase**. Glioblastoma multiforme: possibilities to improve treatment efficacy. Tartu, 2015, 137 p.
233. **Riina Runnel**. Oral health among elementary school children and the effects of polyol candies on the prevention of dental caries. Tartu, 2015, 112 p.
234. **Made Laanpere**. Factors influencing women's sexual health and reproductive choices in Estonia. Tartu, 2015, 176 p.
235. **Andres Lust**. Water mediated solid state transformations of a polymorphic drug – effect on pharmaceutical product performance. Tartu, 2015, 134 p.
236. **Anna Klugman**. Functionality related characterization of pretreated wood lignin, cellulose and polyvinylpyrrolidone for pharmaceutical applications. Tartu, 2015, 156 p.
237. **Triin Laisk-Podar**. Genetic variation as a modulator of susceptibility to female infertility and a source for potential biomarkers. Tartu, 2015, 155 p.
238. **Mailis Tõnisson**. Clinical picture and biochemical changes in blood in children with acute alcohol intoxication. Tartu, 2015, 100 p.
239. **Kadri Tamme**. High volume haemodiafiltration in treatment of severe sepsis – impact on pharmacokinetics of antibiotics and inflammatory response. Tartu, 2015, 133 p.

240. **Kai Part**. Sexual health of young people in Estonia in a social context: the role of school-based sexuality education and youth-friendly counseling services. Tartu, 2015, 203 p.

241. **Urve Paaver**. New perspectives for the amorphization and physical stabilization of poorly water-soluble drugs and understanding their dissolution behavior. Tartu, 2015, 139 p.

242. **Aleksandr Peet**. Intrauterine and postnatal growth in children with HLA-conferred susceptibility to type 1 diabetes. Tartu. 2015, 146 p.

243. **Piret Mitt**. Healthcare-associated infections in Estonia – epidemiology and surveillance of bloodstream and surgical site infections. Tartu, 2015, 145 p.

244. **Merli Saare**. Molecular Profiling of Endometriotic Lesions and Endometria of Endometriosis Patients. Tartu, 2016, 129 p.

245. **Kaja-Triin Laisaar**. People living with HIV in Estonia: Engagement in medical care and methods of increasing adherence to antiretroviral therapy and safe sexual behavior. Tartu, 2016, 132 p.

246. **Eero Merilind**. Primary health care performance: impact of payment and practice-based characteristics. Tartu, 2016, 120 p.

247. **Jaanika Kärner**. Cytokine-specific autoantibodies in AIRE deficiency. Tartu, 2016, 182 p.

248. **Kaido Paapstel**. Metabolomic profile of arterial stiffness and early biomarkers of renal damage in atherosclerosis. Tartu, 2016, 173 p.

249. **Liidia Kiisk**. Long-term nutritional study: anthropometrical and clinico-laboratory assessments in renal replacement therapy patients after intensive nutritional counselling. Tartu, 2016, 207 p.

250. **Georgi Nellis**. The use of excipients in medicines administered to neonates in Europe. Tartu, 2017, 159 p.

251. **Aleksei Rakitin**. Metabolic effects of acute and chronic treatment with valproic acid in people with epilepsy. Tartu, 2017, 125 p.

252. **Eveli Kallas**. The influence of immunological markers to susceptibility to HIV, HBV, and HCV infections among persons who inject drugs. Tartu, 2017, 138 p.

253. **Tiina Freimann**. Musculoskeletal pain among nurses: prevalence, risk factors, and intervention. Tartu, 2017, 125 p.

254. **Evelyn Aaviksoo**. Sickness absence in Estonia: determinants and influence of the sick-pay cut reform. Tartu, 2017, 121 p.

255. **Kalev Nõupuu**. Autosomal-recessive Stargardt disease: phenotypic heterogeneity and genotype-phenotype associations. Tartu, 2017, 131 p.

256. **Ho Duy Binh**. Osteogenesis imperfecta in Vietnam. Tartu, 2017, 125 p.

257. **Uku Haljasorg**. Transcriptional mechanisms in thymic central tolerance. Tartu, 2017, 147 p.

258. **Živile Riispere**. IgA Nephropathy study according to the Oxford Classification: IgA Nephropathy clinical-morphological correlations, disease progression and the effect of renoprotective therapy. Tartu, 2017, 129 p.

259. **Hiie Soeorg**. Coagulase-negative staphylococci in gut of preterm neonates and in breast milk of their mothers. Tartu, 2017, 216 p.

260. **Anne-Mari Anton Willmore**. Silver nanoparticles for cancer research. Tartu, 2017, 132 p.

261. **Ott Laius**. Utilization of osteoporosis medicines, medication adherence and the trend in osteoporosis related hip fractures in Estonia. Tartu, 2017, 134 p.

262. **Alar Aab**. Insights into molecular mechanisms of asthma and atopic dermatitis. Tartu, 2017, 164 p.

263. **Sander Pajusalu**. Genome-wide diagnostics of Mendelian disorders: from chromosomal microarrays to next-generation sequencing. Tartu, 2017, 146 p.

264. **Mikk Jürisson**. Health and economic impact of hip fracture in Estonia. Tartu, 2017, 164 p.

265. **Kaspar Tootsi**. Cardiovascular and metabolomic profiling of osteo-arthritis. Tartu, 2017, 150 p.

266. **Mario Saare**. The influence of AIRE on gene expression – studies of transcriptional regulatory mechanisms in cell culture systems. Tartu, 2017, 172 p.

267. **Piia Jõgi**. Epidemiological and clinical characteristics of pertussis in Estonia. Tartu, 2018, 168 p.

268. **Elle Põldoja**. Structure and blood supply of the superior part of the shoulder joint capsule. Tartu, 2018, 116 p.

269. **Minh Son Nguyen**. Oral health status and prevalence of temporo-mandibular disorders in 65–74-year-olds in Vietnam. Tartu, 2018, 182 p.

270. **Kristian Semjonov**. Development of pharmaceutical quench-cooled molten and melt-electrospun solid dispersions for poorly water-soluble indomethacin. Tartu, 2018, 125 p**.**

271. **Janne Tiigimäe-Saar**. Botulinum neurotoxin type A treatment for sialorrhea in central nervous system diseases. Tartu, 2018, 109 p.

272. **Veiko Vengerfeldt.** Apical periodontitis: prevalence and etiopathogenetic aspects. Tartu, 2018, 150 p.

273. **Rudolf Bichele.** TNF superfamily and AIRE at the crossroads of thymic differentiation and host protection against *Candida albicans* infection. Tartu, 2018, 153 p.

274. **Olga Tšuiko**. Unravelling Chromosomal Instability in Mammalian Pre-implantation Embryos Using Single-Cell Genomics. Tartu, 2018, 169 p.

275. **Kärt Kriisa.** Profile of acylcarnitines, inflammation and oxidative stress in first-episode psychosis before and after antipsychotic treatment. Tartu, 2018, 145 p.

276. **Xuan Dung Ho.** Characterization of the genomic profile of osteosarcoma. Tartu, 2018, 144 p.

277. **Karit Reinson.** New Diagnostic Methods for Early Detection of Inborn Errors of Metabolism in Estonia. Tartu, 2018, 201 p.

278. **Mari-Anne Vals.** Congenital N-glycosylation Disorders in Estonia. Tartu, 2019, 148 p.

279. **Liis Kadastik-Eerme**. Parkinson's disease in Estonia: epidemiology, quality of life, clinical characteristics and pharmacotherapy. Tartu, 2019, 202 p.

280. **Hedi Hunt**. Precision targeting of intraperitoneal tumors with peptide-guided nanocarriers. Tartu, 2019, 179 p.

281. **Rando Porosk**. The role of oxidative stress in Wolfram syndrome 1 and hypothermia. Tartu, 2019, 123 p.

282. **Ene-Ly Jõgeda**. The influence of coinfections and host genetic factor on the susceptibility to HIV infection among people who inject drugs. Tartu, 2019, 126 p.

283. **Kristel Ehala-Aleksejev**. The associations between body composition, obesity and obesity-related health and lifestyle conditions with male reproductive function. Tartu, 2019, 138 p.

284. **Aigar Ottas**. The metabolomic profiling of psoriasis, atopic dermatitis and atherosclerosis. Tartu, 2019, 136 p.

285. **Elmira Gurbanova.** Specific characteristics of tuberculosis in low default, but high multidrug–resistance prison setting. Tartu, 2019, 129 p.

286. **Van Thai Nguyeni.** The first study of the treatment outcomes of patients with cleft lip and palate in Central Vietnam. Tartu, 2019, 144 p.

287. **Maria Yakoreva**. Imprinting Disorders in Estonia. Tartu, 2019, 187 p.

288. **Kadri Rekker**. The putative role of microRNAs in endometriosis pathogenesis and potential in diagnostics. Tartu, 2019, 140 p.

289. **Ülle Võhma**. Association between personality traits, clinical characteristics and pharmacological treatment response in panic disorder. Tartu, 2019, 121 p.

290. **Aet Saar**. Acute myocardial infarction in Estonia 2001–2014: towards risk-based prevention and management. Tartu, 2019, 124 p.

291. **Toomas Toomsoo**. Transcranial brain sonography in the Estonian cohort of Parkinson's disease. Tartu, 2019, 114 p.

292. **Lidiia Zhytnik**. Inter- and intrafamilial diversity based on genotype and phenotype correlations of Osteogenesis Imperfecta. Tartu, 2019, 224 p.

293. **Pilleriin Soodla.** Newly HIV-infected people in Estonia: estimation of incidence and transmitted drug resistance. Tartu, 2019, 194 p.

294. **Kristiina Ojamaa.** Epidemiology of gynecological cancer in Estonia. Tartu, 2020, 133 p.

295. **Marianne Saard.** Modern Cognitive and Social Intervention Techniques in Paediatric Neurorehabilitation for Children with Acquired Brain Injury. Tartu, 2020, 168 p.

296. **Julia Maslovskaja.** The importance of DNA binding and DNA breaks for AIRE-mediated transcriptional activation. Tartu, 2020, 162 p.

297. **Natalia Lobanovskaya.** The role of PSA-NCAM in the survival of retinal ganglion cells. Tartu, 2020, 105 p.

298. **Madis Rahu.** Structure and blood supply of the postero-superior part of the shoulder joint capsule with implementation of surgical treatment after anterior traumatic dislocation. Tartu, 2020, 104 p.

299. **Helen Zirnask**. Luteinizing hormone (LH) receptor expression in the penis and its possible role in pathogenesis of erectile disturbances. Tartu, 2020, 87 p.